

# **IN-RUSH CURRENT MITIGATION ON TOROIDAL TRANSFORMERS WITH COMPOSITE CORES**

Warnakula Patabendige Thushan Sameera Perera

(149318P)

Degree of Master of Science

Department of Electrical Engineering

University of Moratuwa

Sri Lanka

March 2018

# **IN-RUSH CURRENT MITIGATION ON TOROIDAL TRANSFORMERS WITH COMPOSITE CORES**

Warnakula Patabendige Thushan Sameera Perera

(149318P)

Dissertation submitted in partial fulfillment of the requirements for the degree of  
Master of Science in Electrical Installation

Department of Electrical Engineering

University of Moratuwa

Sri Lanka

March 2018

## DECLARATION OF THE CANDIDATE AND SUPERVISORS

I declare that this is my own work and this dissertation does not incorporate without acknowledgment any material previously submitted for a Degree or Diploma in any other University or institute of higher learning and to the best of my knowledge and belief it does not contain any material previously published or written by another person except where the acknowledgement is made in the text.

Also, I hereby grant to University of Moratuwa the non-exclusive right to reproduce and distribute my dissertation, in whole or in part in print, electronic or other medium. I retain the right to use this content in whole or part in future works (such as articles or books).

.....  
Signature of the candidate  
(W. P. T. S. Perera)

Date

The above candidate has carried out research for the Masters dissertation under my supervision.

.....  
Signature of the supervisor  
(Prof. J.P. Karunadasa)

Date

## **ACKNOWLEDGEMENT**

First of all, the pride, praise and perfection belong to the almighty alone.

Then, I would like to express my sincere gratitude to my supervisor Prof. J. P. Karunadasa for the continuous guidance given me to drive this research to the success, through motivation, enthusiasm and with his immense knowledge.

Further, I would like to pay my gratitude to all the lecturers engaged in the MSc course programme, for making our vision broader and providing us the opportunity to improve our knowledge in various fields.

Then I would like to extend my appreciation to the company I am currently working Noratel International (Pvt) Ltd. for providing the necessary research material and facilities required to complete this study.

Warmest thanks go to the prototype division of the company for the support given to me by sampling, which greatly helped me for the collection of required data.

Moreover, I appreciate the help given by my colleagues Sumith and Suresh in my work place and for the continuous encouragement throughout this post graduate programme and in the research work.

Finally my special thanks go to my wife, my mother, my father and my brother for their love, unwavering and resolute support during this eventful period.

W. P. T. S. Perera

## ABSTRACT

Toroidal transformers play an important role in the transformer industry specially in high end applications due to their superior performance, over the conventional laminated transformers. But toroidal transformers lag in performance when comes to high power requirements, specially due to their extremely high inrush currents compared to the laminated transformers.

There are many options that can be used externally to the toroidal transformer to avoid this issue, but due to the reliability concerns, transformer based inrush current mitigation methods are always preferred in the industry. Conventional transformer based inrush current mitigation methods fall short on toroidal transformers, because those methods tend to mitigate their superior performance also, together with the inrush current.

The proposed transformer based inrush current mitigating method with composite cores will reduce the inrush current extensively, while protecting the typical superior performance characteristics of toroidal transformers. Also the proposed method will have better control over the inrush current than the conventional methods, while being competitive in the market.

The proposed method involves two cores; one is lower grade NGOSS (Non Grain Oriented Silicon Steel) core in the centre for the normal operation, and the other is higher grade GOSS (Grain Oriented Silicon Steel) core positioned around the NGOSS core with a controlled air-gap, for inrush current controlling purpose. Due to the uncut NGOSS core in the centre, the composite core retains high performance in the normal operation without compromising.

This dissertation includes practical development of the composite core together with silicon steel types CK37-35H300 and M0H-M103-27P, and then experimental testing on inrush current and finally converge the research findings for developing a new design guideline for the optimized solution, while discussing the cost and the manufacturing aspects.

# TABLE OF CONTENTS

DECLARATION OF THE CANDIDATE AND SUPERVISORS.....	i
ACKNOWLEDGEMENT.....	ii
ABSTRACT .....	iii
LIST OF FIGURES.....	viii
LIST OF TABLES.....	x
LIST OF ABBREVIATIONS.....	xi
LIST OF APPENDICES.....	xii
<b>Chapter 1 – INTRODUCTION</b>	
1.1 Toroidal transformer construction.....	2
1.2 Motivation to the research.....	4
1.3 Objective of the research.....	5
<b>Chapter 2 - INRUSH CURRENT IN TOROIDAL TRANSFORMERS</b>	
2.1 Theoretical background of inrush current.....	7
2.2 Toroidal core.....	9
2.2.1 Silicon steel .....	10
2.2.2 Silicon steel on toroidal core .....	10
2.3 Saturation inductance and inrush current.....	12
<b>Chapter 3 - RESEARCH DESIGN</b>	
3.1 Existing inrush current mitigation methods.....	16
3.1.1 NTC thermistor in primary winding .....	16
3.1.2 Use of NGOSS .....	18
3.1.3 Cut core toroidal transformers .....	21
3.2 Proposed composite core concept for inrush current mitigation ..	23
3.2.1 Design flux density.....	24
3.2.2 Airgap size in cut core.....	25
3.2.2.1 Flux distribution in the composite core.....	26
3.2.2.2 Calculation of saturation inductance $L_s$ .....	30
3.2.2.3 Calculation of inrush current.....	32

3.2.3	Uncut – Cut core cross-sectional area ratio.....	35
3.3	Importance Of Source Impedance On Inrush Current .....	35
3.4	Scope of the research.....	37
<b>Chapter 4 - EXPERIMENTAL DATA COLLECTION</b>		
4.1	Inrush current measurement on samples.....	38
4.2	Finding the optimum air gap for outer core.....	39
4.3	Summary of inrush current measurements.....	47
4.4	Inrush current measurements for different area ratios.....	48
<b>Chapter 5 - ANALYSIS OF DATA</b>		
5.1	Selection of optimum air-gap .....	50
5.2	Calculation of relative permeability .....	52
5.3	Calculation of inrush current for different core cross-sectional area ratios.....	53
5.4	Development of design tool for composite core.....	55
5.5	Comparison between measured and calculated inrush current values.....	57
<b>Chapter 6 - RESULTS DISCUSSION AND MOTIVATION</b>		
6.1	Comparison of electrical parameters .....	60
6.1.1	Comparison of inrush current values.....	60
6.1.2	Comparison of no-load current values.....	62
6.1.3	Comparison of reactive power loss.....	63
6.1.4	Comparison of active power loss.....	64
6.2	Use of recycle steel cores .....	66
6.3	Comparison of manufacturing aspects.....	67
6.3.1	Manufacturing of conventional cut core.....	67
6.3.2	Manufacturing of composite core.....	68
6.4	Comparison of mechanical parameters.....	69
<b>Chapter 7 - CONCLUSION AND SUGGESTIONS FOR FUTURE RESEARCH</b>		
7.1	Conclusion.....	72
7.2	Suggestions for future research.....	73



Reference List.....	74
Appendices.....	75

## LIST OF FIGURES

Figure No.	Description	Page
<b>Figure 1.1:</b>	Inrush current transient waveform .....	2
<b>Figure 1.2:</b>	Toroidal transformer.....	3
<b>Figure 1.3:</b>	EI laminated transformer .....	4
<b>Figure 2.1:</b>	Graphical interpretation of inrush current with remanence .....	9
<b>Figure 2.2:</b>	Silicon steel mother coils .....	10
<b>Figure 2.3:</b>	BH characteristics for AISI CK37 (35H300).....	13
<b>Figure 2.4:</b>	BH characteristics for AISI M-0H M103-27P.....	14
<b>Figure 2.5:</b>	BH characteristics for AISI M-5.....	15
<b>Figure 3.1:</b>	Typical characteristic curve for NTC .....	17
<b>Figure 3.2:</b>	Magnetization characteristics for GOSS-AISI Grade M5.....	18
<b>Figure 3.3:</b>	Core loss curve for GOSS-AISI Grade M5.....	19
<b>Figure 3.4:</b>	Magnetization characteristics for NGOSS 35H300.....	19
<b>Figure 3.5:</b>	Core loss curve for NGOSS 35H300.....	20
<b>Figure 3.6:</b>	BH loops before and after core cut.....	21
<b>Figure 3.7:</b>	Composite core arrangement.....	23
<b>Figure 3.8:</b>	Real manufactured composite core .....	23
<b>Figure 3.9:</b>	Variation of inrush current with outer core airgap.....	26
<b>Figure 3.10:</b>	Flux density distribution between Cut/Uncut cores.....	27
<b>Figure 3.11:</b>	BH curve for AISI MOH - M103-27P.....	28
<b>Figure 3.12:</b>	Experimentally calculated $\mu$ H characteristic curve.....	28
<b>Figure 3.13:</b>	Extract of calculated $\mu$ H characteristic.....	29
<b>Figure 3.14:</b>	Calculated $B_{\mu}$ characteristic .....	30
<b>Figure 3.15:</b>	BH loops at different air-gaps .....	33
<b>Figure 3.16:</b>	BH loop at deep saturation .....	34
<b>Figure 3.17:</b>	Inrush current measured with high source impedance.....	36
<b>Figure 3.18:</b>	Inrush current measured with low source impedance.....	37
<b>Figure 4.1:</b>	Test setup for inrush current measurement.....	38
<b>Figure 4.2:</b>	Variation of inrush current with outer core airgap .....	40

<b>Figure 4.3:</b>	Inrush current wave form TI-173622.....	40
<b>Figure 4.4:</b>	Flux density distribution of Cut/Uncut cores.....	41
<b>Figure 4.5:</b>	Variation of inrush current with outer core airgap.....	42
<b>Figure 4.6:</b>	Inrush current wave form TI-173618C.....	42
<b>Figure 4.7:</b>	Flux density distribution of Cut/Uncut cores .....	43
<b>Figure 4.8:</b>	Variation of inrush current with outer core airgap.....	44
<b>Figure 4.9:</b>	Inrush current wave form TI-173618D.....	44
<b>Figure 4.10:</b>	Flux density distribution of Cut/Uncut cores.....	45
<b>Figure 4.11:</b>	Variation of inrush current with outer core airgap.....	46
<b>Figure 4.12:</b>	Inrush current wave form TI-173618E.....	46
<b>Figure 4.13:</b>	Flux density distribution of Cut/Uncut cores.....	47
<b>Figure 4.14:</b>	Inrush Current ( $\times I_{load}$ ) Vs Steel cross-sectional area ratio.....	49
<b>Figure 5.1:</b>	Optimum air-gap to the cut core cross sectional area.....	51
<b>Figure 5.2:</b>	Relative permeability Vs Cut-core cross-sectional area.....	53
<b>Figure 5.3:</b>	Inrush Current ( $\times I_{load}$ ) Vs Steel cross-sectional area ratio.....	54
<b>Figure 5.4:</b>	Flow chart of Design tool.....	56
<b>Figure 5.5:</b>	Design tool.....	57
<b>Figure 6.1:</b>	Inrush current of composite / conventional designs.....	61
<b>Figure 6.2:</b>	No-load current of composite / conventional designs.....	63
<b>Figure 6.3:</b>	Reactive power loss of composite / conventional designs.....	64
<b>Figure 6.4:</b>	Active power loss of composite / conventional designs.....	65
<b>Figure 6.5:</b>	Recycle core including joints in steel strips.....	66
<b>Figure 6.6:</b>	Conventional cut core.....	67
<b>Figure 6.7:</b>	Composite core.....	68
<b>Figure 6.8:</b>	Humming test set up.....	70

## LIST OF TABLES

<b>Table No.</b>	<b>Description</b>	<b>Page</b>
<b>Table 3.1:</b>	Flux densities at normal/inrush condition .....	27
<b>Table 3.2:</b>	Experimental test data on AISI M0H - M103-27P.....	29
<b>Table 4.1:</b>	Design parameters for TI-173622.....	39
<b>Table 4.2:</b>	Design parameters for TI-173618C.....	41
<b>Table 4.3:</b>	Design parameters for TI-173618D.....	43
<b>Table 4.4:</b>	Design parameters for TI-173618E.....	45
<b>Table 4.5:</b>	Summary of inrush current measurements.....	48
<b>Table 4.6:</b>	Inrush current measurements for different area ratios.....	48
<b>Table 4.7:</b>	Inrush current measurements for all samples.....	49
<b>Table 5.1:</b>	Optimum air-gap to the cut core cross sectional area.....	51
<b>Table 5.2:</b>	Relative permeability to the core cross sectional area.....	52
<b>Table 5.3:</b>	Comparison between measured and calculated inrush current values.....	58
<b>Table 6.1:</b>	Inrush current measurements of composite / conventional designs.....	60
<b>Table 6.2:</b>	No-load current measurements of composite / conventional designs.....	62
<b>Table 6.3:</b>	Reactive power loss measurements of composite/conventional designs.....	63
<b>Table 6.4:</b>	Active power loss measurements of composite / conventional Designs.....	65

## LIST OF ABBREVIATIONS

<b>Abbreviation</b>	<b>Description</b>
AC	Alternative Current
AISI	American Iron and Steel Institute
DC	Direct Current
EMI	Electro Magnetic Interference
GOSS	Grain Oriented Silicon Steel
H	Height
ID	Inner Diameter
IEC	International Electrotechnical Commission
MMF	Magneto Motive Force
MPL	Magnetic Path Length
NC	Nano Crystalline
NGOSS	Non Grain Oriented Silicon Steel
NTC	Negative Temperature Coefficient
OD	Outer Diameter
RMS	Root Mean Square

## LIST OF APPENDICES

Appendix	Description	Page
<b>Appendix A:</b>	Design simulations with ToroidEZE programme for designs with steel area ratio Uncut : Cut – 1.0 : 0.7.....	75
<b>Appendix B:</b>	Design simulations with ToroidEZE programme for designs with different steel area ratios .....	83
<b>Appendix C:</b>	Test equipment details .....	91

## INTRODUCTION

Inrush current (sometimes called input surge current) is defined as maximum peak current drawn by electrical equipment due to driving its core into deep saturation at the time of energization. Inrush current is an undesirable phenomenon to occur and the equipment manufacturers/designers have to take this in to consideration where it is applicable. Elimination of inrush current could be very costly and impossible but mitigation of inrush current is possible [1].

Generally for all cases inrush current does not last for a long time. For example it lasts only for few cycles for alternating current (AC), for transformers and motors. Magnitude of inrush current to its rated current could be several times, or even closer to 30 times in extreme cases, especially with toroidal transformers [2]. The magnitude of the inrush current is based on several parameters like; switching angle, source impedance, magnitude of input voltage, residual flux on the core, saturation inductance, etc. As a result, more often overcurrent protection reacts for these high currents and trips the device from the source resulting inability to energize the equipment. Also the inrush current will result in significant voltage drops, and thus affect the power quality, reliability and stability [2].

Inrush current most of the time is harmless to the device but unwanted tripping could cause undue problems to the electrical system. But in special cases, mostly with toroidal transformers which normally connected at high end applications, it needs to protect the expensive power electronic equipment from the high currents [2].

To understand this phenomenon in transformers and motors it requires sound knowledge of mathematics and magnetism. Inrush current occurrences on transformers are explained in chapter 2 to the extent of the topic being discussed. Typical inrush current transient waveform when a transformer is energized is illustrated in Figure 1.1, which is captured on a single phase 1000VA toroidal transformer.

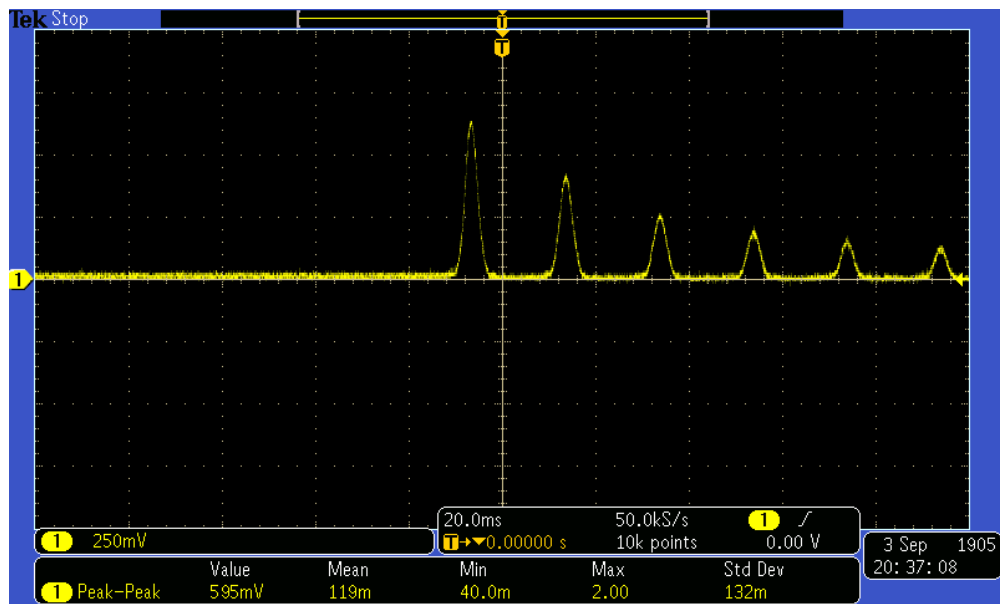


**Figure 1.1:** Inrush current transient waveform

## 1.1 Toroidal Transformer Construction

Toroidal winding is considered to be challenging with respect to winding in laminated transformer, as it required rotating the coil during winding through the inner diameter of the core. Typical toroidal core does not hold any gaps in its magnetic path, which cause the toroidal transformer to be high performing with respect to the laminated transformers. The performance of an ideal transformer can be closely approximated with this most expensive toroidal construction [1].

In the process, first sufficient winding wire must be wound or loaded onto the winding shuttle (or magazine), and then unwound onto the toroidal transformer's core as per the required turns in the particular design. This is repeated as for the number of primary and secondary windings on the transformer. Also it is having the capability to wind several copper wires together to wind several windings at once, hence saving cost. For isolation transformer, insulation is required in between the



primary winding and the secondary winding. Generally the exposed enamel copper (or aluminium) wire is protected by outer wrapping insulation tape for safety purpose. Normally all the insulations are done based on the creep and clearance distance requirements coming under IEC 61558.

Toroidal transformer will not require a bobbin or tube like with the laminated construction, but the insulated core itself act as the bobbin, which is creating better coupling of flux in the core together with the windings.

Toroidal construction is less common and not popular in the industry due to its manufacturing complexity and high cost. However toroidal components can be seen in high end applications regardless of its high costs due to their high performance requirements.

Figure 1.2 shows a single-phase toroidal transformer which goes to a power supply unit for high-end audio amplifier.



**Figure 1.2:** Toroidal transformer

Most common transformer construction is laminated type transformers due to its simplicity in construction. A typical laminated type transformer is illustrated in Figure 1.3. When comes to low power transformers, most of the laminated type

transformers are made with EI shaped core laminations. These are stamped as English letters 'E' and 'I' and these E's and I's are then stacked to form the core. Then the copper/aluminium wire (or foil) winding is done on a bobbin, and the wound bobbin is then inserted into the stacked E and I core parts, and finally they are fixed tightly by suitable mechanism.

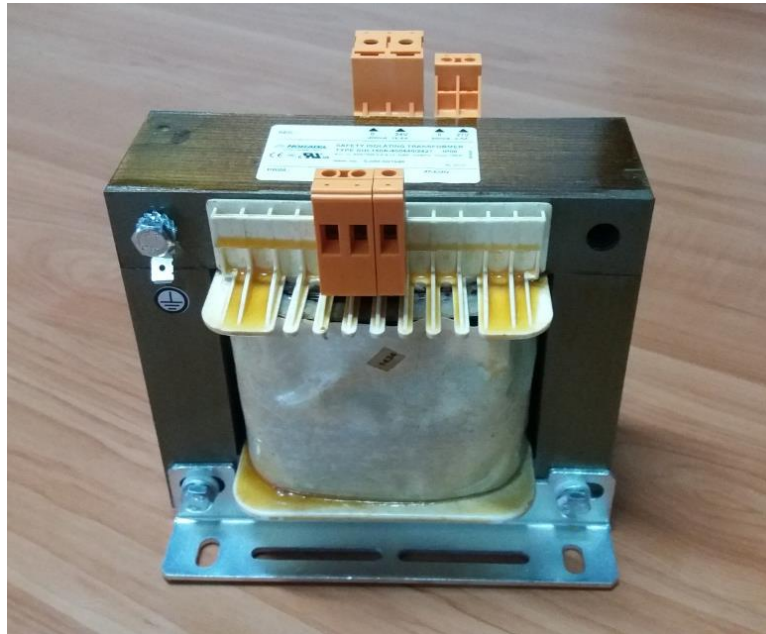


**Figure 1.3:** EI laminated transformer

## 1.2 Motivation to the Research

Toroidal transformer has its advantages over laminated transformers of high efficiency, low weight, low leakage and low Electro Magnetic Interference (EMI), low volume, etc. The core loss in a toroidal transformer is very low since its gapless round shape, and which supports and allows the magnetic flux to travel ideally in a less reluctance magnetic path with minimum stray field. As a result, when designing toroidal transformers, the designers can go for high design flux densities and utilise material effectively than in laminated type [1].

However due to its low reluctance to flux, toroidal transformer exhibits severe inrush currents than standard laminated type transformers. This is one major drawback in toroids and it becomes significant especially considering high power transformers. The situation gets worsen when higher quality grade steel is used, due to even low reluctance in the core to the flux.

High quality grain-oriented silicon steel (GOSS) has steep induction curve against excitation current and also they do have higher residual flux (remanence flux) which cause high inrush of the transformer. This occurrence is further described in chapter 2, also comparing different types of electrical steel grades (Grain-oriented and Non grain-oriented) usually used in toroidal transformer designing.

Presently there are many methods to limit inrush current on toroidal transformers, both using external equipment based and transformer-based solutions. But most of the existing transformer-based mitigation methods are weakening the performance indicators of the toroidal transformer design; even it is more reliable than the external equipment based inrush current mitigation methods [1].

Therefore still there is an industry requirement to search for a more developed and optimized inrush mitigation method to boost the market share on toroidal transformers.

### **1.3 Objective of the Research**

The main objective of this study is to propose a reliable and economical transformer-based inrush current mitigation method for toroidal transformers. The conceptual proposal would be to use a composite core with an uncut inner-core and a gapped outer-core.

Using the proposed composite core method, it is envisaged to increase the performance of transformer by using low grade steel in the un-gapped core in place

of air-gapped high grade steel. With this method, it is expecting to save material costs and labour on the product and overall being competitive in the market.

The ultimate goal of the project is to promote toroidal transformers in the industry over other types of transformers (laminated), even in the high power levels.

Furthermore, limiting the use of high grade materials unworthily in magnetic components is also an objective of this study. General norm is high grade materials are extracted and manufactured with higher energy intense processes, and therefore an environment friendly and resource conservative benefits are secured out of this research. The possibility of using re-cycled steel for composite core method is also an advantage of this regards [1].

---

## INRUSH CURRENT IN TOROIDAL TRANSFORMERS

As stated in the previous Chapter 1, inrush current is a critical problem for toroidal transformers compared to the laminated transformers, especially considering higher power levels. A brief introduction to toroidal transformer is done in previous Chapter 1 under section 1.2, and in this chapter the following main topics are discussed in order to have a better understanding on the inrush current scenario with toroidal transformers.

- 1) Theoretical background of inrush current
- 2) Toroidal core
- 3) Saturation inductance and inrush current

### 2.1 Theoretical Background of Inrush Current

This is a transient scenario, where high saturation of the transformer core originates high inrush current at the point of energization. There are several explanations on this scenario in several sources, but the below will illustrate the basics of the inrush current occurrence in a simpler way.

Basically the input voltage applied to the transformer will be the driving force to the inrush current and that will force the flux to build up double the steady state flux plus the remanence flux. Hence the transformer gets in to deep saturation and that result with creating a high energization current [3].

Inrush current occurrence of a transformer is a transient effect which could be explained with electromagnetism as described follows.

The inrush current phenomenon is governed by Faraday's law [3].

$$v(t) = \frac{d}{dt} \phi'(t) \quad (2.1)$$

Where  $v(t)$  is the instantaneous voltage applied and  $\phi'(t)$  is the instantaneous flux linkage.

Then, 
$$\phi'(t) = \int_0^t v(t) dt \quad (2.2)$$

Neglecting the leakage flux component, the total instantaneous flux  $\Phi(t)$  of the core with  $N$  number of turns of the winding can be written as,

$$\phi'(t) = N\phi(t) \quad (2.3)$$

Then with combining equations (2.2) and (2.3)

$$\phi(t) = \frac{1}{N} \int_0^t v(t) dt \quad (2.4)$$

Consider the supply voltage for the transformer is sinusoidal with switching angle  $\theta$

$$v(t) = V_m \cdot \sin(\omega t + \theta)$$

Then re-write equation (2.4) with sinusoidal supply voltage  $v(t)$

$$\phi(t) = \frac{1}{N} \int_0^t V_m \cdot \sin(\omega t + \theta) dt \quad (2.5)$$

$$\phi(t) = \frac{V_m}{N} \int_0^t \sin(\omega t + \theta) dt$$

$$\phi(t) = \frac{V_m}{N\omega} \cdot [-\cos(\omega t + \theta)]_0^t$$

$$\phi(t) = \frac{V_m}{N\omega} \cdot [-\cos(\omega t + \theta) + \cos \theta] + \phi(0)$$

Considering the remanence flux at  $t=0$  is  $\phi(0) = \phi_r$  (Remanence flux)

Then,

$$\phi(t) = \frac{V_m}{N\omega} \cdot [-\cos(\omega t + \theta) + \cos \theta] + \phi_r$$

The maximum flux  $\phi_{max}$  is generated at zero crossing of the input voltage applied; means  $\theta = 0$

$$\phi_{max} = \frac{V_m}{N\omega} \cdot [2] + \phi_r$$

$$\phi_{max} = \frac{2V_m}{N\omega} + \phi_r$$

$$\phi_{max} = 2\phi_m + \phi_r \quad (2.6)$$

So it is proven that, the inrush transient forces the flux to build up double the steady state flux plus the remanence flux. This scenario can be illustrated in graphical form as per the Figure 2.1 [3].

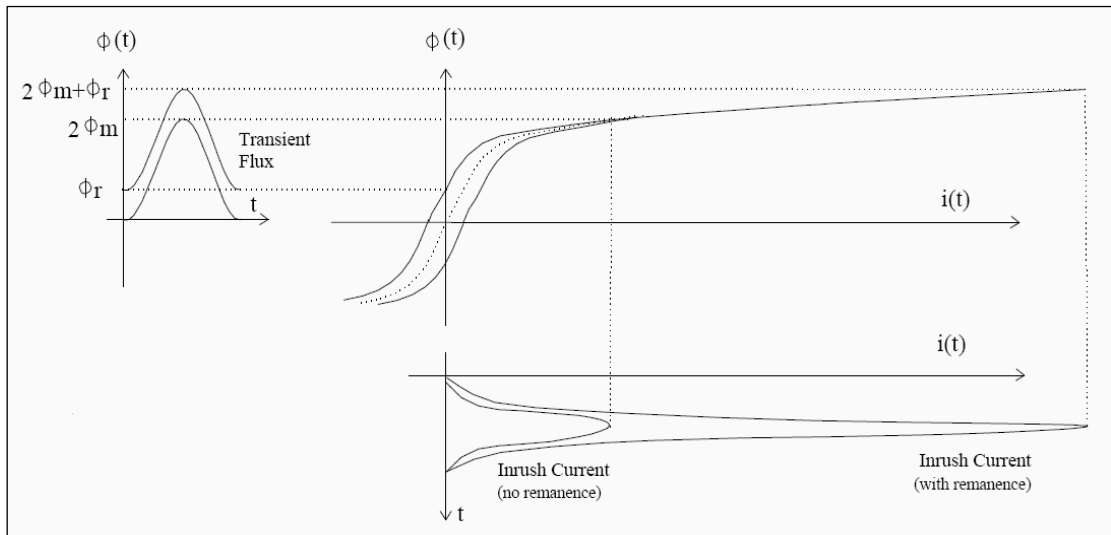


**Figure 2.1:** Graphical interpretation of Inrush current with remanence

## 2.2 Toroidal Core

Toroidal core is having donut shape with no air gaps in the magnetic path, against the laminated transformer cores. These cores are available in many material types; Silicon steel (SiFe), Nickel iron (NiFe), Perm-alloy, Nano-crystalline (NC) and others [1]. Silicon steel and nickel iron mainly available as tape wound cores or laminated pieces. In this research, only Silicon steel types are considered for toroidal transformer cores.

### 2.2.1 Silicon steel

Silicon steel is available as tape wound reels with different types/grades, thicknesses, widths and can be purchased based on the requirements of the relevant designs. Standard available steel widths are varying with the steps of 5mm, but still possible to purchase even other sizes in between, based on the demand. Figure 2.2 shows a silicon steel coil before the slitting process done, and in this form it is called as the ‘Mother coil’. Mother steel coil is commonly available with 350mm width.



**Figure 2.2:** Silicon steel mother coils

### 2.2.2 Silicon steel on toroidal core

Generally the silicon steel contains high permeability ( $\mu$ ) providing low reluctance (R) for a given Magnetic Path Length (MPL). When a transformer core is magnetized to the flux density (B) and the permeability increases as per following basic equation.



$$B = \mu \cdot H \quad (2.7)$$

Where H – Magnetizing force

As per the B-H characteristics of typical silicon steel (refer Figure 2.3), it retains almost linear relationship between B and H up to certain flux density (where it holds maximum permeability) and then the steel starts approaching to the saturation region. Then, if the flux density further increased in the saturation region, the permeability decreases approaching to the value of free space or air. This region is called as deep saturation of the steel core. This is a common scenario for all the silicon steel types, apart from the difference of the flux densities where it start saturation.

Electrical steel comprises of various grades and have different classifications. One of the standard classifications is from its AISI grade. AISI stands for American Iron and Steel Institute [1].

There are mainly three types of silicon steel types discussed in this research; one is non-grain oriented steel type AISI CK37 (35H300) and other two are grain oriented steel types AISI M-5 and AISI M-0H. See Figure 2.3 to 2.5 for the steel characteristic curves taken from Kawasaki Steel data catalogue [4].

Mainly the grain oriented steel type AISI M-5 is used for conventional low inrush designs to retain better performance, even together with fully air-gapped core. The drawbacks of this method are discussed in the next chapter 3.

But in this research, the steel types AISI CK37 (35H300) and AISI M-0H M103-27P are mainly discussed in the composite core. Basically with the proposed composite core method, the steel AISI CK37 is used as the centre core to operate in the normal condition at its unsaturated region, while AISI M-0H is used to dominate in the inrush condition at its “Just unsaturated” condition.

### **2.3 Saturation Inductance and Inrush Current**

In this research, it is proven that the most significant parameter affect to the inrush is saturation induction. In many literatures, they say the input winding resistance mainly affects the inrush current, but in practical scenario the designers do not have much allowance to change the winding resistances having a design is normally bound for particular temperature class.

Therefore in this research, the effects of saturation induction to the inrush current is mainly discussed and go through details on the inrush current variation by changing the air-gap in the outer core, hence changing the saturation induction.

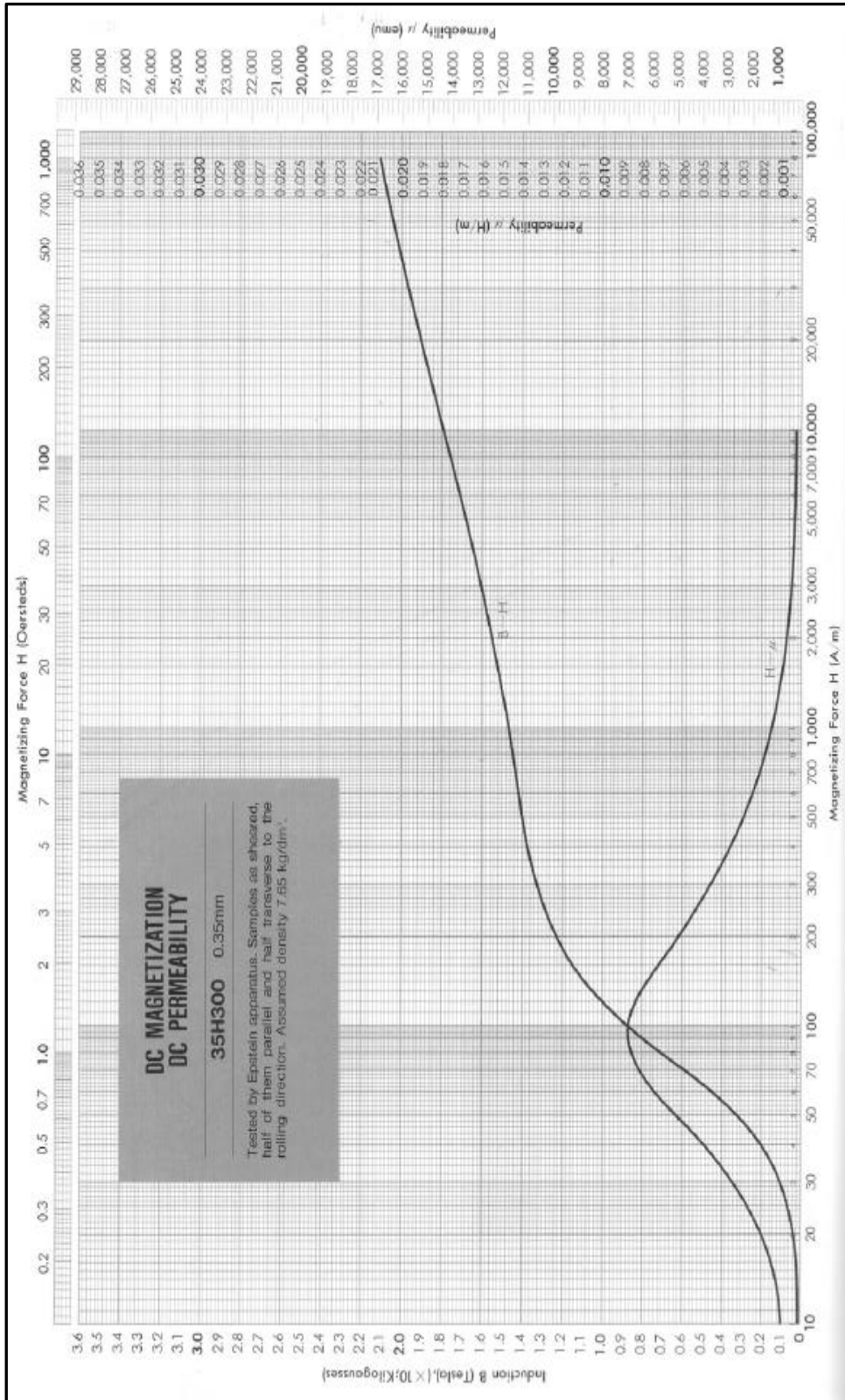


Figure 2.3 : BH characteristics for AISI CK37 (35H300)

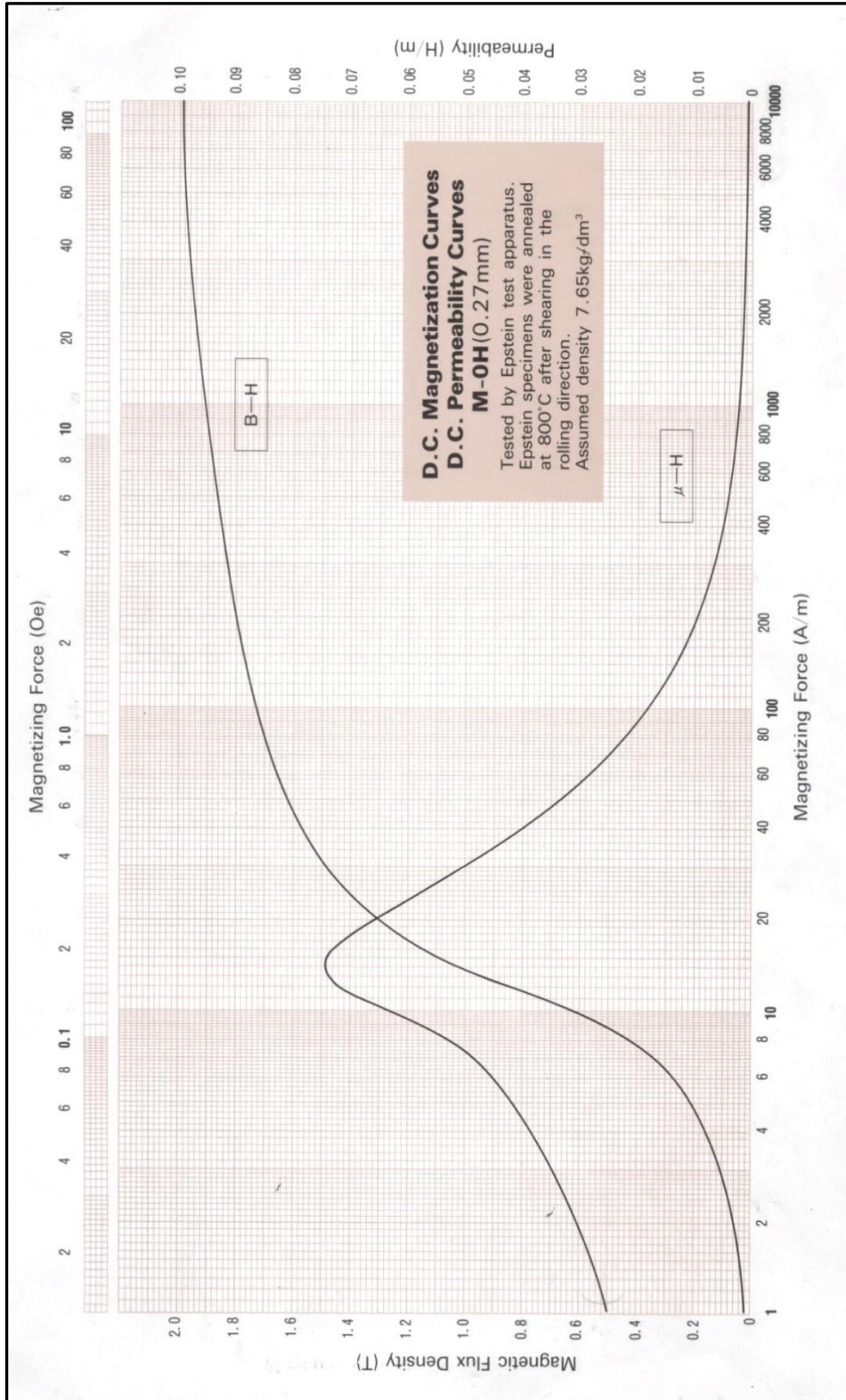


Figure 2.4 : BH characteristics for AISI M-0H M103-27P

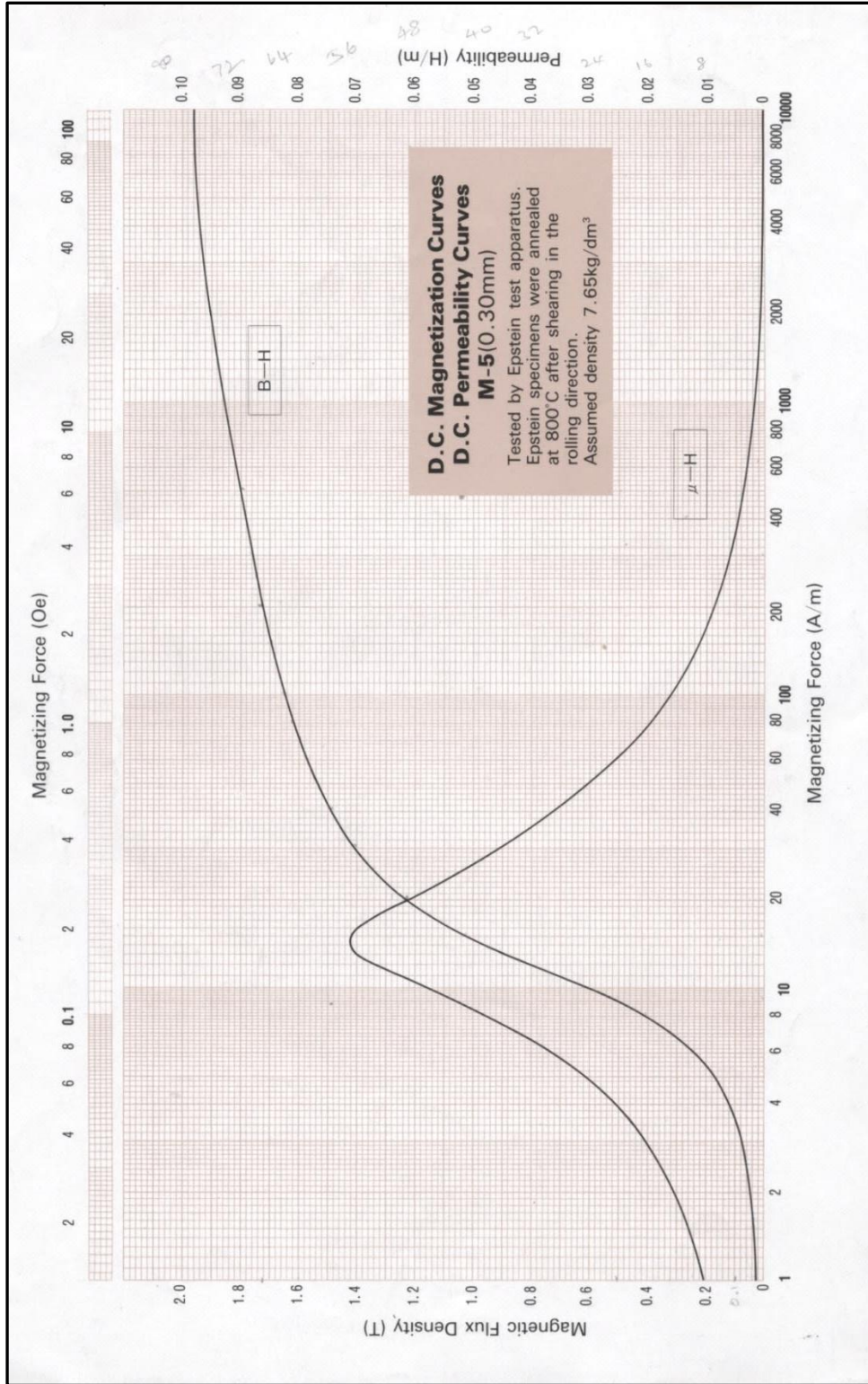


Figure 2.5 : BH characteristics for AISI M-5

---

## RESEARCH DESIGN

In chapter 2, it was discussed about the inrush current phenomenon on toroidal transformers and about the factors that affect the magnitude of inrush transients; mainly the saturation inductance and electrical steel characteristics.

In this chapter following aspects are discussed descriptively.

- 1) Existing inrush current mitigation methods
- 2) Proposed composite core concept for inrush current mitigation
- 3) Importance of source impedance on inrush current
- 4) Scope of the research

### 3.1 Existing Inrush Current Mitigation Methods

Mainly there are two categories of inrush mitigation methods available for toroidal transformers; one is external equipment based inrush current mitigation and the other is transformer-based inrush current mitigation.

Out of these two categories, most of the high end applications prefer the transformer-based solutions for inrush current mitigation, due to their higher reliability [1]. Followings are some of the methods used by designers/manufacturers for mitigation of inrush currents in toroidal transformers.

#### 3.1.1 NTC thermistor in primary winding

This method can be used with general purpose toroidal transformers, where the transformer is not designed intending to mitigate the inrush current. The main advantage of this method is, here the transformer can be designed in higher flux density utilizing the magnetization curve to its maximum possible point. Also the transformer efficiency, weight, dimensions could also be to its optimum and also that lead avoiding complex manufacturing processes, hence finally be economical.

The Negative Temperature Coefficient (NTC) thermistors are thermally sensitive semiconductor resistors which exhibit inverse characteristic between the resistance and the absolute temperature, as shown in Figure 3.1. In typical operation of the NTC thermistor, this is connected in series with the transformer input winding and initially holding high resistance at lower ambient temperature. But after the transformer is powered up, the resistance of the NTC thermistor can be brought down either by a change in the ambient temperature or by self-heating resulting from current flowing through the device [1].

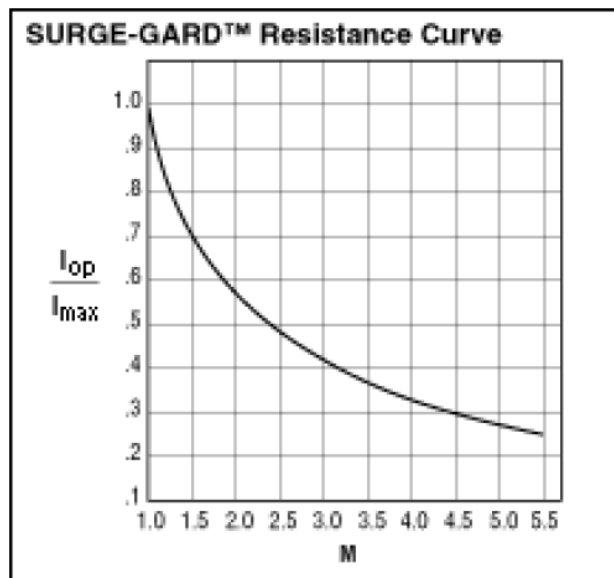


**Figure 3.1:** Typical characteristic curve for NTC

Referring the Figure 3.1, the x-axis is representing the multiplying factor  $M$ , which should multiply with specified nominal resistance of the NTC at  $I_{max}$ , to get the resistance value at each  $I_{op} / I_{max}$ .

$I_{max}$  - The maximum steady state RMS AC or DC

$I_{op}$  - The actual operating current.

The main drawbacks of this method are the addition of primary resistance to normal operation of the transformer and the heat dissipation and ultimately leading to low efficiency of the total equipment. And the next drawback is, it will not do the intended function in successive power interruptions, because due to the thermal

inertia the thermistor may hold high temperature - low resistance stage in the next power up. The other drawback is the reliability. Transformer itself is highly reliable but adding the NTC thermistor in series with the supply makes the combination unreliable.

### 3.1.2 Use of NGOSS

The typical B-H curve for silicon steel presents steep magnetization characteristic after they exceed the maximum unsaturated flux density. This characteristic is far great especially with GOSS types, while it is not that much critical for NGOSS types.

Generally toroidal transformers are wound using high grade GOSS for its common intended performances, but the said steep magnetization curves of GOSS and high design flux density makes easy to saturate the core. See Figure 3.2 and Figure 3.3 for magnetization characteristics with corresponding loss curves for GOSS (AISI M-5) [4].

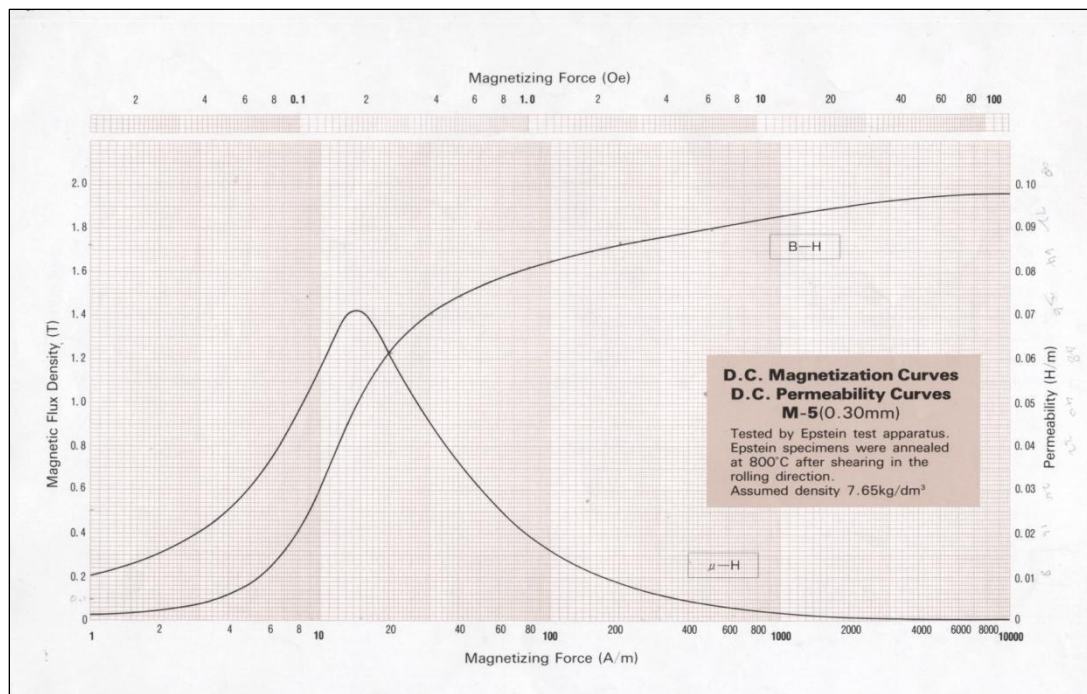


**Figure 3.2:** Magnetization characteristics for GOSS-AISI Grade M5



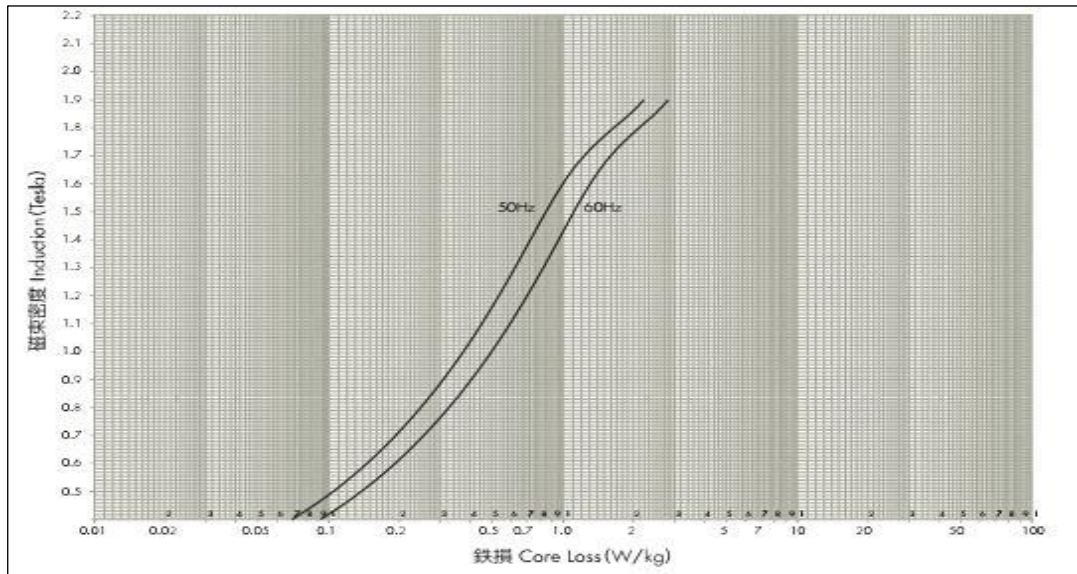


**Figure 3.3:** Core loss curve for GOSS-AISI Grade M5

As a result, designers are using NGOSS for low inrush designs due to lower steep characteristics in magnetization [1]. NGOSS transformers have to be designed in low flux density and then its narrow magnetization characteristics can be used to keep it unsaturated, compared to the GOSS types. Following Figures 3.4 to 3.5 illustrates magnetization characteristics with corresponding loss curves for NGOSS (35H300) [4], for easy understanding of above mentioned point.

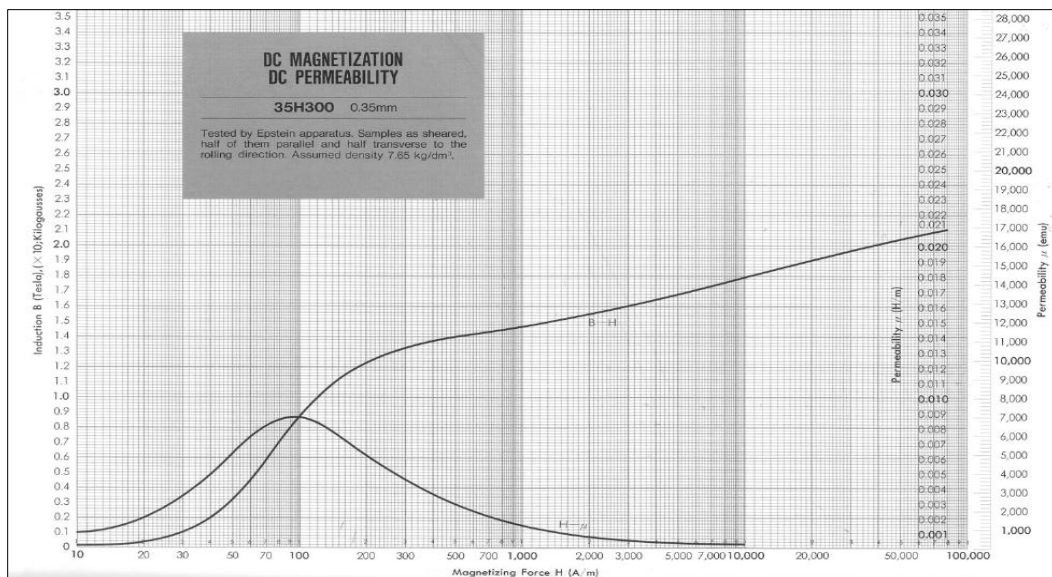


**Figure 3.4:** Magnetization characteristics for NGOSS 35H300

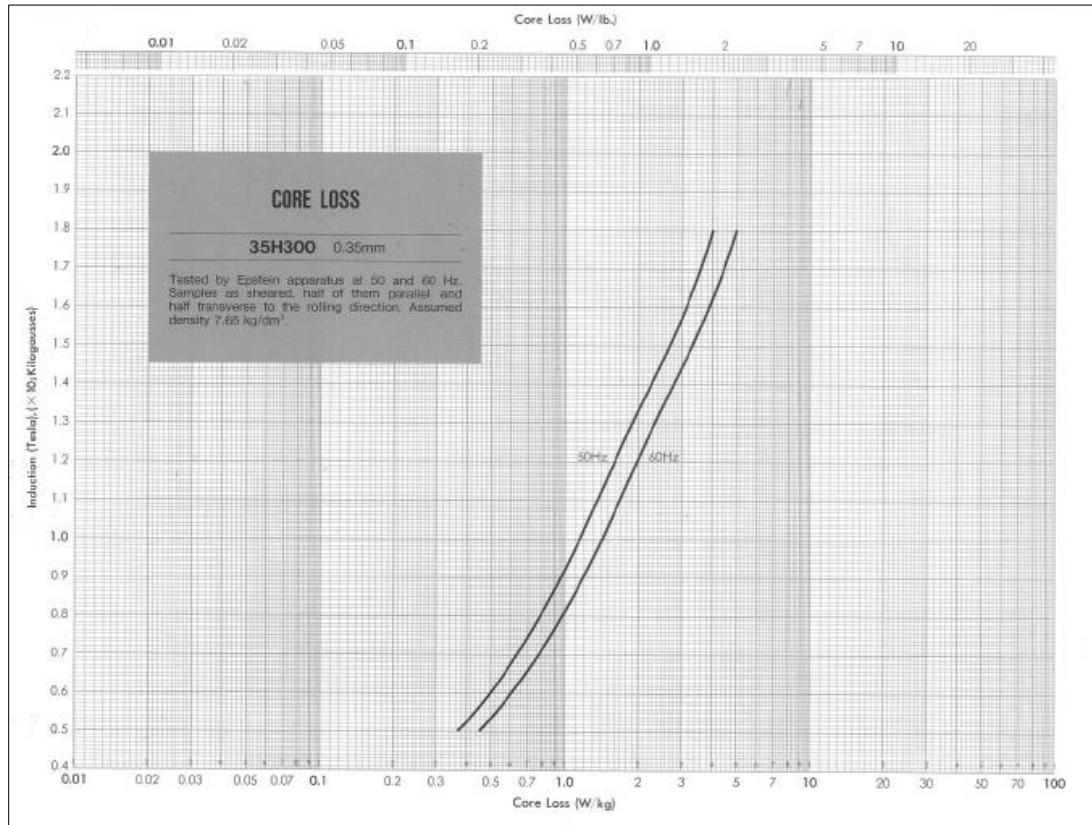


**Figure 3.5:** Core loss curve for NGOSS 35H300

Selection of NGOSS does reduce the inrush current to some extent, but when the application is critical on inrush current, the designers also tend to use above NGOSS without annealing process [1]. Annealing is a special heat treatment process done to regain the magnetic properties back to steel core, after it has been lost in the core manufacturing process (due to stresses exerted on the steel strips).

The main drawback of this method is the less efficiency of the transformer due to high core losses (see Figure 3.5) and high excitation current. These designs are obviously bulky and weight is more than the standard GOSS designs.

However reliability point of view this method is better than the method described in previous section 3.1.1.

### 3.1.3 Cut core toroidal transformers

Introducing a cut (or a small air-gap) to the magnetic path of the toroidal core will change magnetization characteristics of the steel; basically this will increase the unsaturation characteristic even at the high flux densities. Based on the BH characteristics, it will reduce the slope of the curve (or reduce permeability) and bring the knee point to the right side of magnetization curve, while increasing the magnetizing force.

Also the other main purpose is reducing the remanence flux ( $\phi_r$ ). As per the equation 2.6 derived for inrush current (also Figure 2.1), the remanence flux (or remanence flux density,  $B_r$ ) plays an important role in the inrush current. The Figures 3.6 illustrates how the remanence flux density get reduced (by  $\Delta B$ ) together with an air gap in the toroidal core [5].

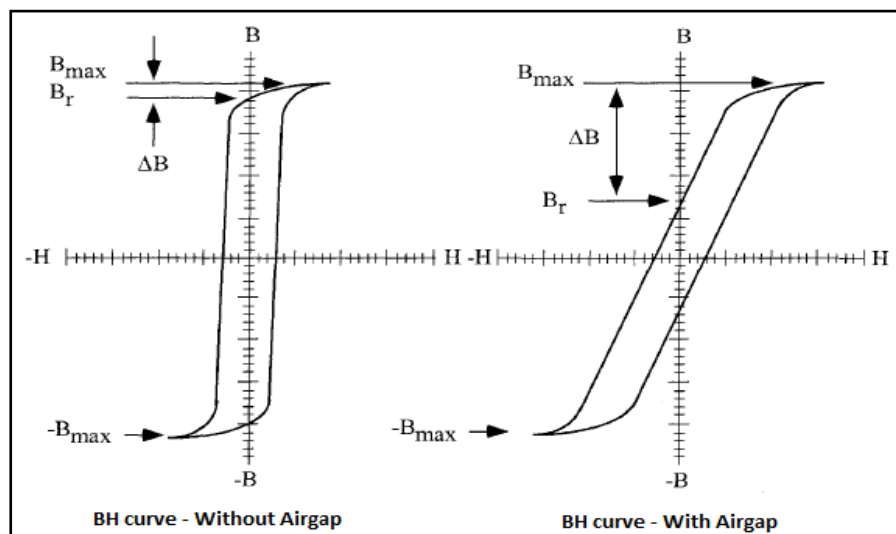


**Figure 3.6:** BH loops before and after core cut

There are several advantages and disadvantages of this method.

First discussing on the advantages; this method does not change the core losses (negligible increment) with respect to the uncut core. Note in Figure 3.6, the areas within the BH loops for with and without air-gap are almost same.

Also this inrush mitigation method is more reliable than the external NTC thermistor option described in previous section 3.1.1.

Regarding the disadvantage; the gapped cores need more Magneto Motive Force (MMF) to magnetise the core than the normal toroidal core, hence it draws higher current in the off-load condition. Due to that reason, the gapped core transformer consumes lot more reactive power loss. Therefore this cannot be designed at its optimum flux density and hence should be designed approximately 30% lower value. Also core vibration due to loose lamination and noise issues could be an issue in the end application [1].

Based on the discussed inrush current mitigation methods, the gapped core option is mostly used in applications due to its reliability and other advantages. But still it is necessary to overcome its disadvantages, and hence the Composite core method introduced.

### 3.2 Proposed Composite Core Concept for Inrush Current Mitigation

As per the concept of the composite core there are two cores positioned concentrically; one is uncut core in the centre and the other is a cut-core around the centre core. The basic arrangement is shown in the Figure 3.7 and Figure 3.8 [5].

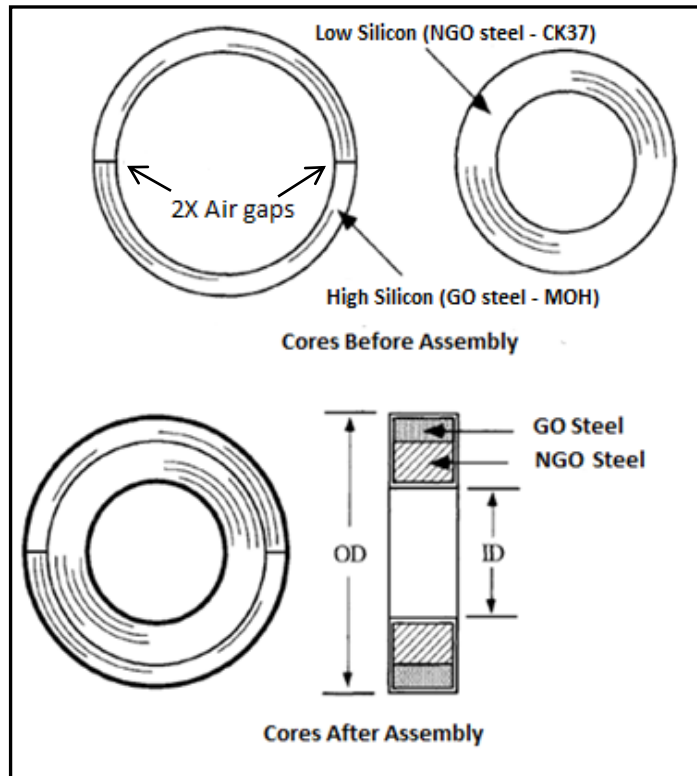


**Figure 3.7:** Composite core arrangement

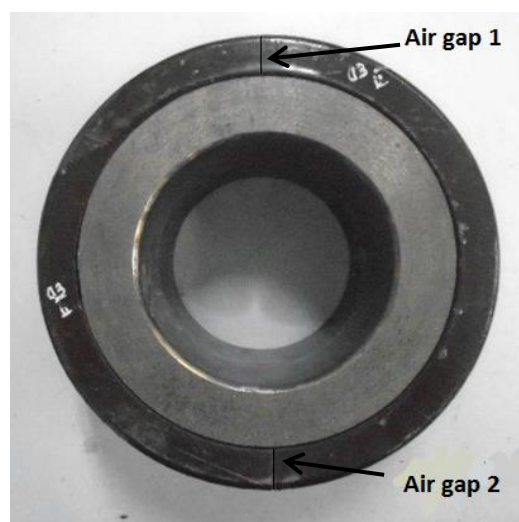


**Figure 3.8:** Real manufactured composite core

In this core arrangement, the centre core is made with lower grade steel type (Steel AISI CK37 - 35H300, which will be used in this research) and the outer core is made with higher graded steel (AISI M0H - M103-27P, which will be used in this research).

According to the basics of magnetism, the majority of flux will concentrate on the lowest magnetic path length (means close to the inner core), and then the flux gets propagate over the whole cross sectional area of the core when the core energization gets higher. Similarly, the centre core will dominate in the normal operation of the transformer, and the outer core will dominate in the inrush current transient.

There are three main design factors considered in the designing process.

- 1) Design flux density
- 2) Airgap size in cut core
- 3) Uncut core – Cut core cross-sectional area ratio

### **3.2.1 Design flux density**

In this research, the design flux density is kept fixed to the inner uncut core to 1.30T, and accordingly the number of turns for the primary winding is calculated (Refer Appendix-A, for ToroidEZE simulations for designs). Then the outer cut core is separately calculated based on the target inrush current requirement. Basically in normal operation, the inner core will be operated slightly below 1.30T flux density, while the outer cut core also will energize around 0.2-0.3T.

This scenario will extensively discuss in section 3.2.2 and 3.2.3.

### 3.2.2 Airgap size in cut core

Air gap is the main design parameter in designing process with composite core. First, the equation 3.1 is showing the general relationship between the maximum inrush current and the impedance of the product [6] [7].

$$I_{max} = \frac{V_m}{\sqrt{(\omega L_s)^2 + R^2}} \cdot \left(1 + \cos \theta + \frac{B_s - B_r}{B_n}\right) \quad (3.1)$$

- $I_{max}$  - Maximum inrush current (peak current)
- $V_m$  - Maximum input voltage (peak voltage)
- $R$  - Winding resistance
- $L_s$  - Saturation inductance
- $\theta$  - Switching angle
- $B_r$  - Residual flux density
- $B_s$  - Saturation flux density
- $B_n$  - Nominal design flux density

According to the equation 3.1, it is obvious that increasing the Saturation inductance ( $L_s$ ) and Winding resistance ( $R$ ) will be the main option to minimize the inrush current. When comes to winding resistance, in practical situation the designer does not have much allowance to changed resistance having the product itself should complied with certain thermal class. Hence changing the winding resistance is not an option to control the inrush current. Therefore, increasing the Saturation inductance will be the only option in this regards.

It is obvious, reducing the airgap will increase the inductance value, but too much lowering the gap will lead saturating the outer core. Note, the outer core dominates in the inrush scenario, so it needs to maintain the outer core unsaturated in the inrush current transient. Therefore it needs to find the **Optimum gap** is such, which holds the maximum  $L_s$ , while keeping the outer core unsaturated.

The following test has been done to the 1000VA transformer, where the inrush current is measured with different air gaps in outer core. See Figure 3.9.

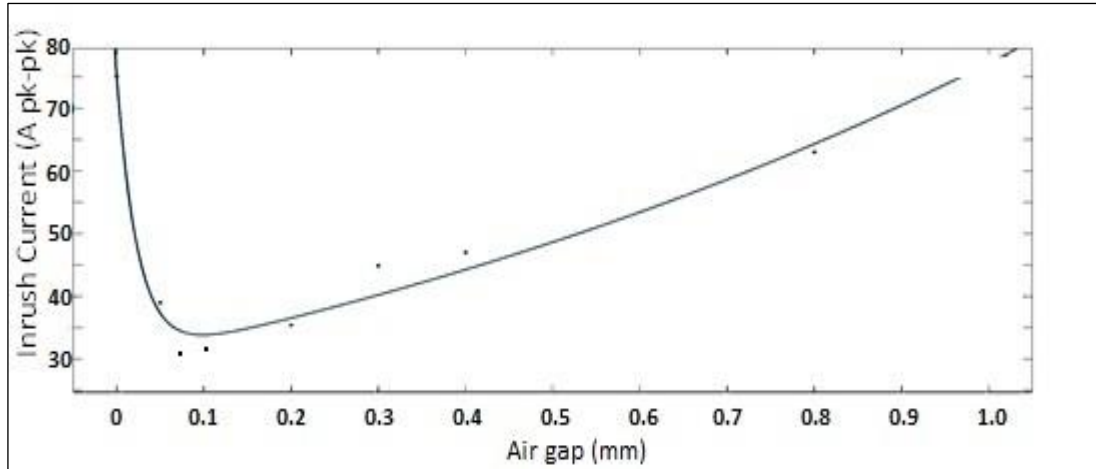


**Figure 3.9:** Variation of inrush current with outer core airgap

According to the Figure 3.9, it shows higher inrush currents in the lower gaps due to saturating the outer cut core. As the air gap increases along the x-axis, the inrush current reduces due to moving the cut-core in to unsaturated region. But too much increase of the air-gap will again increase the inrush current due to drop of Saturation inductance ( $L_s$ ). Means there is a particular air gap which should be maintained to minimize the inrush current, called “Optimum air gap”.

It was experimentally found, that the Optimum airgap changes with the size of the cut-core cross sectional area. The distribution of Optimum airgap with respect to cross sectional area will be discussed in the chapter 4.

### 3.2.2.1 Flux distribution in the composite core

The next important step is analysing the flux distribution within the composite core (between cut core and uncut core), when the composite core is magnetized from the lower voltage to the deep saturation stage. As discussed early of this section, the inner uncut core dominates in the normal operation, while outer cut core share lesser flux. But outer cut core also holds considerable flux density (similar to the uncut core) when the composite core subjected in to deep saturation. Refer Figure 3.10.



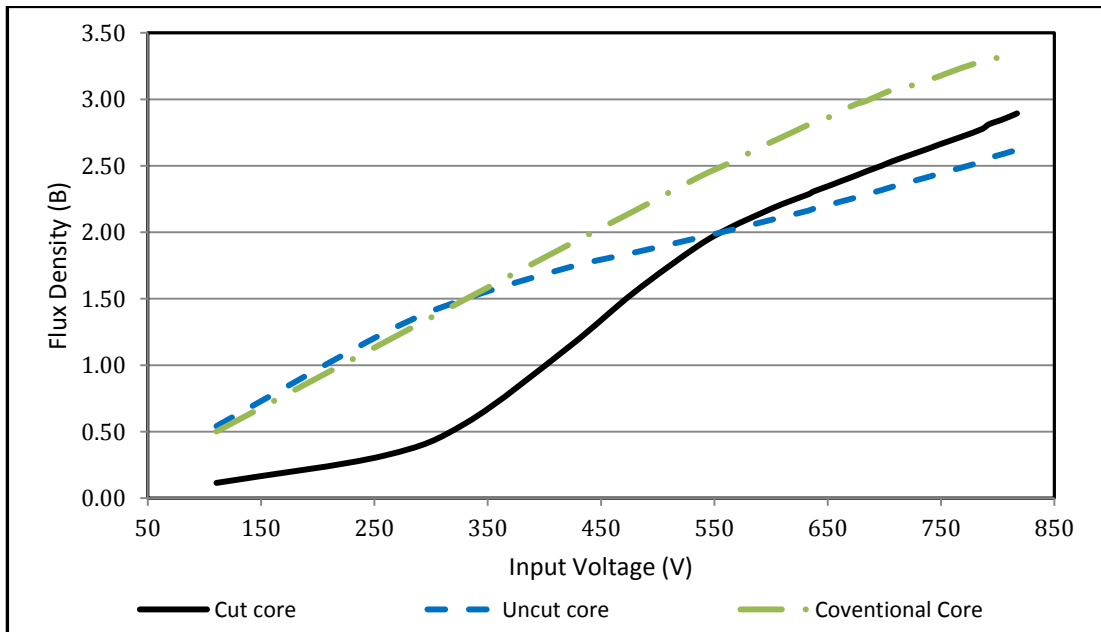


**Figure 3.10:** Flux density distribution between Cut/Uncut cores

The flux densities of the cut core and uncut core at normal operation and at deep saturation stage (at inrush transient, energized 2.65 times to normal operation – Refer Section 3.2.2.3 / equation 3.6) are tabulated as per Table 3.1. The flux density variation of the corresponding conventional core also graphed to compare how the composite core maintain lower flux density at inrush transient to keep the combined core well unsaturated comparatively.

**Table 3.1:** Flux densities at normal/inrush condition

	Flux Density (T)	
	At normal operation	At inrush transient
Uncut core	1.205	2.114
Cut core	0.304	2.215

Finding the flux density of the cut core at inrush transient is the most important outcome of the above exercise. The reason behind is, the flux density of the cut core is needed to find the Relative permeability ( $\mu_r$ ) of the cut core at inrush, and which becomes the most dominant parameter for calculating Saturation inductance ( $L_s$ ). After all,  $L_s$  be the most significant parameter in calculating the inrush current.

In order to extract  $\mu_r$  via the flux density, the steel supplier's BH characteristics of the outer core (AISI M0H - M103-27P) should be used. But, having this scenario interested on  $\mu_r$  at deep saturation level (at flux density 2.215T), the values for  $\mu_r$  will be very low and practically difficult to read the exact values from Figure 3.11[4].

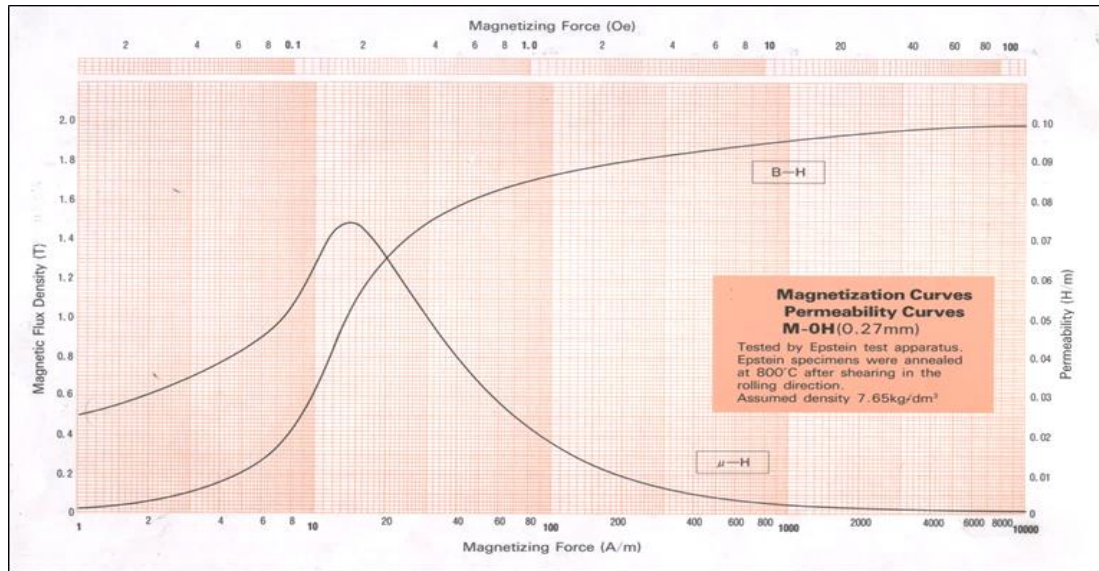


**Figure 3.11:** BH curve for AISI M0H - M103-27P

To overcome this issue, the research will continue with experimentally calculated  $\mu_H$  characteristic curve, Figure 3.12. One advantage of this method is, the experimentally calculated  $\mu_H$  characteristic will reflect the real annealing condition of the manufacturing facility and hence the accuracy becomes higher.

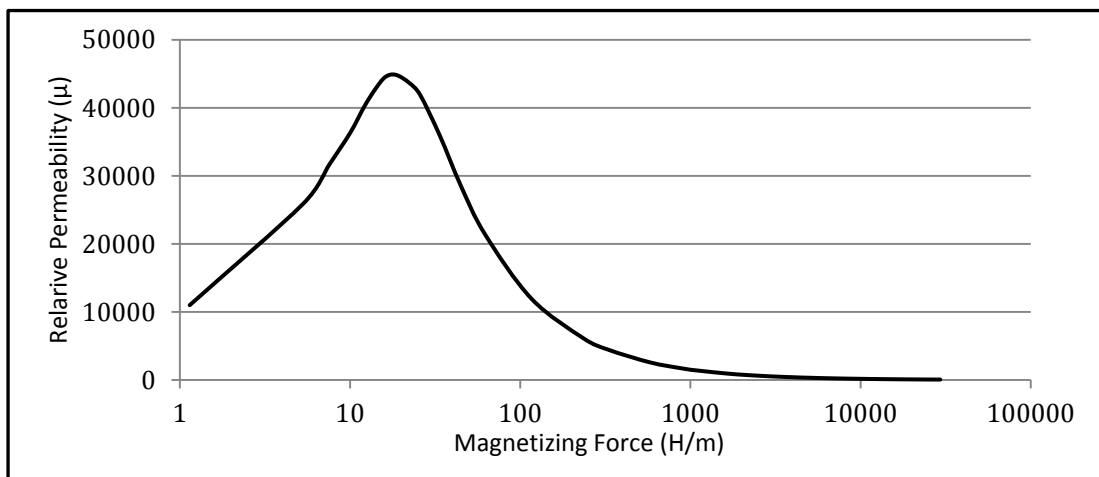


**Figure 3.12:** Experimentally calculated  $\mu_H$  characteristic curve

Then it is possible to extract the deep saturation section of curve (Figure 3.12) to derive Figure 3.13. Together with the experimental results in Table 3.2, it can derive the  $B_{\mu}$  characteristic curve Figure 3.14, which finally helps to calculate the exact values of  $\mu_r$  for closely varying flux densities. Note, the value of  $L_s$  is solely depending on the value of  $\mu_r$ ; hence the accuracy is much important.

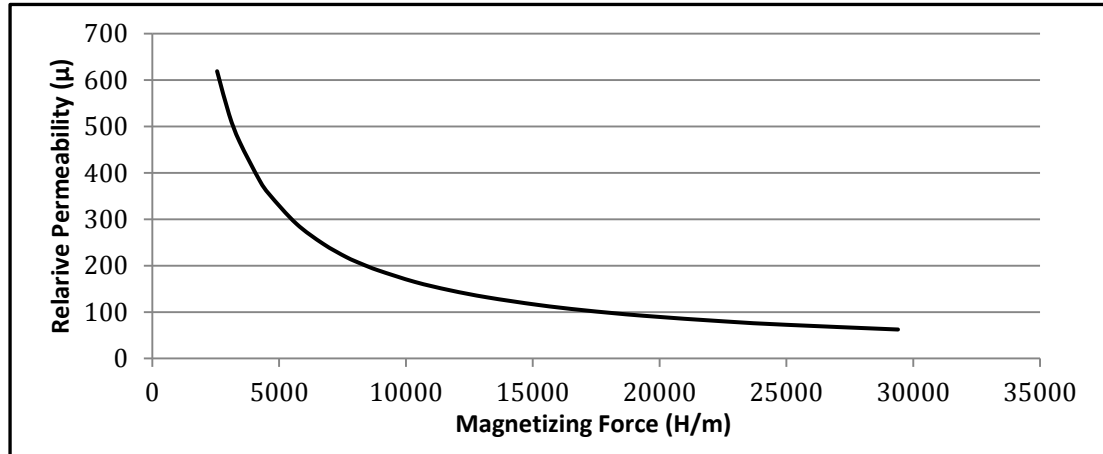


**Figure 3.13:** Extract of calculated  $\mu H$  characteristic

**Table 3.2:** Experimental test data on AISI M0H - M103-27P

Flux Density (T)	Magnetizing Force (A/m)	Relative Permeability
1.99	2555	619.1
2.00	3027	525.9
2.02	3441	467.1
2.04	4229	383.8
2.05	4618	353.4
2.07	5676	290.6
2.09	6736	247.1
2.10	7652	218.4
2.11	8258	203.7
2.13	8906	189.9
2.15	10347	165.0
2.17	11731	147.0
2.19	13200	131.7
2.21	15200	115.4
2.22	17000	104.0
2.24	19350	92.1
2.27	22600	79.8
2.28	25000	72.6
2.31	29400	62.4

Together with Table 3.2 and Figure 3.14, it is possible to find  $\mu_r$  at flux density 2.215T as 109.5.

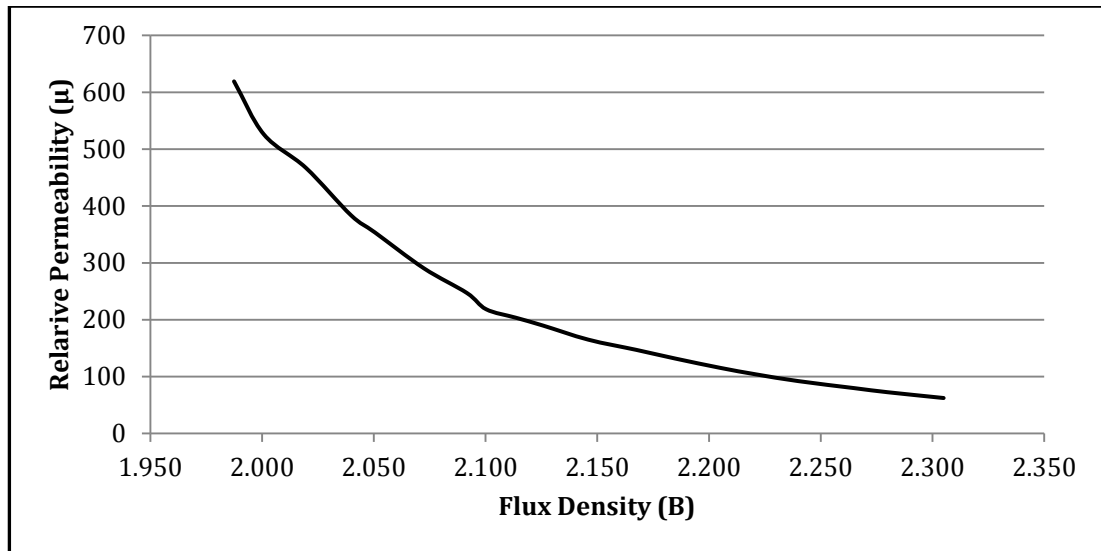


**Figure 3.14:** Calculated  $B\mu$  characteristic

### 3.2.2.2 Calculation of saturation inductance $L_s$

According to the concept, as the composite core subjected to deep saturating condition, the outer cut core will retain in the “Just unsaturated” stage, while the centre uncut core will be saturated.

Hence the inductance of the **inner uncut core** can be considered as the inductance of saturated core (air choke).

$$L_{uncut} = \frac{4\pi \times 10^{-7} \cdot N^2 \cdot A \cdot \mu_r}{MPL_{uncut}} \quad (3.2)$$

- $L_{uncut}$  - Uncut core saturated Inductance
- A - Cross sectional area of core
- $\mu_r$  - Relative Permeability
- MPL - Magnetic path length
- OD/ID – Outer/Inner diameter of core
- N - Number of turns

Where MPL is calculated by,

$$MPL = \frac{\pi \times (OD - ID)}{\ln\left(\frac{OD}{ID}\right)}$$

Considering the 1000VA transformer;

<b>Uncut</b> core dimension (OD x ID x H)	: 133 x 90 x 90 mm
<b>Cut</b> core dimension (OD x ID x H)	: 165 x 135 x 90 mm
Number of turns	: 430 turns

The parameters for the centre “uncut core”;

Saturated (uncut) core area	= 1935 mm <sup>2</sup>
Relative permeability	= 1 (Air)
MPL	= 345.902 mm

Substituting the uncut core data into equation 3.2

$$L_{uncut} = 1.299 \text{ mH}$$

Then the inductance of the **outer cut core** can be calculated from the equation 3.3

$$L_{cut} = \frac{4\pi \times 10^{-7} N^2 A \mu_r}{MPL + \mu l_g} \quad (3.3)$$

$L_{cut}$  - Uncut core un-saturated Inductance

$l_g$  - Air gap

The parameters for the centre “Cut core”;

Un-saturated (cut) core area	= 1350 mm <sup>2</sup>
Relative permeability	= 109.5 ( $\mu_r$ at 2.215T)
MPL	= 469.664 mm
Air gap	= 0.075 mm

Substituting the cut core data into equation 3.3

$$L_{cut} = 0.0718 \text{ H}$$

Then the total Saturation inductance  $L_s$  is;

$$L_s = L_{uncut} + L_{cut}$$

$$L_s = 0.0732 H$$

It shows that the inductance of the uncut saturated core ( $L_{uncut}$ ) is negligible on the resultant inductance  $L_s$ , and hence on the inrush current.

### 3.2.2.3 Calculation of inrush current

Recall the equation 3.1

$$I_{max} = \frac{V_m}{\sqrt{(\omega L_s)^2 + R^2}} \cdot \left(1 + \cos \theta + \frac{B_s - B_r}{B_n}\right) \quad (3.1)$$

Having this research is concentrate only on the Maximum inrush current, which occurs at the zero crossing. Then apply  $\theta = 0$

$$I_{max} = \frac{V_m}{\sqrt{(\omega L_s)^2 + R^2}} \cdot \left(1 + 1 + \frac{B_s - B_r}{B_n}\right)$$

$$I_{max} = \frac{V_m}{\sqrt{(\omega L_s)^2 + R^2}} \cdot \left(2 + \frac{B_s - B_r}{B_n}\right)$$

Also applying  $V_m = \sqrt{2} V_{rms}$

$$I_{max} = \frac{\sqrt{2} V_{rms}}{\sqrt{(\omega L_s)^2 + R^2}} \cdot \left(2 + \frac{B_s - B_r}{B_n}\right) \quad (3.4)$$

As per the experimental data, the value of  $\frac{B_s - B_r}{B_n}$  stays almost constant, irrespective to the air gap size. This is proven as following.

Consider the BH loops of two composite core transformers of 1000VA, which are identical except having different air-gaps 0.05mm and 0.80mm in the outer cut-core.

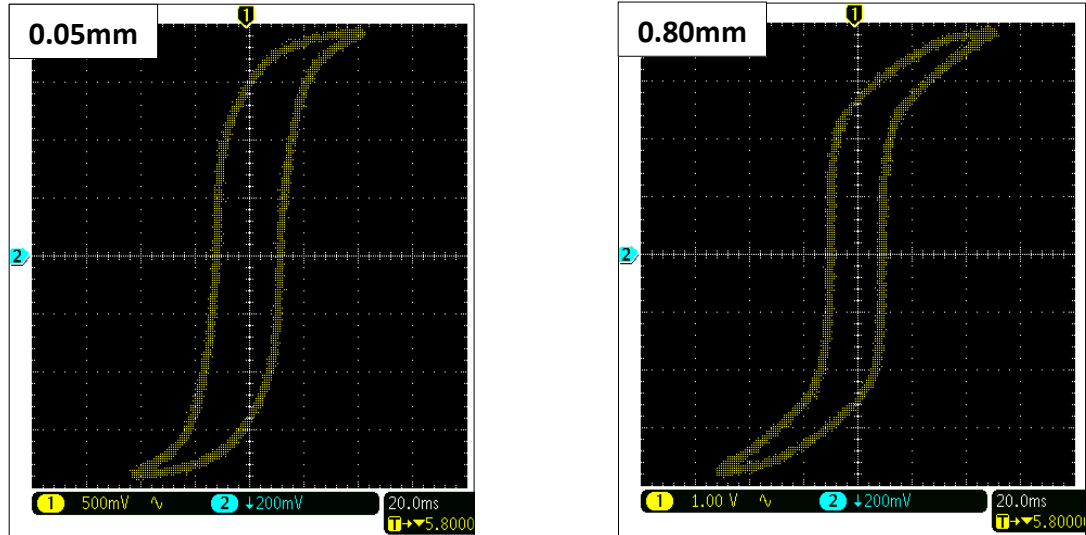


**Figure 3.15:** BH loops at different air-gaps

According to Figure 3.15, the change of the remanence flux is almost negligible even for high variation of air gap size. Hence the ratio between the saturated flux density ( $B_s$ ) and remanence flux density ( $B_r$ ) is considered fixed as following, in this research.

Means,  $B_r = 0.75 B_s$

Therefore we can calculate,

$$B_s - B_r = 0.25 B_s \quad (3.5)$$

Then the composite core of 1000VA (with optimum air-gap) is subjected to deep saturation level and studied its BH loop characteristics. Refer Figure 3.16.

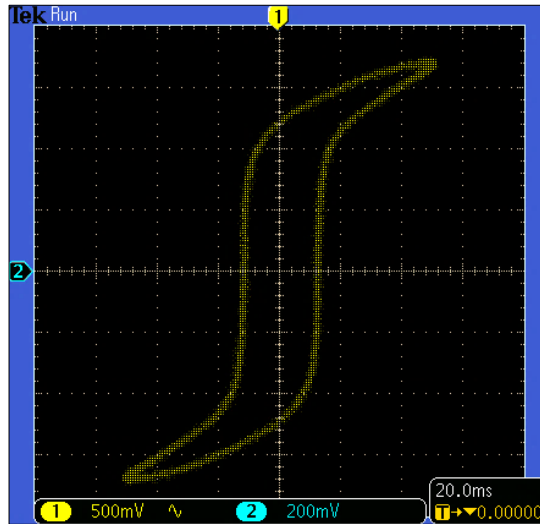


**Figure 3.16:** BH loop at deep saturation

Accordingly it is observed the design starts saturation when the nominal voltage gets nearly 2.65 times, means closer to 610V (230V nominal).

Therefore we can derive,  $B_s : B_n = 2.65 : 1$  (3.6)

From equations (3.5) and (3.6), it is possible to derive,

$$\frac{B_s - B_r}{B_n} \approx 0.65 \quad (3.7)$$

Then substituting the equation 3.7, into equation 3.4.

$$I_{max} = \frac{\sqrt{2}V_{rms}}{\sqrt{(\omega L_s)^2 + R^2}} \cdot (2 + 0.65)$$

$$I_{max} = \frac{3.75 V_{rms}}{\sqrt{(\omega L_s)^2 + R^2}} \quad (3.8)$$

Accordingly it is possible to calculate the  $I_{max}$ , together with the calculated saturation inductance  $L_s$  and calculated winding resistance ( $R = 0.745 \Omega$ )

$$I_{max} = 38.86 \text{ A}$$



But the measured inrush current under the laboratory facility is 36.3A.

There are several factors effecting to this slight deviation between the calculated and measured inrush current values. Some of them are; the level of calibration of the test equipment, estimated assumptions made to simplify the calculation, source impedance to the transformer, etc.

The source impedance to the transformer makes a great effect to the above deviation, over the other factors. The significance of the source impedance will be described in section 3.3

### **3.2.3 Uncut – Cut core cross-sectional area ratio**

It is obvious (and experimentally proven) that increasing the outer cut-core cross sectional area reduces the inrush current. But the drawback of increasing the outer cut-core (which made with M0H - M103-27P) is the cost and the size of the finished product. So the designer shall calculate and decide the steel area ratio required for the target inrush current.

This aspect will be deeply discussed in the chapter 4 and chapter 5, and accordingly this research will be limit for the cross sectional area ratio range 1:0.60 to 1:0.80 (Uncut : Cut).

### **3.3 Importance of Source Impedance on Inrush Current**

In a typical installation, the cable sizes are selected mainly based on the nominal current ratings of the equipment installed, but definitely not considering the transient peak currents (inrush current), having considered those short time transients are not making any harm to the system. Hence in an installation, it is a typical fact that these transient high currents do make significant voltage drops.

Due to the above point, it is evident that the inrush current definitely will not reach to the calculated inrush current in most of practical cases.

Following Figure 3.17 and Figure 3.18 are showing the inrush current measured for the same transformer with two sources; first is having higher source impedance and the second is having negligible source impedance respectively.

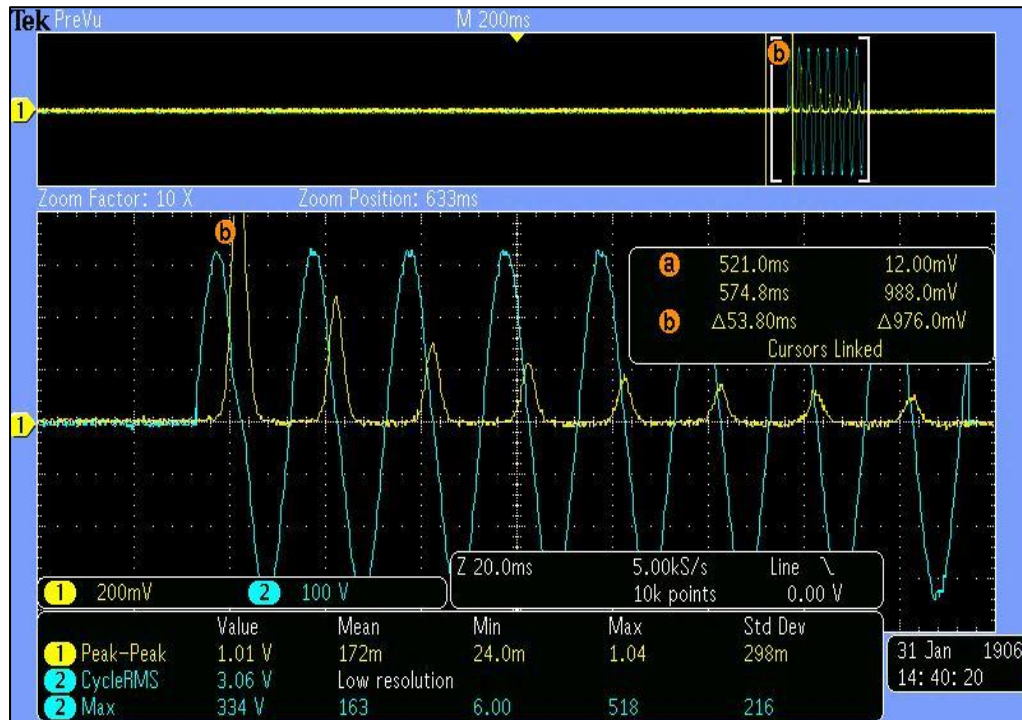


**Figure 3.17:** Inrush current measured with high source impedance

In the Figure 3.17, it shows that the input sinusoidal waveform gets slightly deformed at the zero crossing (where the inrush current generated) and that cause the measured maximum inrush current value near 98.8A (peak).

But in the Figure 3.18, it shows almost no deformation in the input sinusoidal waveform at the zero crossing, and that causes the measured maximum inrush current value near 115.0A (peak).

Therefore, with the purpose of avoiding/neglecting the effect of source impedance, the research is carried out all the important experiments on inrush current measurements with the source having negligible impedance.

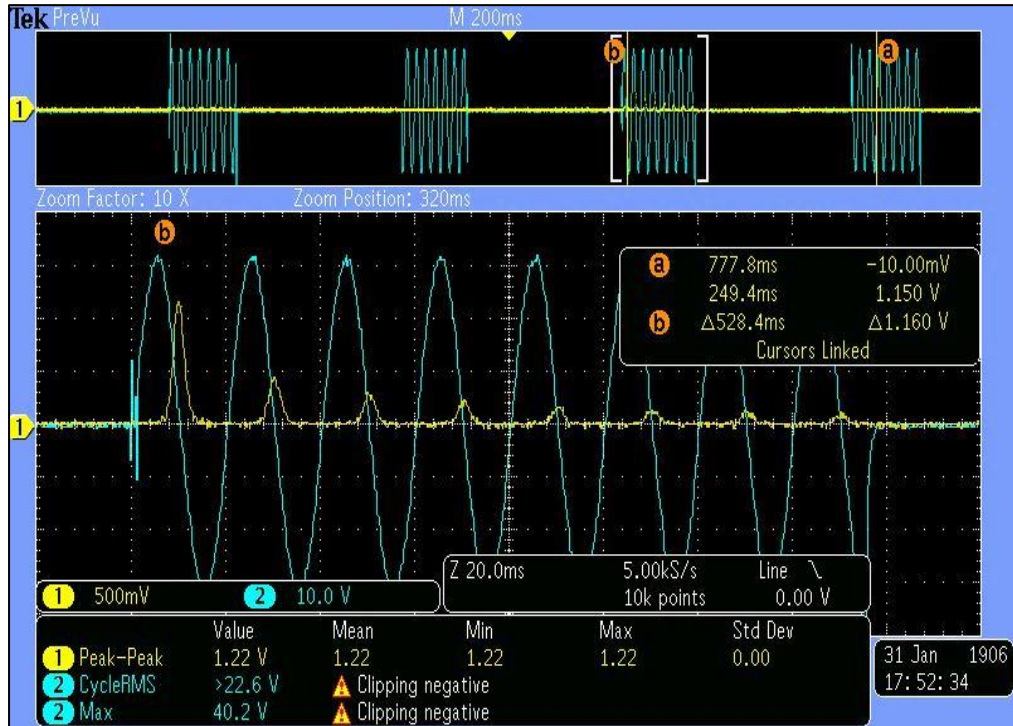


**Figure 3.18:** Inrush current measured with low source impedance

### 3.4 Scope of the Research

Together with the discussions on the section 3.2, this research will be confined into the following scope.

- 1) Design flux density fixed to 1.30T for the inner core and experiments conducted only for 230V mains input
- 2) Considered only the steel types CK37 - 35H300 and M0H - M103-27P for uncut core and cut core respectively
- 3) Considered transformer power range 1kVA to 5kVA
- 4) Considered core cross sectional area ratio range 1:0.60 to 1:0.80 (Uncut: Cut), which covering inrush current range 2 to 8 times of load current.

## EXPERIMENTAL DATA COLLECTION

In chapter 3, the proposed composite core method had been discussed together with 1000VA transformer. This chapter discusses on further details of experimental data collected for composite core designs, covering the transformer power range 1kVA to 5kVA.

Here the following designs are mainly discussed. Note, all the below designs comes with constant core cross sectional area ratio (Cut core: Uncut core = 0.7 : 1.0) and with constant design flux density 1.30T for the inner core.

- 1) TI-173622 (1000VA)
- 2) TI-173618C (2000VA)
- 3) TI-173618D (3000VA)
- 4) TI-173618E (4500VA)

### 4.1 Inrush Current Measurement on Samples

The transformers TI-173622, TI-173618C, TI-173618D and TI-173618E were tested applying alternating rated voltage 230V/50Hz (Sinusoidal) across the primary winding. Then the inrush current transient waveforms are taken to an Oscilloscope (Tektronix DPO3000) connected via a current probe (Tektronix A621) to the circuit. Test set up for this arrangement is shown in Figure 4.1 [1].

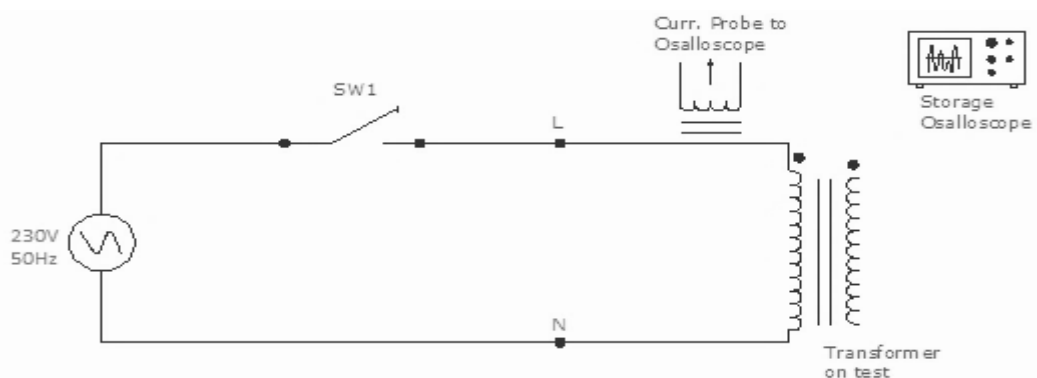


**Figure 4.1:** Test setup for inrush current measurement

In this experiment, the inrush current data collected with two methods. First method is repeating the test several times (minimum 60 times per design), creating the possibility to switch the input wave form at zero crossing, and hence creating the maximum inrush current. The second method is switching the input via zero-point detecting circuit (made with SIEMENS 3RF2050-1AA02), which does monitor and detect the zero crossing of the input wave form and ensure to switch ON the transformer at that point.

Both the options provided almost same maximum inrush current value, for each scenario to be discussed in section 4.2.

## 4.2 Finding the Optimum Air Gap for Outer Core

In this case, each design was tested for inrush current, varying the air-gap size of the outer core, while keeping the other design parameters fixed. Following sections show the maximum inrush current waves and the inrush current varying curves for each air-gap sizes.

### 1) TI-173622 (1000VA)

The design parameters of TI-173622 are as per Table 4.1. Note, the core dimensions typically denoted as “OD x ID x H”. Refer Annex A for more design details.

**Table 4.1:** Design parameters for TI-173622

Product	Cut core dimensions (mm)	Uncut core dimensions (mm)	Primary Turns	Primary Resistance (ohm)	Cut core area $A_{cut}$ (mm <sup>2</sup> )	Uncut core area $A_{uncut}$ (mm <sup>2</sup> )	$A_{cut} / A_{uncut}$	MPL <sub>cut</sub> (mm)	MPL <sub>uncut</sub> (mm)
TI-173622	165x135x90	133x90x90	430	0.745	1350	1935	0.698	469.66	345.90

The design TI-173622 is then tested for the maximum inrush current value at 230V/50Hz, for each air gap in the outer core, as per the Figure 4.2.

Accordingly the “Optimum air gap” is selected as 0.075mm, where the minimum inrush current observed.

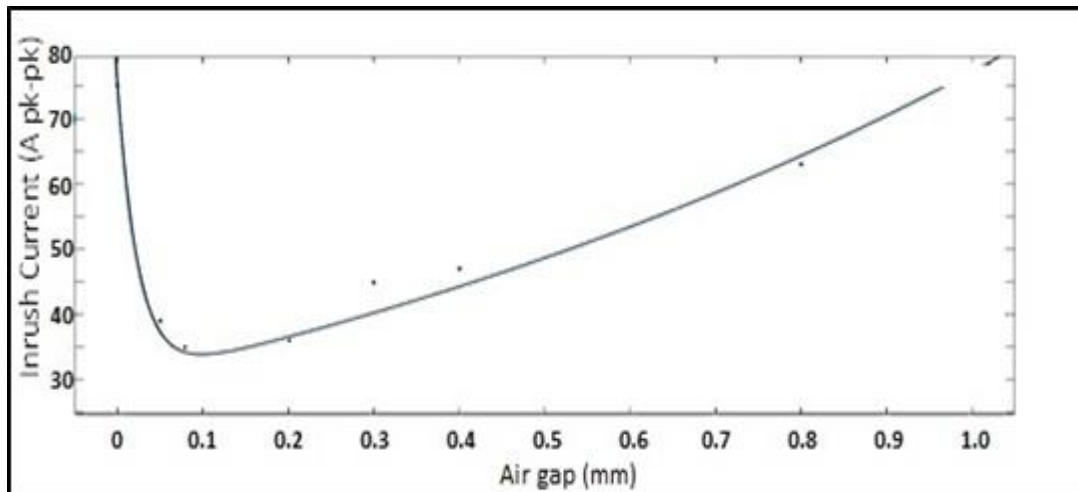


**Figure 4.2:** Variation of inrush current with outer core airgap

The measured inrush current at Optimum air gap is  $36.3A_{pk-pk}$ . Refer Figure 4.3 for the maximum inrush current wave captured through the oscilloscope.

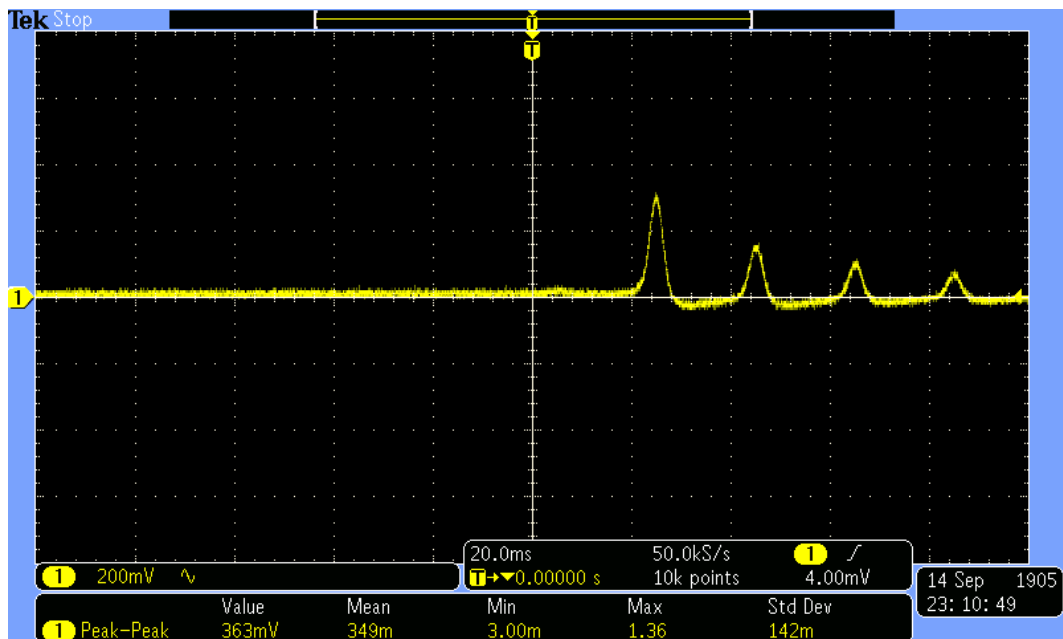


**Figure 4.3:** Inrush current wave form TI-173622

The no load current of this design is measured as 65.7mA and the active and reactive core losses are 8.71 watt and 12.15 var, respectively.

And according to the flux density distribution analysis on the composite core (between the cut core and uncut core) in deep saturation, it is observed that the cut core operates at 2.215T at inrush transient (at 610V). Refer Figure 4.4

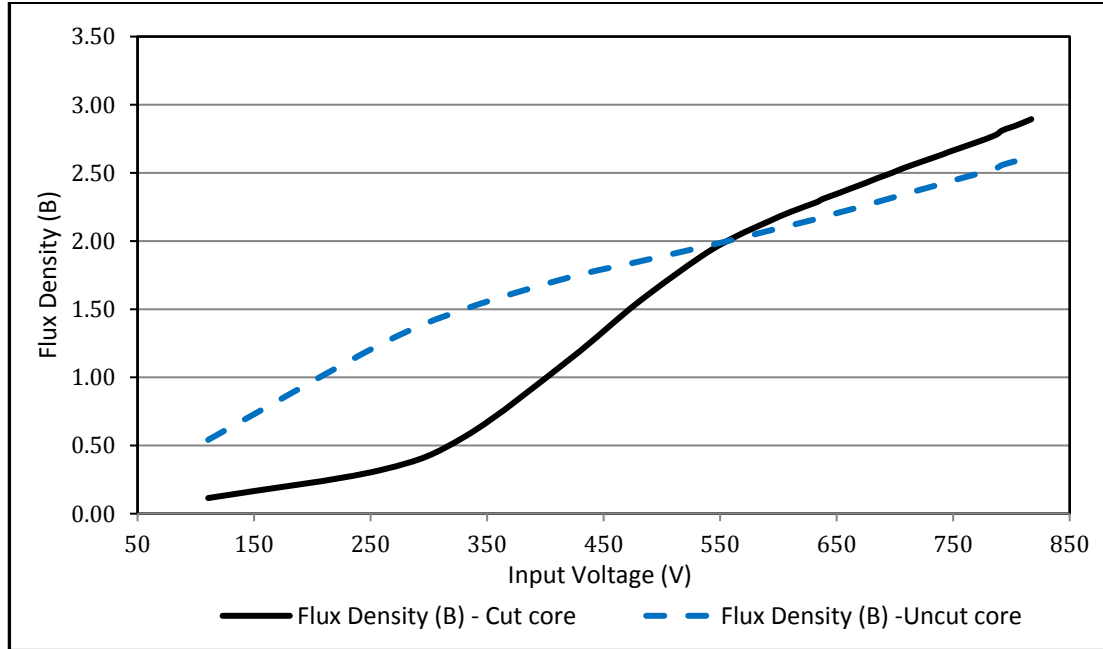


**Figure 4.4:** Flux density distribution of Cut/Uncut cores

**2) TI-173618C (2000VA)**

The design parameters of TI-173618C are as per Table 4.2. Note, the core dimensions typically denoted as “OD x ID x H”. Refer Annex A for more design details.

**Table 4.2:** Design parameters for TI-173618C

Product	Cut core dimensions (mm)	Uncut core dimensions (mm)	Primary Turns	Primary Resistance (ohm)	Cut core area $A_{cut}$ (mm <sup>2</sup> )	Uncut core area $A_{uncut}$ (mm <sup>2</sup> )	$A_{cut} / A_{uncut}$	MPL <sub>cut</sub> (mm)	MPL <sub>uncut</sub> (mm)
TI-173618C	247x184x60	180x90x60	311	0.74	1890	2700	0.700	672.16	407.91

The design TI-173618C is then tested for the maximum inrush current value at 230V/50Hz, for each air gap in the outer core as per the Figure 4.5.

Accordingly the “Optimum air gap” is selected as 0.30mm, where the minimum inrush current observed.

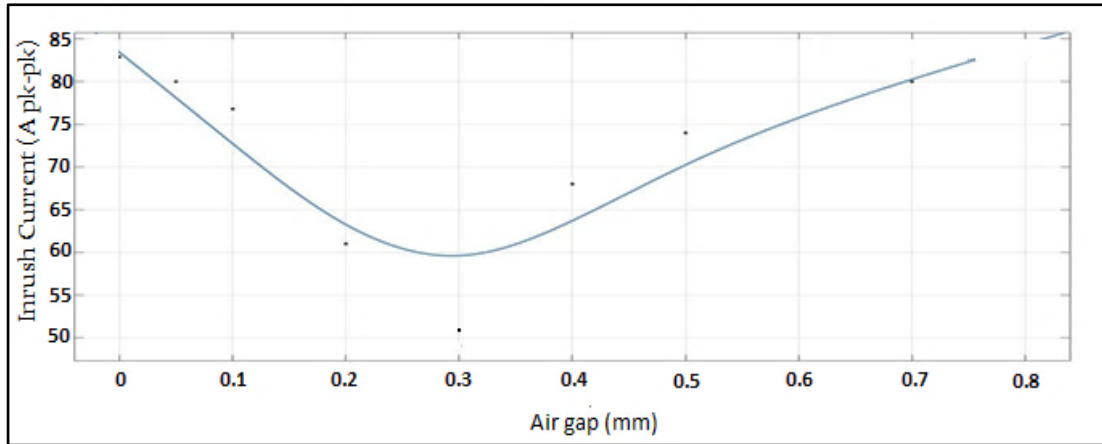


**Figure 4.5:** Variation of inrush current with outer core airgap

The measured inrush current at Optimum air gap is 51.8A<sub>pk-pk</sub>. Refer Figure 4.6 for the maximum inrush current wave captured through the oscilloscope.

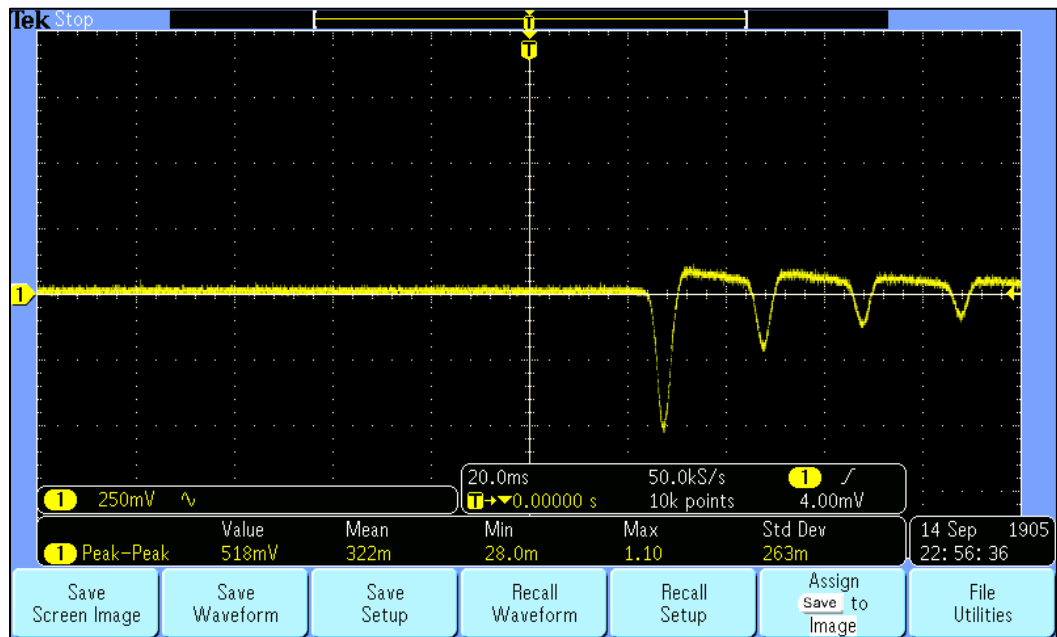


**Figure 4.6:** Inrush current wave form TI-173618C

The no load current of this design is measured as 86.7mA and the active and reactive core losses are 11.12 watt and 15.67 var, respectively.



And according to the flux density distribution analysis on the composite core (between the cut core and uncut core) in deep saturation, it is observed that the cut core is operates at 2.148T at inrush transient (at 610V). Refer Figure 4.7.

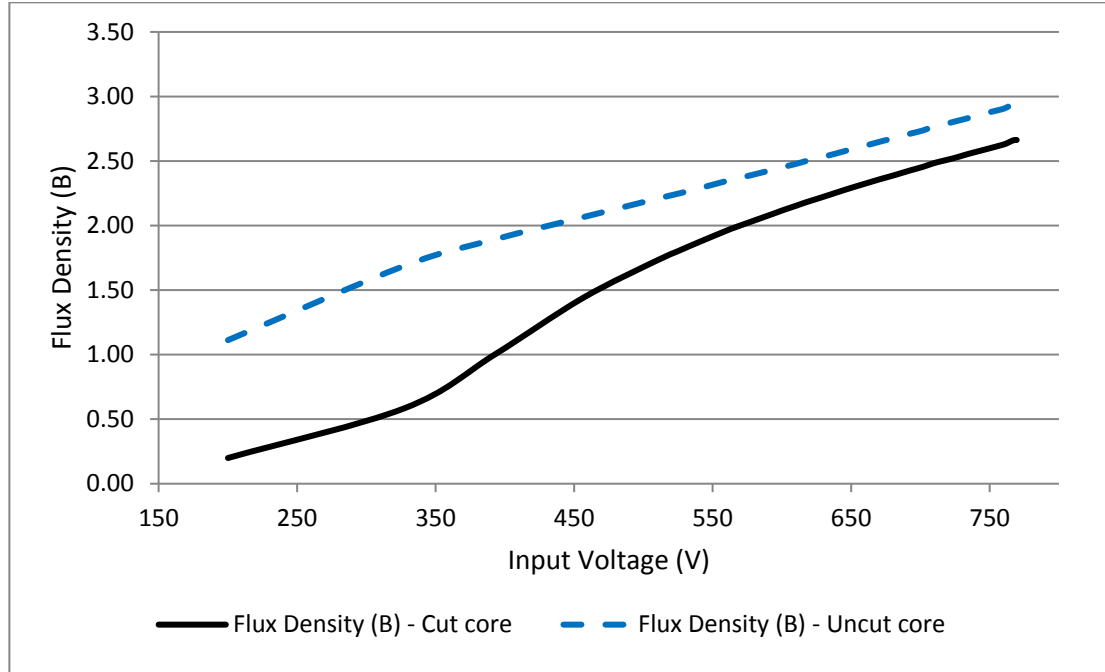


**Figure 4.7:** Flux density distribution of Cut/Uncut cores

**3) TI-173618D (3000VA)**

The design parameters of TI-173618D are as per Table 4.3. Note, the core dimensions typically denoted as “OD x ID x H”. Refer Annex A for more design details.

**Table 4.3:** Design parameters for TI-173618D

Product	Cut core dimensions (mm)	Uncut core dimensions (mm)	Primary Turns	Primary Resistance (ohm)	Cut core area $A_{cut}$ (mm <sup>2</sup> )	Uncut core area $A_{uncut}$ (mm <sup>2</sup> )	$A_{cut} / A_{uncut}$	MPL <sub>cut</sub> (mm)	MPL <sub>uncut</sub> (mm)
TI-173618D	247x184x80	180x90x80	231	0.72	2520	3600	0.700	672.16	407.91

The design TI-173618D is then tested for the maximum inrush current value at 230V/50Hz, for each air gap in the outer core as per the Figure 4.8.

Accordingly, the “Optimum air gap” is selected as 0.60mm, where the minimum inrush current observed.

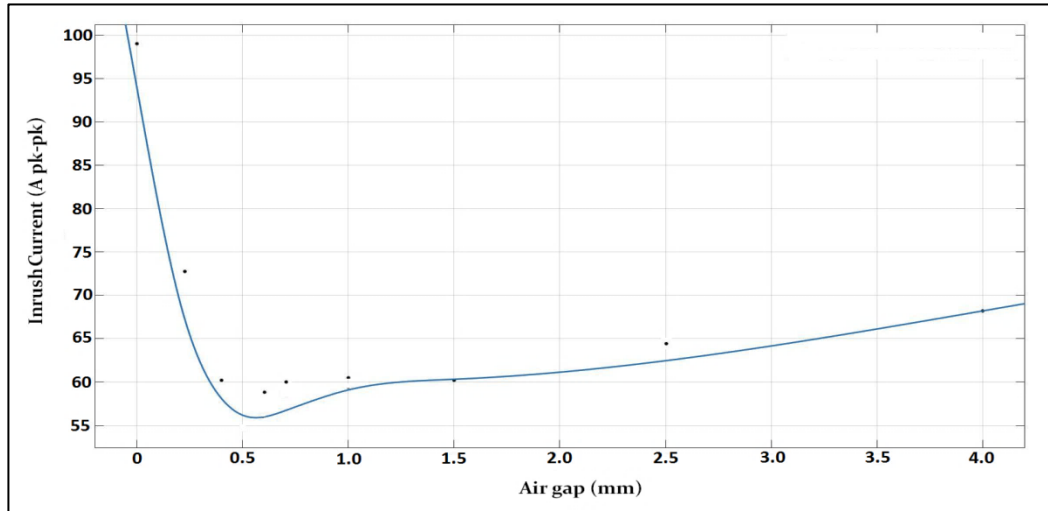


**Figure 4.8:** Variation of inrush current with outer core airgap

The measured inrush current at Optimum air gap is  $58.9A_{pk-pk}$  . Refer Figure 4.9 for the maximum inrush current wave captured through the oscilloscope.

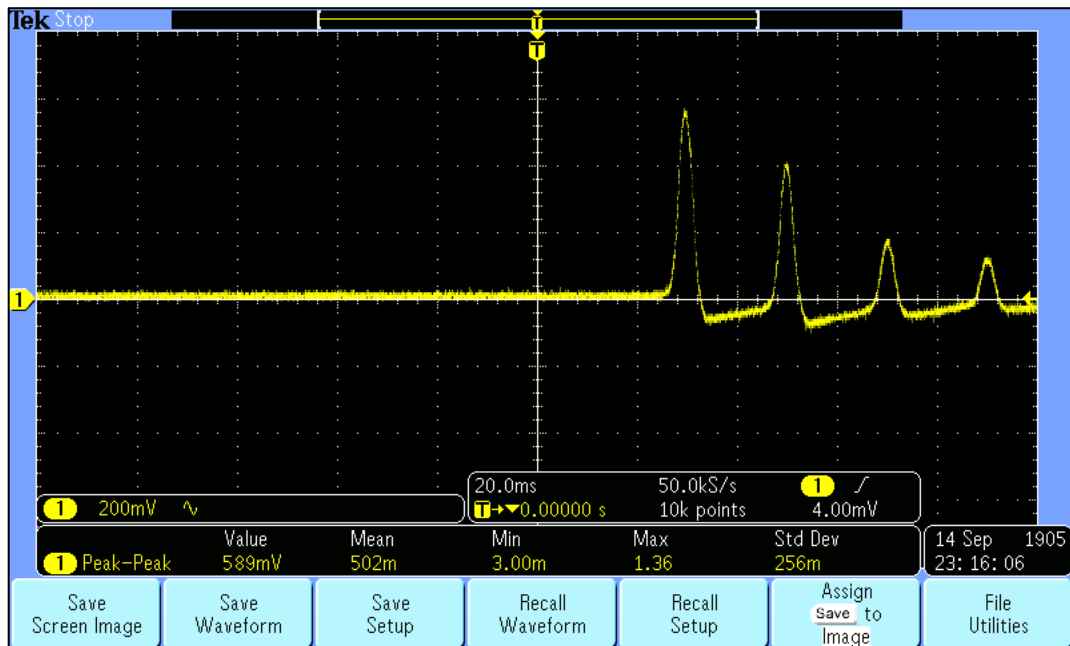


**Figure 4.9:** Inrush current wave form TI-173618D

The no load current of this design is measured as 122mA and the active and reactive core losses are 15.5 watt and 23.39 var, respectively.

And according to the flux density distribution analysis on the composite core (between the cut core and uncut core) in deep saturation, it is observed that the cut core is operates at 2.103T at inrush transient (at 610V). Refer Figure 4.10.

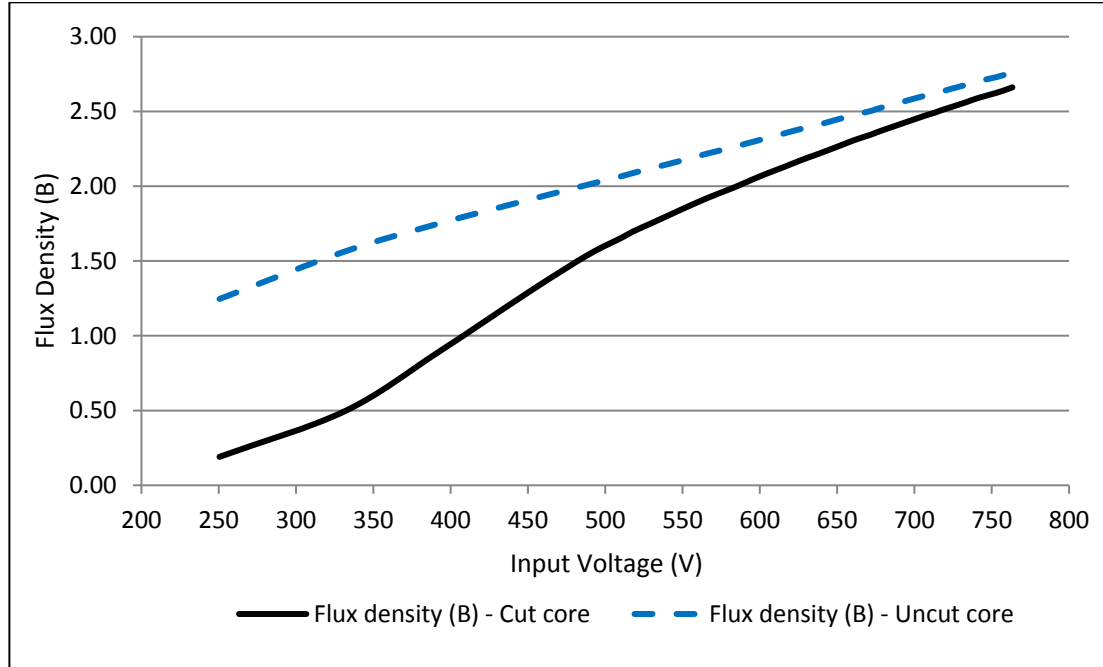


**Figure 4.10:** Flux density distribution of Cut/Uncut cores

**4) TI-173618E (4500VA)**

The design parameters of TI-173618E are as per Table 4.4. Note, the core dimensions typically denoted as “OD x ID x H”. Refer Annex A for more design details.

**Table 4.4:** Design parameters for TI-173618E

Product	Cut core dimensions (mm)	Uncut core dimensions (mm)	Primary Turns	Primary Resistance (ohm)	Cut core area $A_{cut}$ (mm <sup>2</sup> )	Uncut core area $A_{uncut}$ (mm <sup>2</sup> )	$A_{cut} / A_{uncut}$	MPL <sub>cut</sub> (mm)	MPL <sub>uncut</sub> (mm)
TI-173618E	247x184x100	180x90x100	186	0.715	3150	4500	0.700	672.16	407.91

The design TI-173618E is then tested for the maximum inrush current value at 230V/50Hz, for each air gap in the outer core as per the Figure 4.11.

Accordingly, the “Optimum air gap” is selected as 0.70mm, where the minimum inrush current observed.

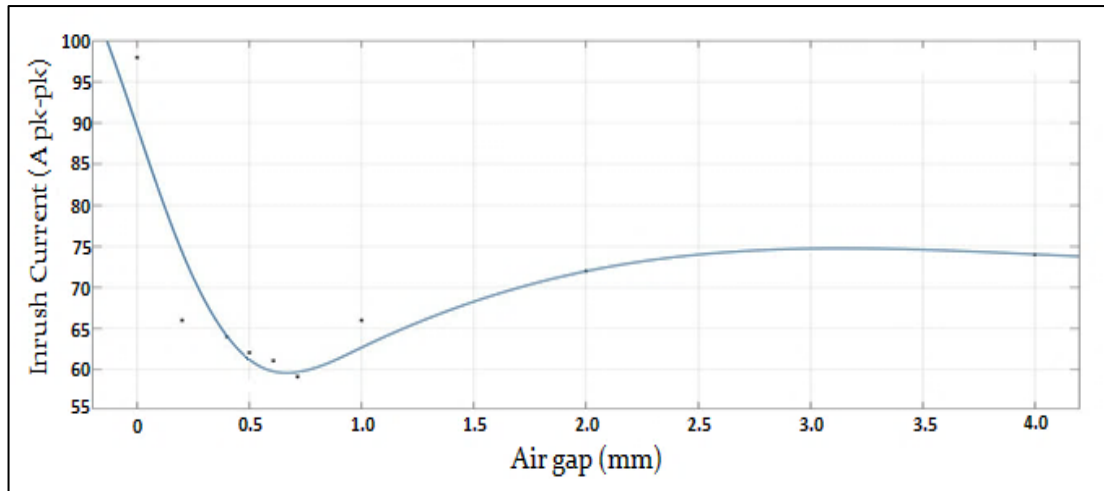


**Figure 4.11:** Variation of inrush current with outer core airgap

The measured inrush current at Optimum air gap is 59.5A<sub>pk-pk</sub>. Refer Figure 4.12 for the maximum inrush current wave captured through the oscilloscope.

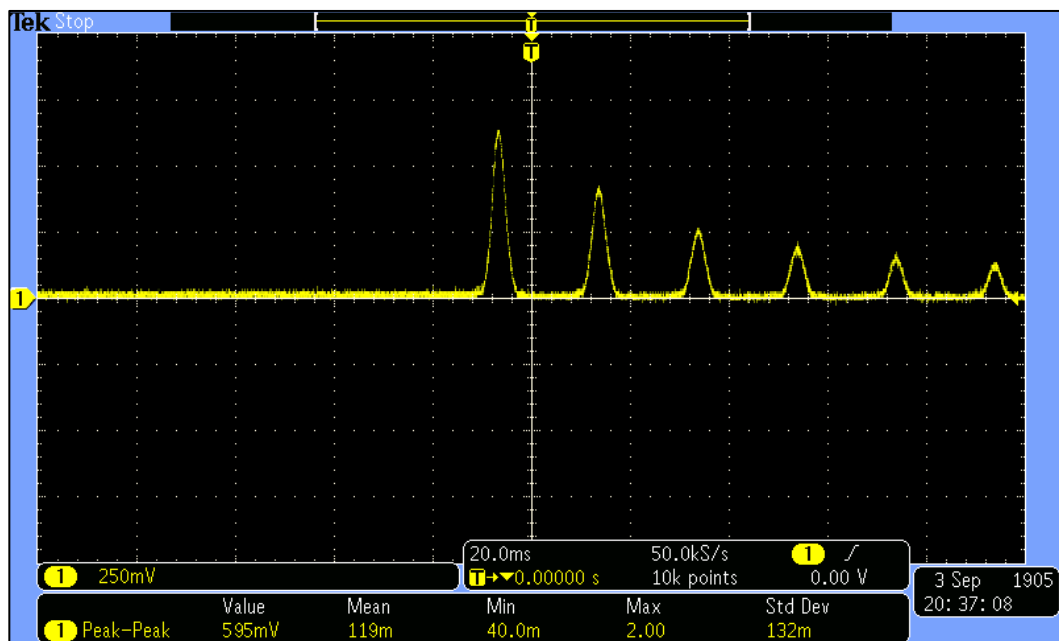


**Figure 4.12:** Inrush current wave form TI-173618E

The no load current of this design is measured as 228mA and the active and reactive core losses are 25.1 watt and 46.08 var, respectively.

And according to the flux density distribution analysis on the composite core (between the cut core and uncut core) in deep saturation, it is observed that the cut core is operates at 2.071T at inrush transient (at 610V). Refer Figure 4.13.

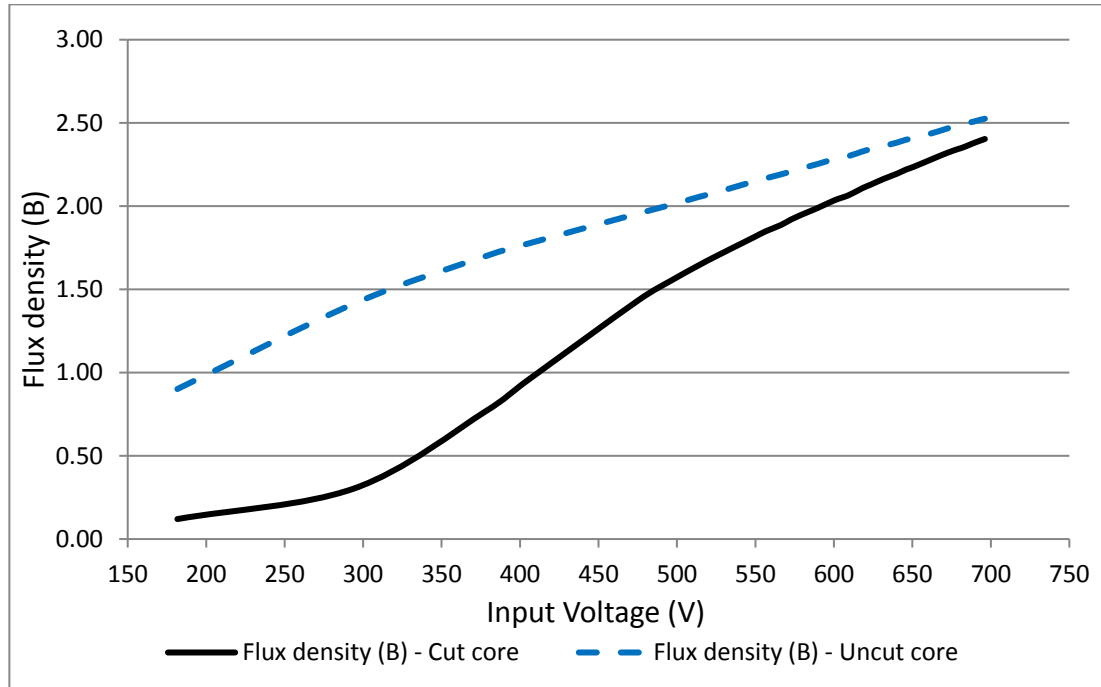


**Figure 4.13:** Flux density distribution of Cut/Uncut cores

### 4.3 Summary of Inrush Current Measurements

Following Table 4.5 comes with the summary of test data, together with the Relative permeability calculated based on the experimentally derived relationship of Figure 3.14 in chapter 3.

These data will be using in chapter 5 to develop some useful characteristics, in order to build up relationships to calculate inrush current.

**Table 4.5:** Summary of inrush current measurements

Product Number	Inrush current (A pk-pk)	Air gap (mm)	Flux Density (B) (cut core at inrush)	Relative permeability
TI-173622 (1000VA)	36.3	0.075	2.215	109.5
TI-173618C (2000VA)	51.8	0.30	2.148	160.0
TI-173618D (3000VA)	58.9	0.60	2.103	220.0
TI-173618E (4500VA)	59.5	0.70	2.071	291.0

#### 4.4 Inrush Current Measurements for Different Area Ratios

In this section, the two designs TI-173622 (1000VA) and TI-173618D (3000VA) are tested for different core cross sectional area ratios (Cut core: Uncut core) while keeping all the other parameters constant. Refer Annex B for design details. The tests are done under the same procedure discussed in the previous sections and the Table 4.6 is showing the test result summary.

**Table 4.6:** Inrush current measurements for different area ratios

Steel area ratio	Inrush Current ( $A_{pk-pk}$ )	
	TI-173618D (3000VA)	TI-173622 (1000VA)
0.60	120.3	72.7
0.65	78.5	47.3
0.70	58.9	36.3
0.75	47.2	28.2
0.80	38.3	24.2

Together with the experimental data in Table 4.6, it was found that the variation of the inrush currents with respect to the area ratio is following the same characteristic curve. In order to illustrate that, the inrush current is graphed as the multiple of load

current with respect to the area ratio. Refer Figure 4.14. The relationship at Figure 4.14 will be used to calculate inrush current for different area ratios in the next chapters.

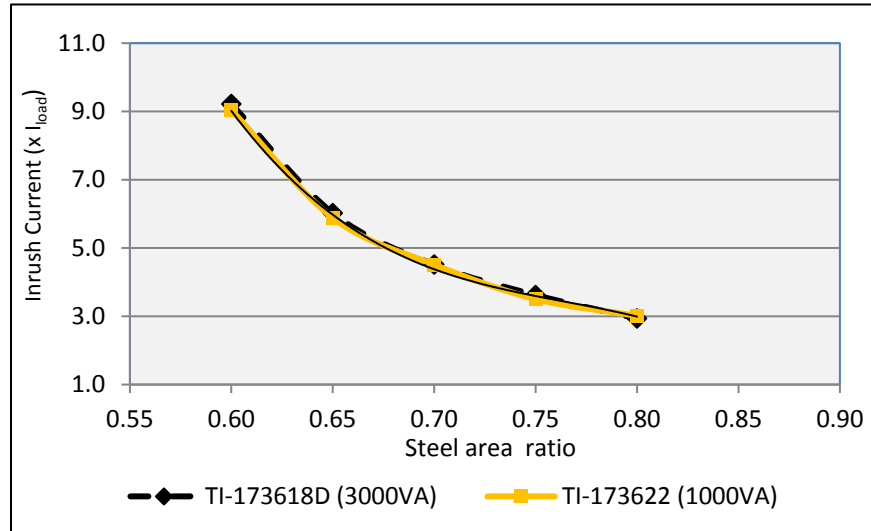


**Figure 4.14:** Inrush Current ( $\times I_{load}$ ) Vs Steel cross-sectional area ratio

Following Table 4.7 shows test results on furthermore designs (having different core cross sectional area ratios) tested in the same way, covering the power range 1kVA to 5kVA.

**Table 4.7:** Inrush current measurements for all samples

Article Number	Measure inrush current ( $A_{pk-pk}$ )
TI-173622 (1000VA)	36.3
TI-173628 (1000VA)	58.3
TI-173630 (1000VA)	21.8
TI-173618C (2000VA)	51.8
TI-173618M (2500VA)	93.4
TI-173618D (3000VA)	58.9
TI-173618N (3500VA)	30.7
TI-173618E (4500VA)	59.5

## ANALYSIS OF DATA

In this chapter, it is mainly focused to build up a methodology to calculate inrush current towards developing a design tool. As discussed in chapter 3, basically the equation 5.1 can be used for inrush calculation. But together with the experimental data collected in chapter 4, there are certain characteristics can be built and embedded in to the calculation towards handling the design parameters.

$$I_{max} = \frac{3.75 V_{rms}}{\sqrt{(\omega L_s)^2 + R^2}} \quad (5.1)$$

In this chapter the following aspects will be discussed together with the data obtained in chapter 4 and the inrush current calculation method discussed in the chapter 3.

- 1) Selection of optimum air-gap
- 2) Calculation of relative permeability
- 3) Calculation of inrush current for different core cross-sectional area ratios
- 4) Development of design tool for composite core
- 5) Comparison between measured and calculated inrush current values

### 5.1 Selection of Optimum Air-Gap

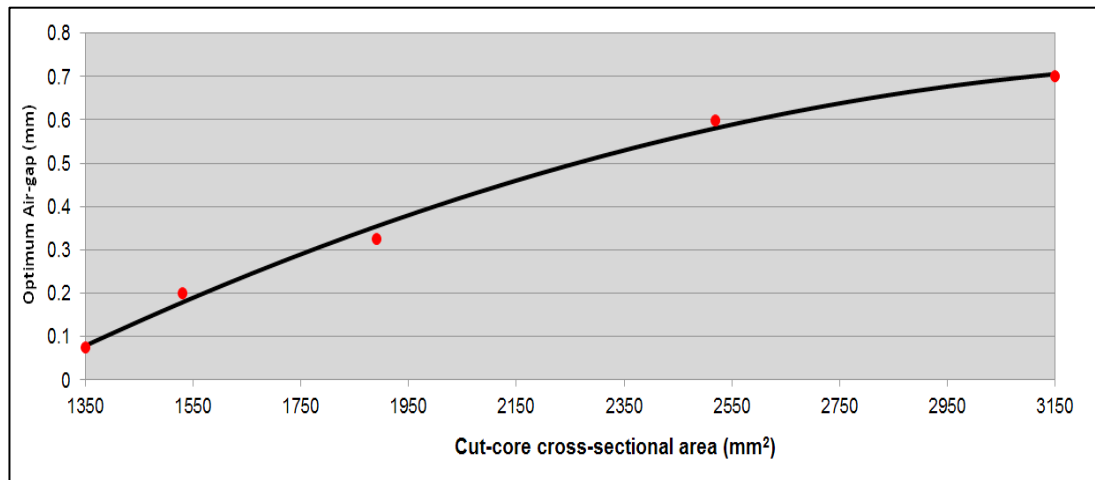
The optimum air-gap of the outer core is found to be related together with the size of the core, or explicitly the cross sectional area of the cut-core. Therefore based on the experimental data discussed in chapter 4, it is possible to derive a direct relationship between the optimum air-gap and the cut-core cross sectional area.

Refer Table 5.1 for the summary of experimental test results extracted from chapter 4 and consequent graph in Figure 5.1.



**Table 5.1:** Optimum air-gap to the cut core cross sectional area

Product	Cut core area (mm <sup>2</sup> )	Optimum air-gap (mm)
TI-173622 (1000VA)	1350	0.075
TI-173618C (2000VA)	1890	0.30
TI-173618D (3000VA)	2520	0.60
TI-173618E (4500VA)	3150	0.70

**Figure 5.1:** Optimum air-gap to the cut core cross sectional area

The respective equation for Figure 5.1 comes as the following equation 5.2

$$Y = -1.2808 \times 10^{-7} X^2 + 0.000924X - 0.93474 \quad (5.2)$$

$$R^2 = 0.9939$$

Accordingly the designers are recommended to stick into the given curve in Figure 5.1 (in contrast the polynomial equation 5.2) for selecting the air-gap.

## 5.2 Calculation of Relative Permeability

As per the proposing design guideline, the designer is expected to follow the air-gap selection with respect to the cut core area as discussed in section 5.1. And also having this research is restricted to a fixed flux density 1.30T (see section 3.2.1) for the inner core, it is possible to make a direct relationship between the cut core cross sectional area and the saturation flux density (and hence the relative permeability) of the outer core. See Table 5.2 arranged based on the experimental data discussed in chapter 4.

**Table 5.2:** Relative permeability to the core cross sectional area

Product	Cut-core area (mm <sup>2</sup> )	Air gap (mm)	Flux density (B) of cut core	Relative permeability
TI-173622 (1000VA)	1350	0.075	2.21	109.5
TI-173618C (2000VA)	1890	0.30	2.15	160.0
TI-173618D (3000VA)	2520	0.60	2.10	220.0
TI-173618E (4500VA)	3150	0.70	2.07	291.0

Based on the data in Table 5.2, it is possible to derive a characteristic curve for Relative permeability with respect to Cut-core cross sectional area as per Figure 5.2.

The respective equation for Figure 5.2 comes as the following equation 5.3

$$Y = 0.1004X - 28.437 \quad (5.3)$$

$$R^2 = 0.9979$$

This characteristics equation 5.3 shall be used in permeability calculation purpose in design tool development, towards inrush calculation.

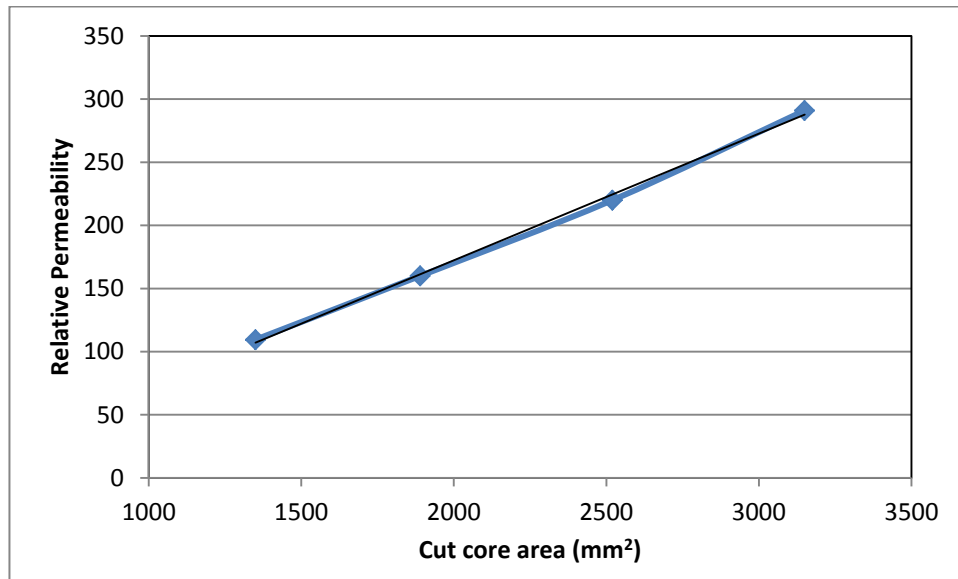


**Figure 5.2:** Relative permeability Vs Cut-core cross-sectional area

Note, the characteristic in Figure 5.2 is strictly valid only for the core cross sectional area ratio 1:0.7 (CK: MOH), and note the four designs discussed here are with the same area ratio, as discussed under chapter 4. This restriction is because, as the area ratio changes, the parameters of Optimum air-gap, Saturation flux density (hence Relative permeability) get changed for particular cross sectional area ratio, means different core cross sectional area ratios result with different characteristics.

### 5.3 Calculation of Inrush Current for Different Core Cross-Sectional Area Ratios

Even the characteristic in Figure 5.2 valid only for finite core cross sectional area ratio 1:0.7 (CK: MOH), it is not admissible fixing the design guideline only for finite core cross sectional area ratio. To meet the flexibility to design in different core cross sectional area ratios, the characteristics in the Figure 5.3 will be used.

Each curve is generated with the transformers having same parameters in all aspects, except changing the core cross sectional area ratio. Note, this characteristic is generated based on the two designs TI-173622 (1000VA) and TI-173618D (3000VA).

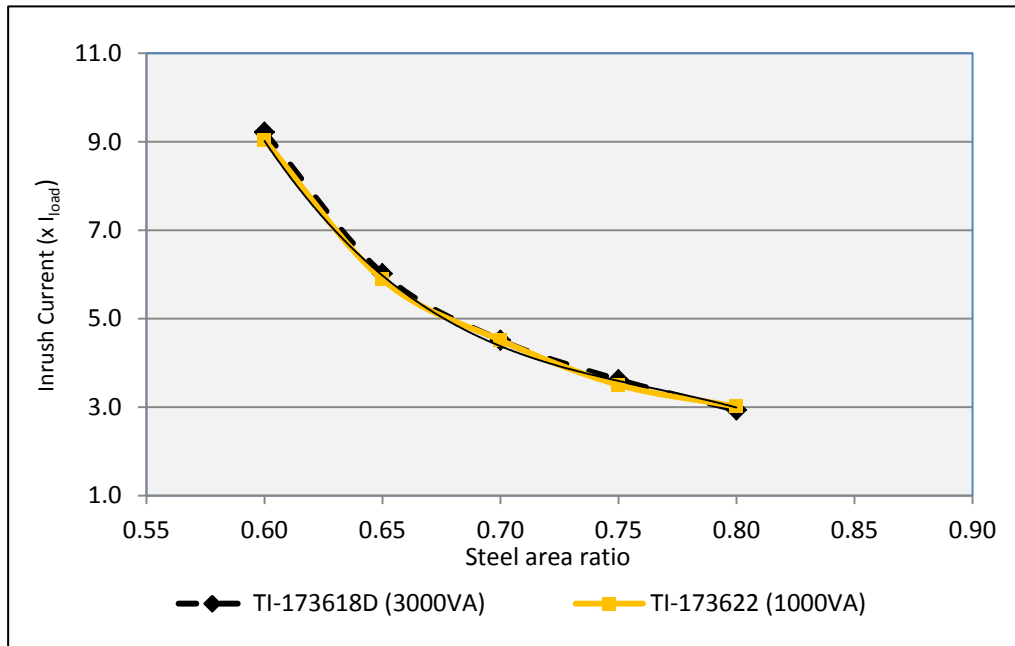


**Figure 5.3:** Inrush Current ( $\times I_{load}$ ) Vs Steel cross-sectional area ratio

Accordingly, once the inrush current is calculated based on core cross sectional area ratio 1:0.7 (CK: MOH), the following polynomial equation 5.4 can be used in calculating inrush currents for different core area ratios.

$$Y = -690X^3 + 1582.4X^2 - 1218.9X + 318.11 \quad (5.4)$$

$$R^2 = 0.9985$$

The research covers the steel ratio range 1:0.60 to 1:0.80 and that will cover the inrush current range approximately 2 to 8 times of load current. This range cover the most of application requirements comes under toroidal transformers.

Having the characteristics curve for Relative permeability and Cut-core cross sectional area (Figure 5.2) is already complied with core cross sectional area ratio 1:0.7 (CK: MOH), the equation 5.4 shall be corrected for  $X = 0.7$  before integrating with equation 5.1, as following.

Consider,

$$Y = -690X^3 + 1582.4X^2 - 1218.9X + 318.11$$

Calculate  $Y_{0.7}$  at  $X = 0.7$

$$Y_{0.7} = -690 \times (0.7)^3 + 1582.4 \times (0.7)^2 - 1218.9 \times (0.7) + 318.11$$

$$Y_{0.7} = 3.586$$

Then the Ratio factor (say  $K_{ratio}$ ) will be derived as following,

$$K_{ratio} = Y / Y_{0.7}$$

$$K_{ratio} = -192.415X^3 + 441.27X^2 - 339.905X + 88.709 \quad (5.5)$$

Accordingly the factor  $K_{ratio}$  can be integrated with the equation 5.1 as following.

$$I_{max} = \frac{3.75 V_{rms}}{\sqrt{(\omega L_s)^2 + R^2}} \times K_{ratio} \quad (5.6)$$

where  $X =$  core cross sectional area ratio

So the equation 5.6 can be used as the general equation for inrush current calculations for different area ratios.

#### 5.4 Development of Design Tool for Composite Core

This section will discuss on development of a design tool for composite core, integrating the equations and characteristics derived in the previous sections.

As discussed in the chapter 3 (section 3.2.1), all the designs considered in this research are done for constant flux density 1.30T considering the centre uncut core. Hence in this design tool the designer will only need to input the core dimensions of the inner core and the outer core (and the input winding resistance), then the design tool itself will calculate the number of turns of the input winding and the other parameters, and finally calculate the inrush current value. The Figure 5.4 shows the simplified flow chart for the calculation tool.

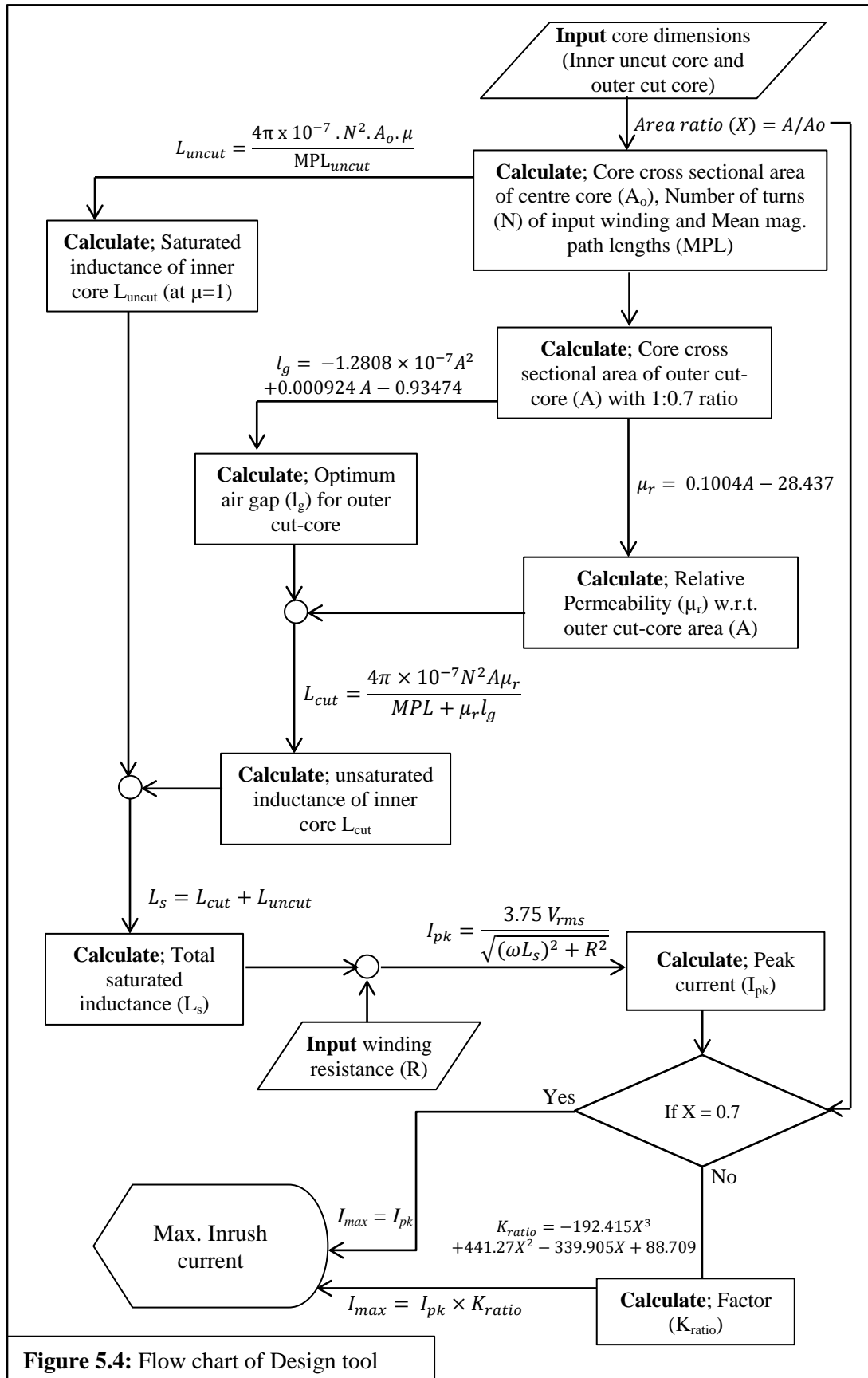


Figure 5.4: Flow chart of Design tool

Then the flow chart can be presented as a design tool, which can be programmed with different software programming languages. The following Figure 5.5 is showing the program which is done on the Flow chart, with Microsoft Excel.

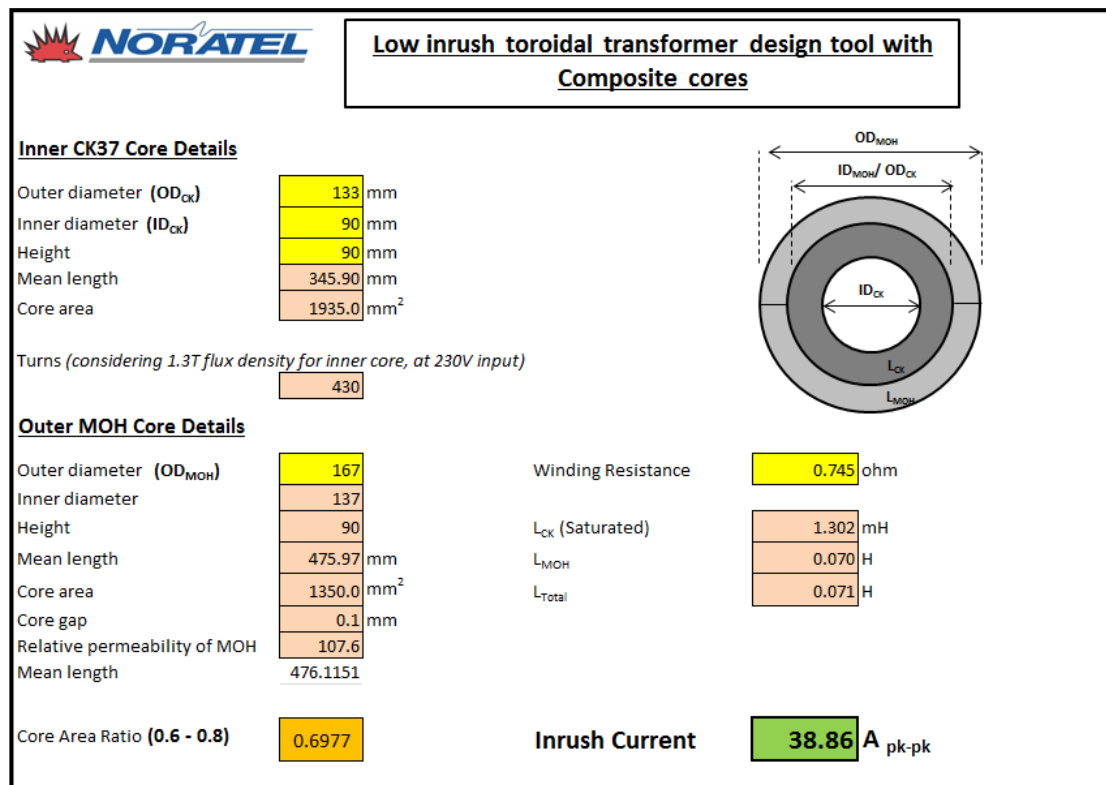


Figure 5.5: Design tool

As shown in the Figure 5.5, the designer will only have to input only the dimensions of the cores and the resistance of the input winding, and the design tool will calculate the maximum inrush current accordingly.

### 5.5 Comparison between Measured and Calculated Inrush Current Values

In this section, it shows the performance of the developed tool comparing together with the measured inrush current values. The Table 5.3 has shown the summary of measured inrush current values and the calculated inrush current values based on the characteristic relationships developed in the previous sections.

**Table 5.3:** Comparison between measured and calculated inrush current values

Article Number	Measure inrush current (A pk-pk)	Calculated inrush current (A pk-pk)	Deviation %
TI-173622 (1000VA)	36.3	38.86	6.6
TI-173628 (1000VA)	58.3	61.40	5.0
TI-173630 (1000VA)	21.8	22.10	1.4
TI-173618C (2000VA)	51.8	54.22	4.5
TI-173618M (2500VA)	93.4	96.10	2.8
TI-173618D (3000VA)	58.9	60.74	3.0
TI-173618N (3500VA)	30.7	31.80	3.5
TI-173618E (4500VA)	59.5	60.84	2.2

In Table 5.3, the deviation in the last column is calculated together with the following equation 5.7.

$$Deviation (\%) = \frac{I_{calculated} - I_{measured}}{I_{measured}} \times 100 \quad (5.7)$$

$I_{calculated}$  - Calculated inrush current  
 $I_{measured}$  - Measured inrush current

Accordingly it is observed that there is only a small deviation between the calculated and measured inrush current values. Means it is evident that the characteristic equations built up for inrush calculation is with high accuracy towards calculating inrush current.

Also it is noted that the deviations are always positive, means the calculated inrush current values are always higher, than the measured inrush current values.

One of the main reasons for that will be the source impedance (section 3.3), which will never be zero in real applications. Note, the above measured values are taken from a source with very low impedance, hence the deviations are minimal.



Therefore considering calculated values as the maximum inrush current is obviously safe, considering all the applications.

Meantime the inrush current values in Table 5.3 evident that the composite core method does have a good control over the inrush current value, rather than the conventional transformer based inrush current mitigation methods. Hence it can be concluded that, together with the composite core method, it is possible to calculate the inrush current values within 10%, including the manufacturing tolerances.

The manufacturing controls will further discussed in chapter 6, under the manufacturing aspects of the composite core.

## RESULTS DISCUSSION AND MOTIVATION

In this chapter, mainly discusses on the results obtained for the composite core designs in chapters 4 and chapter 5; comparing with the corresponding same cost conventional low inrush transformer designs (total cut-core designs). In addition to electrical parameters, transformer manufacturing aspects also briefly discussed. Followings are the main topics to be discussed;

- 1) Comparison of electrical parameters
- 2) Use of recycled steel cores
- 3) Comparison of manufacturing aspects
- 4) Comparison of mechanical parameters

### 6.1 Comparison of Electrical Parameters

Mainly there are four electrical parameters to be discussed under this section. They are Inrush current values, No load current values, Reactive core loss value and Active core loss value.

#### 6.1.1 Comparison of inrush current values

Here the inrush current values obtained from the composite core designs will be compared with the corresponding conventional low inrush designs. The following Table 6.1 shows the measured data on the both options, covering the power range approximately 1kVA to 5kVA.

**Table 6.1:** Inrush current measurements of composite / conventional designs

Power (VA)	Inrush Current - Composite core ( $A_{pk-pk}$ )	Inrush Current – Conventional ( $A_{pk-pk}$ )	Reduction %
1000	36.3	52	30.19
2000	51.8	95	45.47
3000	58.9	125	52.88
4500	59.5	155	61.61

Here the Reduction (%) is calculated by equation 6.1,

$$Reduction (\%) = \frac{I_{conventional} - I_{composite}}{I_{conventional}} \times 100 \quad (6.1)$$

- $I_{conventional}$  - Inrush current from conventional method  
 $I_{composite}$  - Inrush current from composite core method

Also these findings can be graphed as per the Figure 6.1.

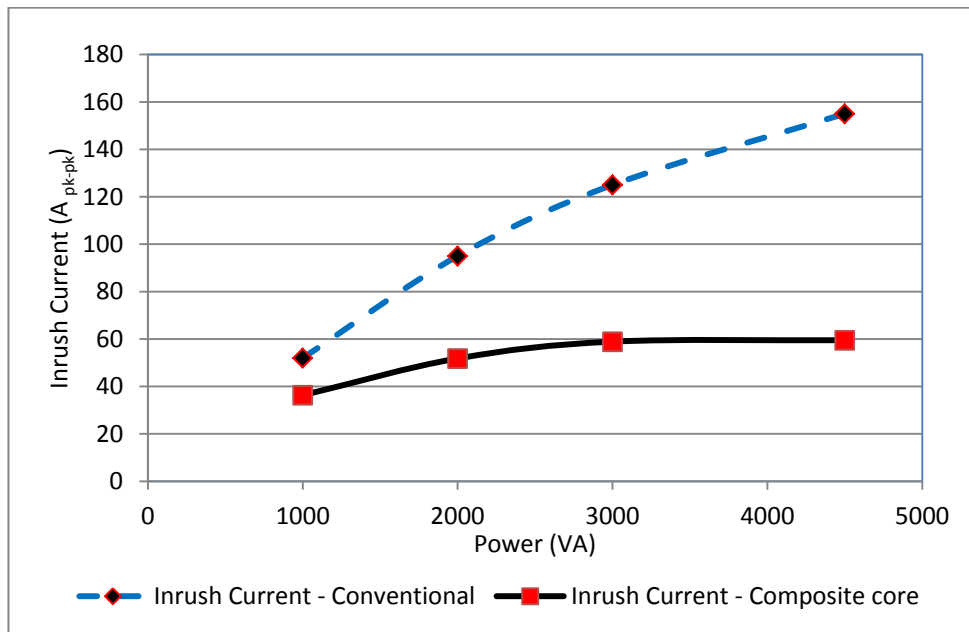


**Figure 6.1:** Inrush current of composite / conventional designs

The Figure 6.1 illustrates that the inrush current values of conventional method increases as the power level increases, but the composite core method do have much control over inrush currents, especially in higher power levels. So basically it can conclude that the composite core method do reduce the inrush current by around 40-60%, compared to conventional method, within the power range 1kVA to 5kVA.

Also if the same inrush current level considered, the composite core method will reduce the transformer cost by 5% for 1000VA power level with respect to the corresponding conventional core transformer, and this saving will further increase even up to 10% considering 5000VA.

### 6.1.2 Comparison of no-load current values

Here the no-load current values obtained from the composite core designs will be compared with the corresponding conventional low inrush designs. The following Table 6.2 shows the measured data on the both options, covering the approximately power range approximately 1kVA to 5kVA.

**Table 6.2:** No-load current measurements of composite / conventional designs

Power (VA)	No-load Current - Composite core (mA)	No-load Current – Conventional (mA)	Reduction %
1000	65.7	208	68.41
2000	86.7	240	63.85
3000	122.0	287	57.49
4500	228.1	410	44.39

Here the Reduction (%) is calculated by equation 6.2,

$$Reduction (\%) = \frac{I_{conventional} - I_{composite}}{I_{conventional}} \times 100 \quad (6.2)$$

$I_{conventional}$  - No-load current from conventional method

$I_{composite}$  - No-load current from composite core method

Also these findings can be graphed as per the Figure 6.2

As the Figure 6.2 illustrates, the no-load current values in conventional method is much higher, but with the composite core method it can be reduce by more than 50%. The basic reason for higher currents in the conventional method is, it cut the total core resulting higher magnetic force requirement in normal operation, while in composite core method the centre uncut core keeps the required magnetic force lower.

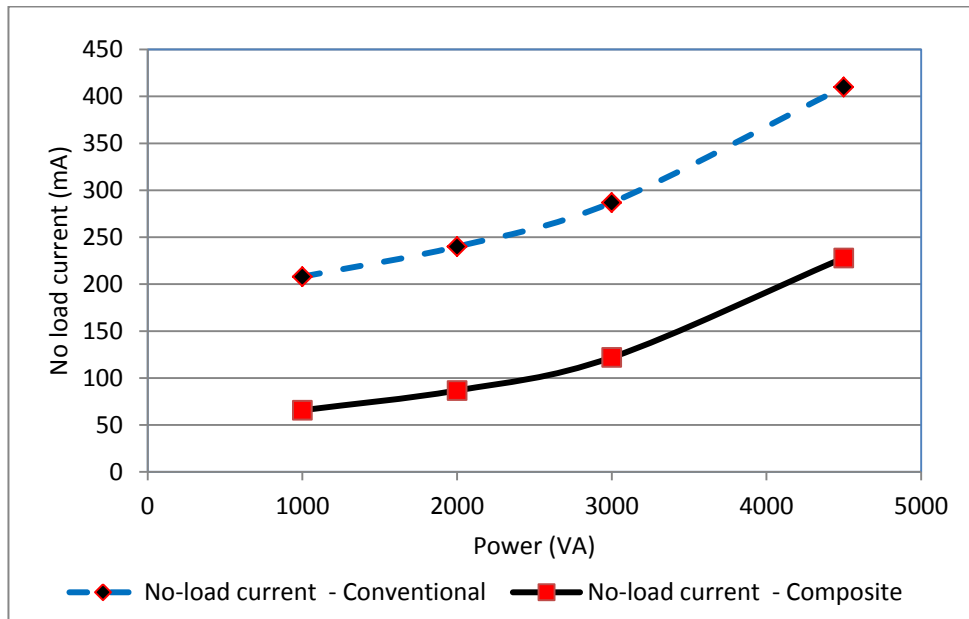


**Figure 6.2:** No-load current of composite / conventional designs

### 6.1.3 Comparison of reactive power loss

Here the reactive power loss values obtained from the composite core designs will be compared with the corresponding conventional low inrush designs. The following Table 6.3 shows the measured data on the both options, covering the power range approximately 1kVA to 5kVA.

**Table 6.3:** Reactive power loss measurements of composite/conventional designs

Power (VA)	Reactive power loss - Composite core (Var)	Reactive power loss – Conventional (Var)	Reduction %
1000	12.15	47.6	74.45
2000	15.67	53.4	70.63
3000	23.39	65.5	64.27
4500	46.08	93.5	50.70

Here the Reduction (%) is calculated by equation 6.3,

$$Reduction (\%) = \frac{var_{conventional} - var_{composite}}{var_{conventional}} \times 100 \quad (6.3)$$

- $\text{var}_{\text{conventional}}$  - Reactive power loss conventional method
- $\text{var}_{\text{composite}}$  - Reactive power loss composite core method

Also these findings can be graphed as per the Figure 6.3.

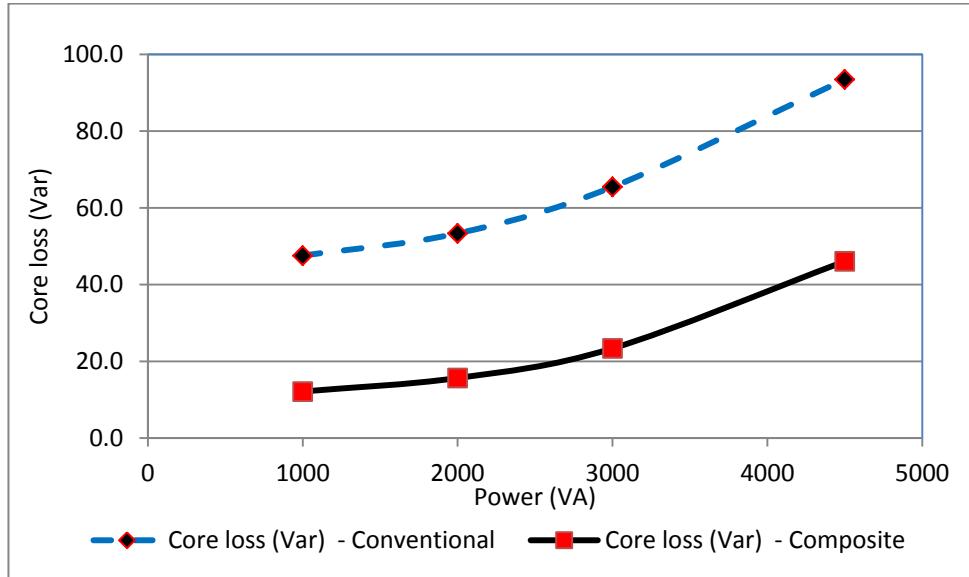


**Figure 6.3:** Reactive power loss of composite / conventional designs

As discussed in section 6.1.2, the transformers with conventional method shows significantly higher no load current, and consequently that shows a higher reactive power loss. Typically it maintains over 50% reduction of reactive power loss in composite core method within power range 1kVA-5kVA.

#### 6.1.4 Comparison of active power loss

Here the active power loss values obtained from the composite core designs will be compared with the corresponding conventional low inrush designs. The following Table 6.4 shows the measured data on the both options, covering the power range approximately 1kVA to 5kVA.

**Table 6.4:** Active power loss measurements of composite / conventional designs

Power (VA)	Active power loss - Composite core (watt)	Active power loss – Conventional (watt)	Increment %
1000	8.71	5.2	40.30
2000	11.12	6.1	45.14
3000	15.5	8.2	47.10
4500	25.1	12.5	50.00

Here the Loss increment (%) is calculated by equation 6.4,

$$Increment (\%) = \frac{watt_{composite} - watt_{conventional}}{watt_{composite}} \times 100 \quad (6.4)$$

watt<sub>conventional</sub> - Active power loss conventional method

watt<sub>composite</sub> - Active power loss composite core method

Also these findings can be graphed as per the Figure 6.4.

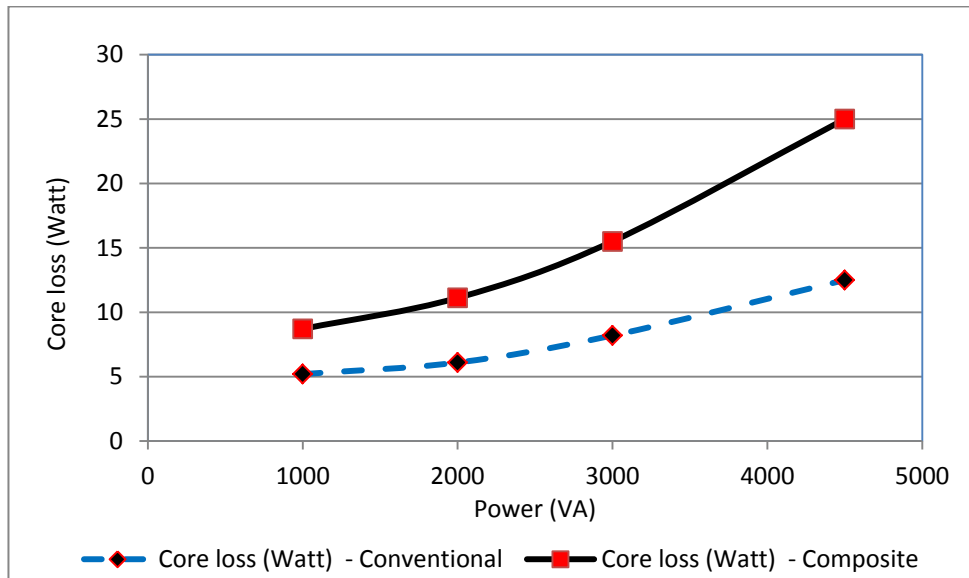


**Figure 6.4:** Active power loss of composite / conventional designs

As Figure 6.4 illustrates, the composite core method is having significantly higher active power loss in normal operation compared to the conventional method. The reason for this is, the composite core uses low graded steel in place of high graded steel for cost saving purpose. But still note, considering the transformer power range 1kVA to 5kVA, this active power loss increment will drop the transformer efficiency only by 0.25% to 0.35% considering the off-load condition.

## 6.2 Use of Recycled Steel Cores

The disadvantage of active power loss increment (discussed in section 6.1.4) can be overcome by use of low cost “Recycled steel cores” for inner core. Recycle cores are typically made with small strips of used high grade steel types (and varnished), instead of virgin steel. Due to this reason, the cost of recycle cores are very low, even closer to the cost of low grade NGOSS cores made with virgin steel. But still recycle cores are holding very low core losses, as they are made with high grade steel.

The specialty of the recycle cores are, they cannot be cut to separate due to its piece-like structure (see Figure 6.5), because that will lead to loose the strips and then gets mechanically unstable. Hence it is difficult to use these recycle cores with conventional low inrush designs due to manufacturability issues.

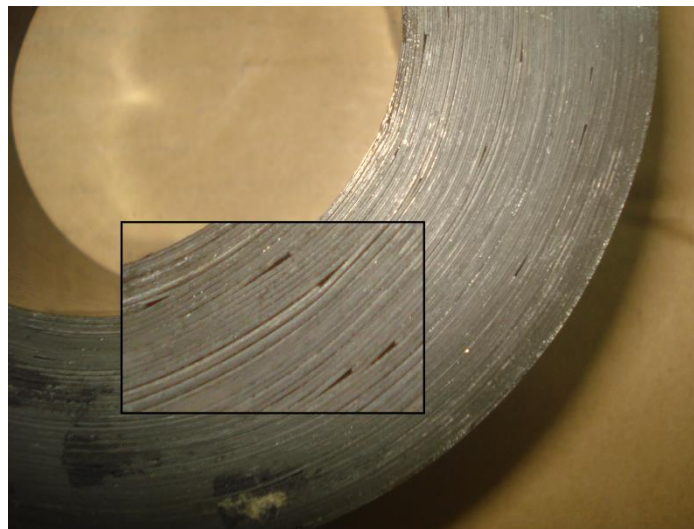


**Figure 6.5:** Recycle core including joints in steel strips



The advantage of the composite core method is, it does not need to cut the centre core, and hence the recycle cores can be used in the place of centre uncut core without any manufacturing issue, while reducing the active core loss.

### 6.3 Comparison of Manufacturing Aspects

This section describes the pros and cons between the core manufacturing of composite core and conventional cut core.

#### 6.3.1 Manufacturing of conventional cut core

Typically the conventional cores are totally made with high grade steel (GOSS-AISI Grade M5) in order to keep the core losses lower as possible, due to these cores are incorporated with a full cut radially. See Figure 6.6.

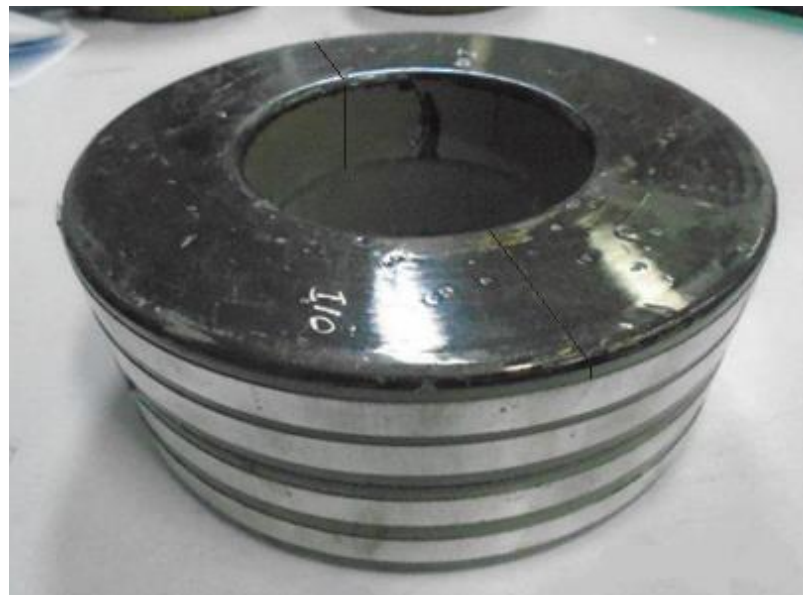


**Figure 6.6:** Conventional cut core

To keep the core loss lower, these cores require special attention in the cutting process, to have a smooth finish on the cutting surfaces. In critical applications, it might require additional polishing process on the surfaces to get them smoother. Also

note, having this method required to cut the total core, it needs to varnish the total core as well. Due to the criticalness of the cutting process, this process consumes more labour time and also will result considerable material wastage, hence finally affect to the product cost.

After it is cut, the core fixing also need to be processed with much attention as it needs to ensure the cutting surfaces are ideally aligned and fixed minimizing the core losses in normal process. Then the core needs to be reinforced together with the steel bands, glue etc. to make it rigid during manufacturing process and also most importantly in continuous operation. Note, this core operates at flux density around  $1.10 - 1.20T$  in normal operation, hence the level of reinforcement affect to the transformer performance (vibration issues).

### 6.3.2 Manufacturing of composite core

The composite core is comprised with two cores, one is uncut core in the centre made with a low grade steel type (NGOSS- AISI Grade 35H300) and other is cut core made with higher grade steel type (GOSS- AISI Grade MOH). See Figure 6.7.



**Figure 6.7:** Composite core

The advantage of the composite core is, it does not need to cut the total core, and hence it does not need to varnish the total core either. Most importantly the outer cut core does not need to have extreme smooth cutting surfaces, because in case of composite core scenario it needs to maintain a certain gap in the outer core. Therefore in this case, it consumes much lower labour time and minimizes material wastage.

But maintaining the air gap is critical in composite core scenario, where it may use specially made spacers or commonly available Intek sticky tapes (Class H graded) with thickness steps 0.05mm.

One more advantage of the composite core method is, the outer core does not need much of reinforcement together with the steel bands similarly in conventional cut core, because the outer core is already supported by the inner uncut core for reinforcement, in both manufacturing process and normal operation. Means this construction is more mechanically stable over the total cut core method.

Hence it is possible to avoid steel bands under this construction in most of the applications (but need to use glue) and reduce cost. Note, the outer cut core operated at flux density around 0.2-0.3T in normal operation, and hence the said bonding level will not affect to the performance at transformer normal operation.

#### **6.4 Comparison of Mechanical Parameters**

In order to measure the mechanical stability of composite core, the only factory available methodology is Humming test. Here same sized two transformers made with the two methods (conventional and composite cores) are tested for humming at their normal operation.

Note, it is difficult to measure the absolute humming level under the factory condition, but only possible to “compare” the sound levels under the same ambient noise condition.

Here the sound level measuring equipment Extech SL130G is used for measuring humming level, together with the wooden box with sound sealing material in the inner surfaces to install the transformer specimen. See Figure 6.8 for humming test set up.



**Figure 6.8:** Humming test set up

Here the first step is calculating the ambient noise level and it was measured as approximately 30dB.

Then consequently the noise levels of the conventional core transformer & composite core transformer (which are made for same power level) are measured under the same mains input within limited time duration to keep the harmonics level of the mains as same as possible.

The noise levels measured are 32.9dB and 33.1dB for the conventional core transformer & composite core transformer respectively. So it is evident that the core bonding mechanism suggested in section 6.2.2 is sufficient for the composite core.

Apart from the humming comparisons, one of the drawbacks in the composite core method is, it occupies slightly larger space (about 8% increment in diameter compared to respective conventional design) in the lower power ranges (1kVA to 2kVA). But this disadvantage get mitigated moving towards higher power ranges (4kVA to 5kVA), comparing together with the respective conventional transformer.

In contrast this increment of volume results in increment of the weight of the final product, compared to the conventional transformer.

---

## CONCLUSION AND SUGGESTIONS FOR FUTURE RESEARCH

### 7.1 Conclusion

In this research study, it emphasized that the transformer based inrush mitigation methods are more reliable over the external equipment based (i.e. connecting NTC thermistor, start-up resistive load) inrush mitigation methods. Further, this research established the use of composite cores as the best option over the existing transformer based solutions to mitigate inrush current and several other drawbacks of the conventional solutions.

The proposed method has the advantages of higher performance; lower inrush current, lower no-load current, low reactive core loss, mechanically stable reinforced structure, easier manufacturing and hence reduced material wastage. So the proposed method saves costs and also the resources. The composite core is highly reliable on inrush mitigation for the 1kVA to 5kVA range of test transformers, the reduction in inrush current was 40-60%, reduction in no load current was over 50%, and reduction in reactive core loss was over 50% compared to the corresponding conventional transformers.

The main disadvantage of composite core was the increment of the active core loss, but which can be mitigated by using recycle cores. So this opportunity of using recycled steel core also an added advantage on saving the resource on the planet.

The composite transformer is slightly larger and heavier, but still that will not cause much of a problem as the increase is small, about 8%. This too would diminish when the transformer capacity goes up.

## 7.2 Suggestions for Future Research

Followings are the future research suggestions, on the composite core method discussed.

- 1) This research is confined to particular steel types, steel area ratio range and transformer power range. So the same calculation methodology can be used to expand the ranges of above parameters while introducing new steel types.
- 2) This research has done experiments only for 230V main input. But it will be useful building the same concept for the other common input voltages of other countries / applications (110V, 120V, 200V, 400V etc.), expanding the design calculation.
- 3) Also there will be more easier and economical manufacturing methods on composite cores; like introducing welding on cut core for bonding purpose together with the centre uncut core, for more stable construction instead gluing etc.

Also it will be worth experimenting for other constructional methods, which could be economical and might be high performing.

## REFERENCE LIST

- [1] H.K. Ekanayake, “Methodology to limit inrush current of toroidal transformers”, Charted Engineering IESL Sri Lanka, 2012
- [2] Rasim Dogan, Saeed Jazebi, ”Investigation of Transformer-Based Solutions for the Reduction of Inrush and Phase-Hop Currents”, IEEE Transactions on Power Electronics, Vol. 31, Iss 5, pp 3506 – 3516, July 2015
- [3] Francisco de L, Brian G, “Transformer Based Solutions to Power Quality Problems”, Plitron Manufacturing Inc. Canada, 2001
- [4] KAWASAKI STEEL CORPORATION, “PLASMA CORE RGHPJ RGH AND RG CORE”, Grain-Oriented Magnetic Steel Strip, Japan: 1991.
- [5] Colonel MW, T. Mcllyman, “Transformer and inductor design handbook”, Third Edition, Kg Magnetics, Inc. California, USA, 2004, pp. 96-100
- [6] Saeed Jazebi, Nicholas Wu, “Enhanced analytical method for the calculation of the maximum inrush current of single phase power transformer”, IEEE Transactions on Power Delivery, Vol. 30, Iss 6, pp 2590 - 2599, June 2015
- [7] Yunfei Wang, Sami G., “Analytical formula to estimate the maximum inrush current”, IEEE Translations on Power Delivery, Vol. 23, No 2, pp 1266 - 1268, April 2008



# APPENDICES

**Appendix A** – Design simulations with ToroidEZE programme for designs with steel area ratio Uncut : Cut – 1.0 : 0.7

## TI-173622 (1000VA) – Uncut centre core

<u>TOROIDAL TRANSFORMER DESIGN SUMMARY .</u>		
Design No	: TI-173622 (1000VA) - Uncut core	Printed : 2017-10-31
Customer	:	Designer : Sameera
Customer P/N	:	Noratel SL
<b>Notes:</b>		
Design File : 173622- un-cut core.tfx		
Core : 133 x 90 x 90 mm CK-37	Iron Loss : 9.2 W	Finished Dim's : 153 x 57 x 116 mm
Fe Weight : 5.1 kg	Coil Weight : 5.66 kg	Tot. Weight : 10.827 kg
Induction : 1.311 T	Load Loss : 34.69 W	Tot. Power : 999 VA
Frequency : 50 Hz	Sec Loss : 18.45 W	Temp. Rise : 42/50 deg.C
Excitation: 110.9 mA	Fri Loss : 16.24 W	Optimized : 1:0.36 Wdg+
Core/Coil : 0.9:1 kg	Window Fill : 83.6 %	Wire Fill : 38.3 %
<b>Windings.</b>	<b>Primary</b>	<b>Sec 1</b>
	0	0
Rated Volts rms.	230v	222v
Rated Amps rms.	4.54A	4.5A
Duty Cycle %.	-	100%
	-	-
VA rms.	-	999
Conductor.	Cu	Cu
Turns.	430ts	430ts
Wire Gauge.	1.900mm	1.900mm
Filars.	-	-
	-	-
Ohms @ 20°C.	0.641	0.74
	-	-
Copper grams.	2629	3035
	-	-
Full-Load Volts.	-	222.9v
No-Load Volts.	-	230v
Regulation %.	1.5%	3.1%
	-	-
Watts Loss Hot.	16.24	18.45
	-	-
Insulation Tape.	-	-
Width. mm.	-	13
Thickness. mm.	-	0.05
Layers.	-	3
	-	-
Screening Tape.	-	-
Width. mm.	-	-
Thickness. mm.	-	-
Layers.	-	-
	-	-
A/mm <sup>2</sup> .	1.6	1.59
Copper Fill %.	19.16%	19.16%
ToroidEZE-AL v.2.6.1		
Page 1 of 1.		

## TI-173622 (1000VA) – Composite core

<u>TOROIDAL TRANSFORMER DESIGN SUMMARY.</u>		
Design No	: TI-173622 (1000VA) - Composite core	Printed : 2017-10-31
Customer	:	Designer : Sameera
Customer P/N	:	Noratel SL
<u>Notes:</u>		
Design File : 173622.tfx		
Core : 165 x 90 x 90 mm 27-M0H	Iron Loss : 2.13 W	Finished Dim's : 182 x 57 x 114 mm
Fe Weight : 10.17 kg	Coil Weight : 6.27 kg	Tot. Weight : 16.521 kg
Induction : 0.751 T	Load Loss : 37.25 W	Tot. Power : 999 VA
Frequency : 50 Hz	Sec Loss : 19.64 W	Temp. Rise : 34/41 deg.C
Excitation: 13.7 mA	Pri Loss : 17.61 W	Optimized : 1:0.65 Wdg+
Core/Coil : 1.6:1 kg	Window Fill : 83.6 %	Wire Fill : 38.3 %
<b>Windings.</b>	<b>Primary</b>	<b>Sec 1</b>
	0	0
Rated Volts rms.	230v	222v
Rated Amps rms.	4.51A	4.5A
Duty Cycle %.	-	100%
	-	-
VA rms.	-	999
Conductor.	Cu	Cu
Turns.	430ts	430ts
Wire Gauge.	1.900mm	1.900mm
Filars.	-	-
	-	-
Ohms @ 20°C.	0.72	0.808
	-	-
Copper grams.	2954	3315
	-	-
Full-Load Volts.	-	222.3v
No-Load Volts.	-	230v
Regulation %.	1.6%	3.3%
	-	-
Watts Loss Hot.	17.61	19.64
	-	-
Insulation Tape.	-	-
Width. mm.	-	13
Thickness. mm.	-	0.05
Layers.	-	3
	-	-
Screening Tape.	-	-
Width. mm.	-	-
Thickness. mm.	-	-
Layers.	-	-
	-	-
A/mm <sup>2</sup> .	1.59	1.59
Copper Fill %.	19.16%	19.16%
ToroidEZE-AL v.2.6.1		Page 1 of 1.

## TI-173618C (2000VA) – Uncut centre core

TOROIDAL TRANSFORMER DESIGN SUMMARY.		
Design No : TI-173618C (2000VA) - Uncut core	Printed : 2017-10-31	
Customer :	Designer : Sameera	
Customer P/N :	Noratel SL	
 <b>Notes:</b>		
Design File : 173618C- un-cut core.tfx		
Core : 180 x 90 x 60 mm CK-37	Iron Loss : 15.21 W	Finished Dim's : 195 x 61 x 81 mm
Fe Weight : 8.61 kg	Coil Weight : 4.43 kg	Tot. Weight : 13.11 kg
Induction : 1.299 T	Load Loss : 101.4 W	Tot. Power : 2000 VA
Frequency : 50 Hz	Sec Loss : 35.01 W	Temp. Rise : 97/116 deg.C
Excitation: 178.1 mA	Pri Loss : 66.41 W	Optimized : 1:0.78 Wdg+
Core/Coil : 1.9:1 kg	Window Fill : 75.2 %	Wire Fill : 33.1 %
Windings.	Primary	Sec 1
	0	0
Rated Volts rms.	230v	222v
Rated Amps rms.	9.2A	9.01A
Duty Cycle %.	-	100%
	-	-
VA rms.	-	2000
Conductor.	Cu	Cu
Turns.	311ts	314ts
Wire Gauge.	1.180mm	1.700mm
Filars.	(x2)	(x2)
	-	-
Ohms @ 20°C.	0.537	0.295
	-	-
Copper grams.	1315	3113
	-	-
Full-Load Volts.	-	222v
No-Load Volts.	-	232.2v
Regulation %.	3%	4.4%
	-	-
Watts Loss Hot.	66.41	35.01
	-	-
Insulation Tape.	-	-
Width. mm.	-	13
Thickness. mm.	-	0.05
Layers.	-	3
	-	-
Screening Tape.	-	-
Width. mm.	-	-
Thickness. mm.	-	-
Layers.	-	-
	-	-
A/mm <sup>2</sup> .	4.21	1.98
Copper Fill %.	10.69%	22.41%
ToroidEZE-AL v.2.6.1 <span style="float: right;">Page 1 of 1.</span>		

## TI-173618C (2000VA) – Composite core

<u>TOROIDAL TRANSFORMER DESIGN SUMMARY</u>			
Design No	: TI-173618C (2000VA) - Composite core	Printed	: 2017-10-31
Customer	:	Designer	: Sameera
Customer P/N	:	Noratel SL	
<u>Notes:</u>			
Design File : ED-173618C total core.tfx			
Core	: 247 x 90 x 60 mm 27-M0H	Iron Loss	: 3.87 W
Fe Weight	: 18.75 kg	Coil Weight	: 5.66 kg
Induction	: 0.745 T	Load Loss	: 127.2 W
Frequency	: 50 Hz	Sec Loss	: 42.67 W
Excitation	: 25 mA	Pri Loss	: 84.57 W
Core/Coil	: 3.3:1 kg	Window Fill	: 75.2 %
Finished Dim's	: 259 x 61 x 80 mm	Tot. Weight	: 24.524 kg
Tot. Power	: 2000 VA	Temp. Rise	: 84/100 deg.C
Optimized	: 1:1.32 Fe+	Wire Fill	: 33.1 %
Windings.	Primary	Sec 1	
	0	0	
Rated Volts rms.	230v	222v	
Rated Amps rms.	9.27A	9.01A	
Duty Cycle %.	-	100%	
VA rms.	-	2000	
Conductor.	Cu	Cu	
Turns.	311ts	314ts	
Wire Gauge.	1.180mm	1.700mm	
Filars.	(x2)	(x2)	
Ohms @ 20°C.	0.701	0.374	
Copper grams.	1716	3941	
Full-Load Volts.	-	219.4v	
No-Load Volts.	-	232.2v	
Regulation %.	3.7%	5.5%	
Watts Loss Hot.	84.57	42.67	
Insulation Tape.	-	-	
Width. mm.	-	13	
Thickness. mm.	-	0.05	
Layers.	-	3	
Screening Tape.	-	-	
Width. mm.	-	-	
Thickness. mm.	-	-	
Layers.	-	-	
A/mm^2.	4.24	1.98	
Copper Fill %.	10.69%	22.41%	
ToroidEZE-AL v.2.6.1			Page 1 of 1.

# TI-173618D (3000VA) – Uncut centre core

<u>TOROIDAL TRANSFORMER DESIGN SUMMARY.</u>			
Design No	: TI-173618D (3000VA) - Uncut core	Printed	: 2017-10-31
Customer	:	Designer	: Sameera
Customer P/N	:	Noratel SL	
<u>Notes:</u>			
Design File : 173618D- un-cut core.tfx			
Core	: 180 x 90 x 80 mm CK-37	Iron Loss	: 20.75 W
Fe Weight	: 11.48 kg	Coil Weight	: 6.57 kg
Induction	: 1.311 T	Load Loss	: 201.6 W
Frequency	: 50 Hz	Sec Loss	: 36.33 W
Excitation	: 250.3 mA	Pri Loss	: 165.2 W
Core/Coil	: 1.7:1 kg	Window Fill	: 86.1 %
Finished Dim's	: 197 x 56 x 105 mm	Tot. Weight	: 18.139 kg
Tot. Power	: 2999 VA	Temp. Rise	: 140/168 deg.C
Optimized	: 1:0.7 Wdg+	Wire Fill	: 41.5 %
Windings.	Primary	Sec 1	
	0	0	
Rated Volts rms.	230v	222v	
Rated Amps rms.	14.01A	13.51A	
Duty Cycle %.	-	100%	
VA rms.	-	2999	
Conductor.	Cu	Cu	
Turns.	231ts	231ts	
Wire Gauge.	1.600mm	2.000mm	
Filars.	-	(x3)	
Ohms @ 20°C.	0.513	0.121	
Copper grams.	1060	5511	
Full-Load Volts.	-	216.7v	
No-Load Volts.	-	230v	
Regulation %.	4.8%	5.8%	
Watts Loss Hot.	165.2	36.33	
Insulation Tape.	-	-	
Width. mm.	-	13	
Thickness. mm.	-	0.05	
Layers.	-	3	
Screening Tape.	-	-	
Width. mm.	-	-	
Thickness. mm.	-	-	
Layers.	-	-	
A/mm <sup>2</sup> .	6.97	1.43	
Copper Fill %.	7.3%	34.22%	
ToroidEZE-AL v.2.6.1			Page 1 of 1.

## TI-173618D (3000VA) – Composite core

TOROIDAL TRANSFORMER DESIGN SUMMARY.					
Design No	: TI-173618D (3000VA) - Composite core		Printed	: 2017-10-31	
Customer	:		Designer	: Sameera	
Customer P/N	:		Noratel SL		
<b>Notes:</b>					
Design File : ED-173618D - total core.tfx					
Core	: 247 x 90 x 80 mm 27-M0H	Iron Loss	: 5.25 W	Finished Dim's	: 261 x 56 x 103 mm
Fe Weight	: 25.01 kg	Coil Weight	: 8.07 kg	Tot. Weight	: 33.219 kg
Induction	: 0.752 T	Load Loss	: 245.5 W	Tot. Power	: 2999 VA
Frequency	: 50 Hz	Sec Loss	: 42.6 W	Temp. Rise	: 124/149 deg.C
Excitation	: 33.8 mA	Pri Loss	: 202.9 W	Optimized	: 1:1.24 Fe+
Core/Coil	: 3.1:1 kg	Window Fill	: 86.1 %	Wire Fill	: 41.5 %
Windings.	Primary	Sec 1			
	0	0			
Rated Volts rms.	230v	222v			
Rated Amps rms.	14.13A	13.51A			
Duty Cycle %.	-	100%			
	-	-			
VA rms.	-	2999			
Conductor.	Cu	Cu			
Turns.	231ts	231ts			
Wire Gauge.	1.600mm	2.000mm			
Filars.	-	(x3)			
	-	-			
Ohms @ 20°C.	0.645	0.148			
	-	-			
Copper grams.	1334	6738			
	-	-			
Full-Load Volts.	-	213.9v			
No-Load Volts.	-	230v			
Regulation %.	5.9%	7%			
	-	-			
Watts Loss Hot.	202.9	42.6			
	-	-			
Insulation Tape.	-	-			
Width. mm.	-	13			
Thickness. mm.	-	0.05			
Layers.	-	3			
	-	-			
Screening Tape.	-	-			
Width. mm.	-	-			
Thickness. mm.	-	-			
Layers.	-	-			
	-	-			
A/mm <sup>2</sup> .	7.03	1.43			
Copper Fill %.	7.3%	34.22%			
ToroidEZE-AL v.2.6.1				Page 1 of 1.	

TI-173618E (4500VA) – Uncut centre core

TOROIDAL TRANSFORMER DESIGN SUMMARY.			
Design No	: TI-173618E (4500VA) - Uncut core	Printed	: 2017-10-31
Customer	:	Designer	: Sameera
Customer P/N	:	Noratel SL	
<u>Notes:</u>			
Design File : 173618E- un-cut core.tfx			
Core	: 180 x 90 x 100 mm CK-37	Iron Loss	: 25.54 W
Fe Weight	: 14.36 kg	Coil Weight	: 7.88 kg
Induction	: 1.303 T	Load Loss	: 509.3 W
Frequency	: 50 Hz	Sec Loss	: 74.02 W
Excitation	: 302.1 mA	Pri Loss	: 435.3 W
Core/Coil	: 1.8:1 kg	Window Fill	: 87.6 %
Finished Dim's	: 198 x 55 x 126 mm	Tot. Weight	: 22.338 kg
		Tot. Power	: 4500 VA
		Temp. Rise	: 163/185 deg.C
		Optimized	: 1:0.73 Wdg+
		Wire Fill	: 42.8 %
Windings.	Primary	Sec 1	
	0	0	
Rated Volts rms.	230v	222v	
Rated Amps rms.	21.89A	20.27A	
Duty Cycle %.	-	100%	
	-	-	
VA rms.	-	4500	
Conductor.	Cu	Cu	
Turns.	186ts	183ts	
Wire Gauge.	1.700mm	2.000mm	
Filars.	-	(x4)	
	-	-	
Ohms @ 20°C.	0.422	0.084	
	-	-	
Copper grams.	1112	6767	
	-	-	
Full-Load Volts.	-	204.7v	
No-Load Volts.	-	226.3v	
Regulation %.	8.2%	9.5%	
	-	-	
Watts Loss Hot.	435.3	74.02	
	-	-	
Insulation Tape.	-	-	
Width. mm.	-	13	
Thickness. mm.	-	0.05	
Layers.	-	3	
	-	-	
Screening Tape.	-	-	
Width. mm.	-	-	
Thickness. mm.	-	-	
Layers.	-	-	
	-	-	
A/mm <sup>2</sup> .	9.64	1.61	
Copper Fill %.	6.64%	36.15%	
ToroidEZE-AL v.2.6.1			Page 1 of 1.

## TI-173618E (4500VA) – Composite core

TOROIDAL TRANSFORMER DESIGN SUMMARY.					
Design No	: TI-173618E (4500VA) - Composite core		Printed	: 2017-10-31	
Customer	:		Designer	: Sameera	
Customer P/N	:		Noratel SL		
<b>Notes:</b>					
Special!!!- cut core					
Design File : ED-173618E - total core.tfx					
Core	: 247 x 90 x 100 mm 27-MOH	Iron Loss	: 6.48 W	Finished Dim's	: 261 x 55 x 124 mm
Fe Weight	: 31.26 kg	Coil Weight	: 9.39 kg	Tot. Weight	: 40.8 kg
Induction	: 0.747 T	Load Loss	: 605.1 W	Tot. Power	: 4500 VA
Frequency	: 50 Hz	Sec Loss	: 83.49 W	Temp. Rise	: 137/185 deg.C
Excitation	: 41.8 mA	Pri Loss	: 521.6 W	Optimized	: 1:1.33 Fe+
Core/Coil	: 3.3:1 kg	Window Fill	: 87.6 %	Wire Fill	: 42.8 %
Windings.	Primary	Sec 1			
	0	0			
Rated Volts rms.	230v	222v			
Rated Amps rms.	22.22A	20.27A			
Duty Cycle %.	-	100%			
	-	-			
VA rms.	-	4500			
Conductor.	Cu	Cu			
Turns.	186ts	183ts			
Wire Gauge.	1.700mm	2.000mm			
Filars.	-	(x4)			
	-	-			
Ohms @ 20°C.	0.716	0.099			
	-	-			
Copper grams.	1360	8029			
	-	-			
Full-Load Volts.	-	201v			
No-Load Volts.	-	226.3v			
Regulation %.	9.6%	11.2%			
	-	-			
Watts Loss Hot.	521.6	83.49			
	-	-			
Insulation Tape.	-	-			
Width. mm.	-	13			
Thickness. mm.	-	0.05			
Layers.	-	3			
	-	-			
Screening Tape.	-	-			
Width. mm.	-	-			
Thickness. mm.	-	-			
Layers.	-	-			
	-	-			
A/mm <sup>2</sup> .	9.79	1.61			
Copper Fill %.	6.64%	36.15%			
ToroidEEE-AL v.2.6.1			Page 1 of 1.		



**Appendix B** – Design simulations with ToroidEZE programme for designs with different steel area ratios

TI-173628 (1000VA with Cut:Uncut ratio = 0.6:1.0) – Uncut centre core

TOROIDAL TRANSFORMER DESIGN SUMMARY.		
Design No	: TI-173628 (1000VA) - Uncut core	
Customer	:	
Customer P/N	:	
		Printed : 2017-11-03
		Designer : Sameera
		Noratel SL
<u>Notes:</u>		
Design File : 173628- un-cut core.tfx		
Core	: 133 x 90 x 90 mm CK-37	Iron Loss : 9.2 W
Fe Weight	: 5.1 kg	Coil Weight : 5.66 kg
Induction	: 1.311 T	Load Loss : 34.7 W
Frequency	: 50 Hz	Sec Loss : 18.45 W
Excitation	: 110.9 mA	Pri Loss : 16.24 W
Core/Coil	: 0.9:1 kg	Window Fill : 83.6 %
		Finished Dim's : 153 x 57 x 116 mm
		Tot. Weight : 10.827 kg
		Tot. Power : 999 VA
		Temp. Rise : 42/50 deg.C
		Optimized : 1:0.36 Wdg+
		Wire Fill : 38.3 %
Windings.	Primary	Sec 1
	0	0
Rated Volts rms.	230v	222v
Rated Amps rms.	4.54A	4.5A
Duty Cycle %.	-	100%
	-	-
VA rms.	-	999
Conductor.	Cu	Cu
Turns.	430ts	430ts
Wire Gauge.	1.900mm	1.900mm
Filars.	-	-
	-	-
Ohms @ 20°C.	0.641	0.74
	-	-
Copper grams.	2629	3035
	-	-
Full-Load Volts.	-	222.9v
No-Load Volts.	-	230v
Regulation %.	1.5%	3.1%
	-	-
Watts Loss Hot.	16.24	18.45
	-	-
Insulation Tape.	-	-
Width. mm.	-	13
Thickness. mm.	-	0.05
Layers.	-	3
	-	-
Screening Tape.	-	-
Width. mm.	-	-
Thickness. mm.	-	-
Layers.	-	-
	-	-
A/mm <sup>2</sup> .	1.6	1.59
Copper Fill %.	19.16%	19.16%
ToroidEZE-AL v.2.6.1		
Page 1 of 1.		

TI-173628 (1000VA with Cut:Uncut ratio = 0.6:1.0) – Composite core

<u>TOROIDAL TRANSFORMER DESIGN SUMMARY.</u>			
Design No	: TI-173628 (1000VA) - Composite core	Printed	: 2017-11-03
Customer	:	Designer	: Sameera
Customer P/N	:	Noratel SL	
<b>Notes:</b>			
Special!!			
Design File : ED-173628.tfx			
<hr/>			
Core	: 161 x 90 x 90 mm 27-M0H	Iron Loss	: 2.18 W
Fe Weight	: 9.48 kg	Coil Weight	: 6.18 kg
Induction	: 0.794 T	Load Loss	: 36.75 W
Frequency	: 50 Hz	Sec Loss	: 19.39 W
Excitation	: 14.1 mA	Pri Loss	: 17.35 W
Core/Coil	: 1.5:1 kg	Window Fill	: 83.6 %
Finished Dim's	: 179 x 57 x 115 mm	Tot. Weight	: 15.743 kg
		Tot. Power	: 999 VA
		Temp. Rise	: 34/41 deg.C
		Optimized	: 1:0.61 Wdg+
		Wire Fill	: 38.3 %
<hr/>			
Windings.	Primary	Sec 1	
	0	0	
Rated Volts rms.	230v	222v	
Rated Amps rms.	4.51A	4.5A	
Duty Cycle %.	-	100%	
	-	-	
VA rms.	-	999	
Conductor.	Cu	Cu	
Turns.	430ts	430ts	
Wire Gauge.	1.900mm	1.900mm	
Filars.	-	-	
	-	-	
Ohms @ 20°C.	0.71	0.798	
	-	-	
Copper grams.	2912	3273	
	-	-	
Full-Load Volts.	-	222.4v	
No-Load Volts.	-	230v	
Regulation %.	1.6%	3.3%	
	-	-	
Watts Loss Hot.	17.35	19.39	
	-	-	
Insulation Tape.	-	-	
Width. mm.	-	13	
Thickness. mm.	-	0.05	
Layers.	-	3	
	-	-	
Screening Tape.	-	-	
Width. mm.	-	-	
Thickness. mm.	-	-	
Layers.	-	-	
	-	-	
A/mm^2.	1.59	1.59	
Copper Fill %.	19.16%	19.16%	
<hr/>			
ToroidEZE-AL v.2.6.1			Page 1 of 1.

TI-173630 (1000VA with Cut:Uncut ratio = 0.8:1.0) – Uncut centre core

TOROIDAL TRANSFORMER DESIGN SUMMARY.			
Design No	: TI-173630 (1000VA) - Uncut core	Printed	: 2017-11-03
Customer	:	Designer	: Sameera
Customer P/N	:	Noratel SL	
<b>Notes:</b>			
Design File : TI-173630- un-cut core.tfx			
Core	: 133 x 90 x 90 mm CK-37	Iron Loss	: 9.2 W
Fe Weight	: 5.1 kg	Coil Weight	: 5.66 kg
Induction	: 1.311 T	Load Loss	: 34.69 W
Frequency	: 50 Hz	Sec Loss	: 18.45 W
Excitation	: 110.9 mA	Pri Loss	: 16.24 W
Core/Coil	: 0.9:1 kg	Window Fill	: 83.6 %
Finished Dim's	: 153 x 57 x 116 mm	Tot. Weight	: 10.827 kg
Tot. Power	: 999 VA	Temp. Rise	: 42/50 deg.C
Optimized	: 1:0.36 Wdg+	Wire Fill	: 38.3 %
Windings.	Primary	Sec 1	
	0	0	
Rated Volts rms.	230v	222v	
Rated Amps rms.	4.54A	4.5A	
Duty Cycle %.	-	100%	
VA rms.	-	999	
Conductor.	Cu	Cu	
Turns.	430ts	430ts	
Wire Gauge.	1.900mm	1.900mm	
Filars.	-	-	
Ohms @ 20°C.	0.641	0.74	
Copper grams.	2629	3035	
Full-Load Volts.	-	222.9v	
No-Load Volts.	-	230v	
Regulation %.	1.5%	3.1%	
Watts Loss Hot.	16.24	18.45	
Insulation Tape.	-	-	
Width. mm.	-	13	
Thickness. mm.	-	0.05	
Layers.	-	3	
Screening Tape.	-	-	
Width. mm.	-	-	
Thickness. mm.	-	-	
Layers.	-	-	
A/mm^2.	1.6	1.59	
Copper Fill %.	19.16%	19.16%	
ToroidEZE-AL v.2.6.1			Page 1 of 1.

TI-173630 (1000VA with Cut:Uncut ratio = 0.80:1.0) – Composite core

<u>TOROIDAL TRANSFORMER DESIGN SUMMARY.</u>		
Design No : TI-173630 (1000VA) - Composite core		Printed : 2017-11-03
Customer :		Designer : Sameera
Customer P/N :		Noratel SL
<b>Notes:</b>		
<i>Special!!</i>		
Design File : TI-173630 - Composite.tfx		
<hr/>		
Core : 169 x 90 x 90 mm 27-MOH	Iron Loss : 2.08 W	Finished Dim's : 186 x 57 x 114 mm
Fe Weight : 10.88 kg	Coil Weight : 6.34 kg	Tot. Weight : 17.304 kg
Induction : 0.713 T	Load Loss : 37.65 W	Tot. Power : 999 VA
Frequency : 50 Hz	Sec Loss : 19.87 W	Temp. Rise : 34/41 deg.C
Excitation: 13.5 mA	Pri Loss : 17.78 W	Optimized : 1:0.69 Wdg+
Core/Coil : 1.7:1 kg	Window Fill : 83.6 %	Wire Fill : 38.3 %
<hr/>		
Windings.	Primary	Sec 1
	0	0
Rated Volts rms.	230v	222v
Rated Amps rms.	4.52A	4.5A
Duty Cycle %.	-	100%
	-	-
VA rms.	-	999
Conductor.	Cu	Cu
Turns.	430ts	430ts
Wire Gauge.	1.900mm	1.900mm
Filars.	-	-
	-	-
Ohms @ 20°C.	0.727	0.819
	-	-
Copper grams.	2982	3358
	-	-
Full-Load Volts.	-	222.2v
No-Load Volts.	-	230v
Regulation %.	1.6%	3.4%
	-	-
Watts Loss Hot.	17.78	19.87
	-	-
Insulation Tape.	-	-
Width. mm.	-	13
Thickness. mm.	-	0.05
Layers.	-	3
	-	-
Screening Tape.	-	-
Width. mm.	-	-
Thickness. mm.	-	-
Layers.	-	-
	-	-
A/mm <sup>2</sup> .	1.59	1.59
Copper Fill %.	19.16%	19.16%
<hr/>		
ToroidEZE-AL v.2.6.1		Page 1 of 1.

TI-173618M (2500VA with Cut:Uncut ratio = 0.6:1.0) – Uncut centre core

<u>TOROIDAL TRANSFORMER DESIGN SUMMARY.</u>			
Design No	: TI-173618M (2500VA) - Uncut core	Printed	: 2017-11-03
Customer	:	Designer	: Sameera
Customer P/N	:	Noratel SL	
<b>Notes:</b>			
Design File : 173618M- uncut core.tfx			
<hr/>			
Core	: 180 x 90 x 80 mm CK-37	Iron Loss	: 20.75 W
Fe Weight	: 11.48 kg	Coil Weight	: 6.42 kg
Induction	: 1.311 T	Load Loss	: 140.8 W
Frequency	: 50 Hz	Sec Loss	: 23.11 W
Excitation	: 250.3 mA	Pri Loss	: 117.7 W
Core/Coil	: 1.8:1 kg	Window Fill	: 84.7 %
Finished Dim's	: 197 x 57 x 105 mm	Tot. Weight	: 17.991 kg
Tot. Power	: 2500 VA	Temp. Rise	: 108/130 deg.C
Optimized	: 1:0.71 Wdg+	Wire Fill	: 40.6 %
<hr/>			
Windings.	Primary	Sec 1	
	0	0	
Rated Volts rms.	230v	222v	
Rated Amps rms.	11.57A	11.26A	
Duty Cycle %.	-	100%	
VA rms.	-	2500	
Conductor.	Cu	Cu	
Turns.	231ts	231ts	
Wire Gauge.	1.500mm	2.000mm	
Filars.	-	(x3)	
Ohms @ 20°C.	0.582	0.121	
Copper grams.	930.2	5494	
Full-Load Volts.	-	218.8v	
No-Load Volts.	-	230v	
Regulation %.	4.2%	4.9%	
Watts Loss Hot.	117.7	23.11	
Insulation Tape.	-	-	
Width. mm.	-	13	
Thickness. mm.	-	0.05	
Layers.	-	3	
Screening Tape.	-	-	
Width. mm.	-	-	
Thickness. mm.	-	-	
Layers.	-	-	
A/mm^2.	6.55	1.19	
Copper Fill %.	6.42%	34.22%	
ToroidEZE-AL v.2.6.1			Page 1 of 1.

TI-173618M (2500VA with Cut:Uncut ratio = 0.6:1.0) – Composite core

<u>TOROIDAL TRANSFORMER DESIGN SUMMARY.</u>		
Design No : TI-173618M (2500VA) - Composite core		
Customer :		
Customer P/N :		
		Printed : 2017-11-03
		Designer : Sameera
		Noratel SL
<b>Notes:</b>		
Special!!!- cut core		
Design File : ED-173618M - composite core.tfx		
<hr/>		
Core : 238 x 90 x 80 mm 27-M0H	Iron Loss : 5.33 W	Finished Dim's : 252 x 57 x 103 mm
Fe Weight : 22.94 kg	Coil Weight : 7.71 kg	Tot. Weight : 30.776 kg
Induction : 0.797 T	Load Loss : 165.6 W	Tot. Power : 2500 VA
Frequency : 50 Hz	Sec Loss : 26.5 W	Temp. Rise : 93/112 deg.C
Excitation: 34.3 mA	Pri Loss : 139.1 W	Optimized : 1:1.19 Fe+
Core/Coil : 3:1 kg	Window Fill : 84.7 %	Wire Fill : 40.6 %
<hr/>		
Windings.	Primary	Sec 1
	0	0
Rated Volts rms.	230v	222v
Rated Amps rms.	11.61A	11.26A
Duty Cycle %.	-	100%
	-	-
VA rms.	-	2500
Conductor.	Cu	Cu
Turns.	231ts	231ts
Wire Gauge.	1.500mm	2.000mm
Filars.	-	(x3)
	-	-
Ohms @ 20°C.	0.713	0.144
	-	-
Copper grams.	1139	6569
	-	-
Full-Load Volts.	-	216.9v
No-Load Volts.	-	230v
Regulation %.	4.9%	5.7%
	-	-
Watts Loss Hot.	139.1	26.5
	-	-
Insulation Tape.	-	-
Width. mm.	-	13
Thickness. mm.	-	0.05
Layers.	-	3
	-	-
Screening Tape.	-	-
Width. mm.	-	-
Thickness. mm.	-	-
Layers.	-	-
	-	-
A/mm^2.	6.57	1.19
Copper Fill %.	6.42%	34.22%
<hr/>		
ToroidEZE-AL v.2.6.1		Page 1 of 1.

TI-173618N (3500VA with Cut:Uncut ratio = 0.8:1.0) – Uncut core

<u>TOROIDAL TRANSFORMER DESIGN SUMMARY.</u>		
Design No : TI-173618N (3500VA) - Uncut core	Printed : 2017-11-03	
Customer :	Designer : Sameera	
Customer P/N :	Noratel SL	
<u>Notes:</u>		
Design File : TI-173618N- uncut core.tfx		
Core : 180 x 90 x 80 mm CK-37	Iron Loss : 20.75 W	Finished Dim's : 197 x 57 x 105 mm
Fe Weight : 11.48 kg	Coil Weight : 6.42 kg	Tot. Weight : 17.991 kg
Induction : 1.311 T	Load Loss : 423.6 W	Tot. Power : 3501 VA
Frequency : 50 Hz	Sec Loss : 63.19 W	Temp. Rise : 151/301 deg.C
Excitation: 250.3 mA	Pri Loss : 360.4 W	Optimized : 1:0.71 Wdg+
Core/Coil : 1.8:1 kg	Window Fill : 84.7 %	Wire Fill : 40.6 %
<u>Windings.</u>	<u>Primary</u>	<u>Sec 1</u>
	0	0
Rated Volts rms.	230v	222v
Rated Amps rms.	17.15A	15.77A
Duty Cycle %.	-	100%
	-	-
VA rms.	-	3501
Conductor.	Cu	Cu
Turns.	231ts	231ts
Wire Gauge.	1.500mm	2.000mm
Filars.	-	(x3)
	-	-
Ohms @ 20°C.	0.582	0.121
	-	-
Copper grams.	930.2	5494
	-	-
Full-Load Volts.	-	207.1v
No-Load Volts.	-	230v
Regulation %.	8.6%	10%
	-	-
Watts Loss Hot.	360.4	63.19
	-	-
Insulation Tape.	-	-
Width. mm.	-	13
Thickness. mm.	-	0.05
Layers.	-	3
	-	-
Screening Tape.	-	-
Width. mm.	-	-
Thickness. mm.	-	-
Layers.	-	-
	-	-
A/mm^2.	9.71	1.67
Copper Fill %.	6.42%	34.22%
ToroidEZE-AL v.2.6.1		
Page 1 of 1.		

TI-173618N (3500VA with Cut:Uncut ratio = 0.8:1.0) – Composite core

<u>TOROIDAL TRANSFORMER DESIGN SUMMARY.</u>		
Design No : TI-173618N (3500VA) - Composite core	Printed : 2017-11-03	
Customer :	Designer : Sameera	
Customer P/N :	Noratel SL	
<u>Notes:</u>		
Design File : ED-173618N - Composite core.tfx		
Core : 256 x 90 x 80 mm 27-MOH	Iron Loss : 5.16 W	Finished Dim's : 269 x 57 x 103 mm
Fe Weight : 27.14 kg	Coil Weight : 8.09 kg	Tot. Weight : 35.378 kg
Induction : 0.711 T	Load Loss : 560.3 W	Tot. Power : 3501 VA
Frequency : 50 Hz	Sec Loss : 77.3 W	Temp. Rise : 138/286 deg.C
Excitation: 33.6 mA	Pri Loss : 483 W	Optimized : 1:1.34 Fe+
Core/Coil : 3.4:1 kg	Window Fill : 84.7 %	Wire Fill : 40.6 %
<b>Windings.</b>	<b>Primary</b>	<b>Sec 1</b>
	0	0
Rated Volts rms.	230v	222v
Rated Amps rms.	17.68A	15.77A
Duty Cycle %.	-	100%
	-	-
VA rms.	-	3501
Conductor.	Cu	Cu
Turns.	231ts	231ts
Wire Gauge.	1.500mm	2.000mm
Filars.	-	(x3)
	-	-
Ohms @ 20°C.	0.753	0.152
	-	-
Copper grams.	1204	6891
	-	-
Full-Load Volts.	-	200.5v
No-Load Volts.	-	230v
Regulation %.	11.2%	12.8%
	-	-
Watts Loss Hot.	483	77.3
	-	-
Insulation Tape.	-	-
Width. mm.	-	13
Thickness. mm.	-	0.05
Layers.	-	3
	-	-
Screening Tape.	-	-
Width. mm.	-	-
Thickness. mm.	-	-
Layers.	-	-
	-	-
A/mm^2.	10	1.67
Copper Fill %.	6.42%	34.22%
ToroidEZE-AL v.2.6.1		
Page 1 of 1.		

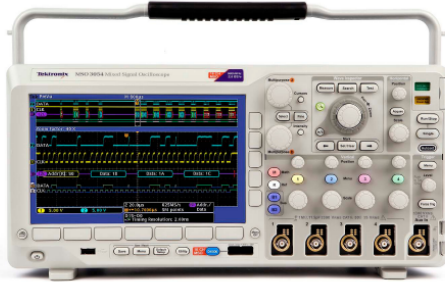


## Appendix C – Test equipment details

### Mixed Signal Oscilloscope (DPO3000)

## Mixed Signal Oscilloscopes

### MSO3000 Series, DPO3000 Series Data Sheet



#### Features & Benefits

##### Key Performance Specifications

- 500, 300, 100 MHz Bandwidth Models
- 2 and 4 Analog Channel Models
- 16 Digital Channels (MSO Series)
- 2.5 GS/s Sample Rate on All Channels
- 5 Megapoint Record Length on All Channels
- >50,000 wfm/s Maximum Waveform Capture Rate
- Suite of Advanced Triggers

##### Ease of Use Features

- Wave Inspector® Controls provide Easy Navigation and Automated Search of Waveform Data
- 29 Automated Measurements, and FFT Analysis for Simplified Waveform Analysis
- TekVPI® Probe Interface Supports Active, Differential, and Current Probes for Automatic Scaling and Units
- 9 in. (229 mm) WVGA Widescreen Color Display
- Small Footprint and Lightweight – Only 5.8 in. (147 mm) deep and 9 lb. (4 kg)

##### Connectivity

- USB 2.0 Host Port on both the Front Panel and Rear Panel for Quick and Easy Data Storage, Printing, and Connecting a USB Keyboard
- USB 2.0 Device Port on Rear Panel for Easy Connection to a PC or Direct Printing to a PictBridge®-compatible Printer
- Integrated 10/100 Ethernet Port for Network Connection and Video Out Port to Export the Oscilloscope Display to a Monitor or Projector

##### Optional Serial Triggering and Analysis

- Automated Serial Triggering, Decode, and Search Options for I<sup>2</sup>C, SPI, CAN, LIN, RS-232/422/485/UART, and I<sup>2</sup>S/L/R/J/TDM

##### Mixed Signal Design and Analysis (MSO Series)

- Automated Triggering, Decode, and Search on Parallel Buses
- Multichannel Setup and Hold Triggering
- MagniVu™ High-speed Acquisition Provides 121.2 ps Fine Timing Resolution on Digital Channels


##### Optional Application Support

- Power Analysis
- HDTV and Custom Video Analysis

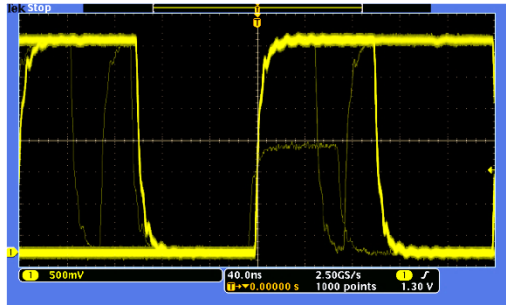
##### Feature-rich Tools for Debugging Mixed Signal Designs

With the MSO/DPO3000 Mixed Signal Oscilloscope Series, you can analyze up to 20 analog and digital signals with a single instrument to quickly find and diagnose problems in complex designs. Bandwidths up to 500 MHz and a minimum of 5X oversampling on all channels ensure you have the performance you need for many of today's mainstream applications. To capture long windows of signal activity while maintaining fine timing resolution, the MSO/DPO3000 offers a deep record length of 5 Mpoints standard on all channels.

With Wave Inspector® controls for rapid waveform navigation, automated serial and parallel bus analysis, and automated power analysis – the MSO/DPO3000 Oscilloscope Series from Tektronix provides the feature-rich tools you need to simplify and speed debug of your complex design.



## Data Sheet



Discover – Fast waveform capture rate - over 50,000 wfms/s - maximizes the probability of capturing elusive glitches and other infrequent events.

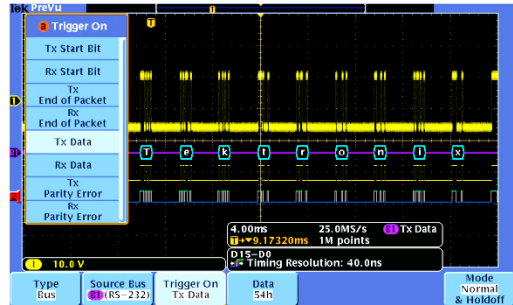
### Comprehensive Features Speed Every Stage of Debug

The MSO/DPO3000 Series offers a robust set of features to speed every stage of debugging your design – from quickly discovering an anomaly and capturing it, to searching your waveform record for the event and analyzing its characteristics and your device's behavior.

#### Discover

To debug a design problem, first you must know it exists. Every design engineer spends time looking for problems in their design, a time-consuming and frustrating task without the right debug tools.

The MSO/DPO3000 Series offers the industry's most complete visualization of signals, providing fast insight into the real operation of your device. A fast waveform capture rate – greater than 50,000 waveforms per second – enables you to see glitches and other infrequent transients within seconds, revealing the true nature of device faults. A digital phosphor display with intensity grading shows the history of a signal's activity by intensifying areas of the signal that occur more frequently, providing a visual display of just how often anomalies occur.



Capture – Triggering on a specific transmit data packet going across an RS-232 bus. A complete set of triggers, including triggers for specific serial packet content, ensures you quickly capture your event of interest.

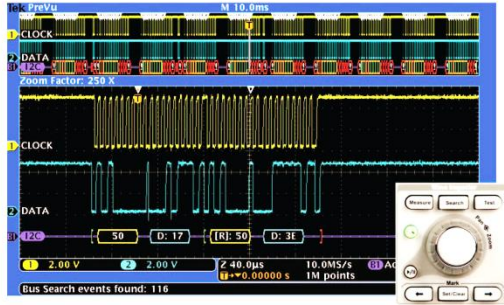
#### Capture

Discovering a device fault is only the first step. Next, you must capture the event of interest to identify root cause.

The MSO/DPO3000 Series provides a complete set of triggers – including runt, logic, pulse width/glitch, setup/hold violation, serial packet, and parallel data – to help quickly find your event. With up to a 5 Mpoint record length, you can capture many events of interest, even thousands of serial packets, in a single acquisition for further analysis while maintaining high resolution to zoom in on fine signal details.

From triggering on specific packet content to automatic decode in multiple data formats, the MSO/DPO3000 Series provides integrated support for the industry's broadest range of serial buses – I<sup>2</sup>C, SPI, CAN, LIN, RS-232/422/485/UART, and I<sup>2</sup>S/LJ/RJ/TDM. The ability to decode up to two serial and/or parallel buses simultaneously means you gain insight into system-level problems quickly.

To further help troubleshoot system-level interactions in complex embedded systems, the MSO3000 Series offers 16 digital channels in addition to its analog channels. Since the digital channels are fully integrated into the oscilloscope, you can trigger across all input channels, automatically time-correlating all analog, digital, and serial signals. The MagniVu™ high-speed acquisition enables you to acquire fine signal detail (up to 121.2 ps resolution) around the trigger point for precision measurements. MagniVu is essential for making accurate timing measurements for setup and hold measurements, clock delay, signal skew, and glitch characterization.

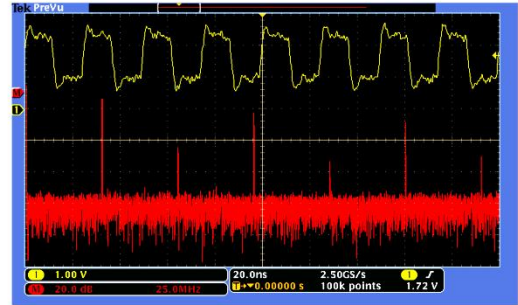


Search – I<sup>2</sup>C decode showing results from a Wave Inspector search for Address value 50. Wave Inspector controls provide unprecedented efficiency in viewing and navigating waveform data.

### Search

Finding your event of interest in a long waveform record can be time consuming without the right search tools. With today's record lengths pushing beyond a million data points, locating your event can mean scrolling through thousands of screens of signal activity.

The MSO/DPO3000 Series offers the industry's most comprehensive search and waveform navigation with its innovative Wave Inspector® controls. These controls speed panning and zooming through your record. With a unique force-feedback system, you can move from one end of your record to the other in just seconds. User marks allow you to mark any location that you may want to reference later for further investigation. Or, automatically search your record for criteria you define. Wave Inspector will instantly search your entire record, including analog, digital, and serial bus data. Along the way it will automatically mark every occurrence of your defined event so you can quickly move between events.



Analyze – FFT analysis of a pulsed signal. A comprehensive set of integrated analysis tools speeds verification of your design's performance.

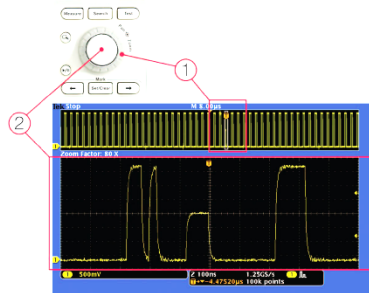
### Analyze

Verifying that your prototype's performance matches simulations and meets the project's design goals requires analyzing its behavior. Tasks can range from simple checks of rise times and pulse widths to sophisticated power loss analysis and investigation of noise sources.

The MSO/DPO3000 Series offers a comprehensive set of integrated analysis tools including waveform- and screen-based cursors, 29 automated measurements, advanced waveform math including arbitrary equation editing, FFT analysis, and trend plots for visually determining how a measurement is changing over time. Specialized application support for serial bus analysis, power supply design, and video design and development is also available.

For extended analysis, National Instrument's LabVIEW SignalExpress™ Tektronix Edition provides over 200 built-in functions including time and frequency domain analysis, limit testing, data logging, and customizable reports.

## Data Sheet



Wave Inspector controls provide unprecedented efficiency in viewing, navigating, and analyzing waveform data. Zip through your 5 Mpoint record by turning the outer pan control (1). Get from the beginning to end in seconds. See something of interest and want to see more details? Just turn the inner zoom control (2).

### Wave Inspector® Navigation and Search

A 5 Mpoint record length represents thousands of screens of information. The MSO/DPO3000 Series enables you to find your event in seconds with Wave Inspector, the industry's best tool for navigation and search.

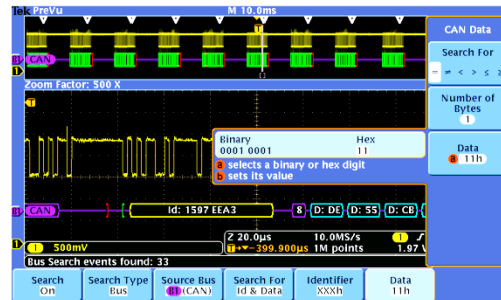
Wave Inspector offers the following innovative controls:

#### Zoom/Pan

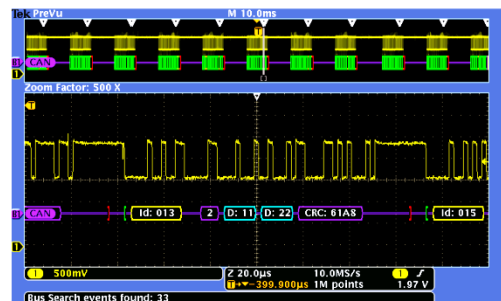
A dedicated, two-tier front-panel control provides intuitive control of both zooming and panning. The inner control adjusts the zoom factor (or zoom scale); turning it clockwise activates zoom and goes to progressively higher zoom factors, while turning it counterclockwise results in lower zoom factors and eventually turning zoom off. No longer do you need to navigate through multiple menus to adjust your zoom view. The outer control pans the zoom box across the waveform to quickly get to the portion of waveform you are interested in. The outer control also utilizes force-feedback to determine how fast to pan on the waveform. The farther you turn the outer control, the faster the zoom box moves. Pan direction is changed by simply turning the control the other way.

#### Play/Pause

A dedicated **Play/Pause** front-panel button scrolls the waveform across the display automatically while you look for anomalies or an event of interest. Playback speed and direction are controlled using the intuitive pan control. Once again, turning the control further makes the waveform scroll faster and changing direction is as simple as turning the control the other way.



Search step 1: You define what you would like to find.



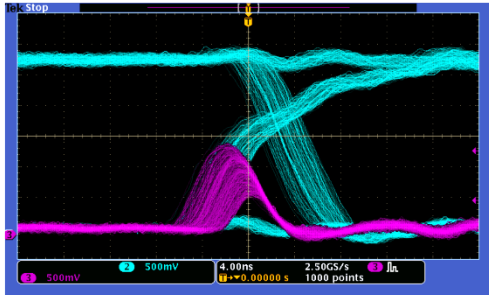
Search step 2: Wave Inspector automatically searches through the record and marks each event with a hollow white triangle. You can then use the **Previous** and **Next** buttons to jump from one event to the next.

#### User Marks

Press the **Set Mark** front-panel button to place one or more marks on the waveform. Navigating between marks is as simple as pressing the **Previous** (←) and **Next** (→) buttons on the front panel.

#### Search Marks

The **Search** button allows you to automatically search through your long acquisition looking for user-defined events. All occurrences of the event are highlighted with search marks and are easily navigated to, using the front-panel **Previous** (←) and **Next** (→) buttons. Search types include edge, pulse width/glitch, runt, logic, setup and hold, rise/fall time parallel bus, and I<sup>2</sup>C, SPI, CAN, LIN, RS-232/422/485/UART, and I<sup>2</sup>S/LJ/RJ/TDM packet content.



Digital phosphor technology enables greater than 50,000 wfms capture rate and real-time intensity grading on the MSO/DPO3000 Series.

### Digital Phosphor Technology

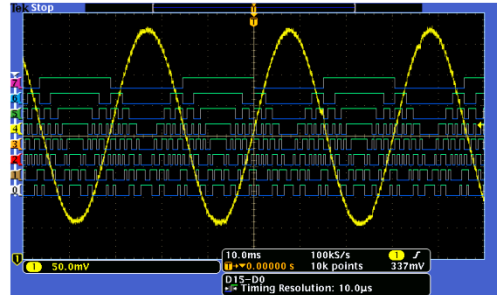
The MSO/DPO3000 Series' digital phosphor technology provides you with fast insight into the real operation of your device. Its fast waveform capture rate – greater than 50,000 wfms/s – gives you a high probability of quickly seeing the infrequent problems common in digital systems: runt pulses, glitches, timing issues, and more.

Waveforms are superimposed with one another and waveform points that occur more frequently are intensified. This quickly highlights the events that over time occur more often or, in the case of infrequent anomalies, occur less often.

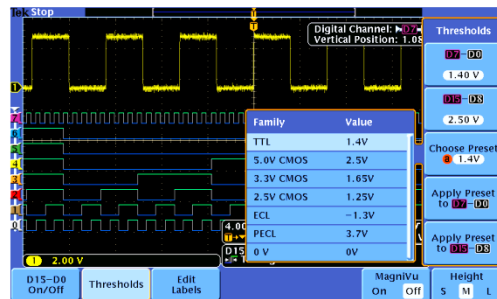
With the MSO/DPO3000 Series, you can choose infinite persistence or variable persistence, determining how long the previous waveform acquisitions stay on-screen. This allows you to determine how often an anomaly is occurring.

### Mixed Signal Design and Analysis (MSO Series)

The MSO3000 Series Mixed Signal Oscilloscopes provide 16 digital channels. These channels are tightly integrated into the oscilloscope's user interface, simplifying operation and making it possible to solve mixed-signal issues easily.



The MSO Series provides 16 integrated digital channels enabling you to view and analyze time-correlated analog and digital signals.



With the color-coded digital waveform display, groups are created by simply placing digital channels together on the screen, allowing the digital channels to be moved as a group. You can set threshold values for each pod of eight channels, enabling support for up to two different logic families.

### Color-coded Digital Waveform Display

The MSO3000 Series has redefined the way you view digital waveforms. One common problem shared by both logic analyzers and mixed-signal oscilloscopes is determining if data is a one or a zero when zoomed in far enough that the digital trace stays flat all the way across the display. The MSO3000 Series has color-coded digital traces, displaying ones in green and zeros in blue.

## Characteristics

### Vertical System Analog Channels

Characteristic	MSO3012 DPO3012	MSO3014 DPO3014	MSO3032 DPO3032	MSO3034 DPO3034	DPO3052	MSO3054 DPO3054
Input Channels	2	4	2	4	2	4
Analog Bandwidth (-3 dB)	100 MHz	100 MHz	300 MHz	300 MHz	500 MHz	500 MHz
Calculated Rise Time 5 mV/div (typical)	3.5 ns	3.5 ns	1.17 ns	1.17 ns	700 ps	700 ps
Hardware Bandwidth Limits	20 MHz		20 MHz, 150 MHz			
Input Coupling	AC, DC, GND					
Input Impedance	1 M $\Omega$ $\pm$ 1%, 75 $\Omega$ $\pm$ 1%, 50 $\Omega$ $\pm$ 1%					
Input Sensitivity Range, 1 M $\Omega$	1 mV/div to 10 V/div					
Input Sensitivity Range, 75 $\Omega$ 50 $\Omega$	1 mV/div to 1 V/div					
Vertical Resolution	8 bits (11 bits with Hi Res)					
Maximum Input Voltage, 1 M $\Omega$	300 V <sub>RMS</sub> with peaks $\leq$ $\pm$ 450 V					
Maximum Input Voltage, 75 $\Omega$ 50 $\Omega$	5 V <sub>RMS</sub> with peaks $\leq$ $\pm$ 20 V					
DC Gain Accuracy	$\pm$ 1.5% for 5 mV/div and above $\pm$ 2.0% for 2 mV/div $\pm$ 2.5% for 1 mV/div					
Channel-to-Channel Isolation (Any Two Channels at Equal Vertical Scale)	$\geq$ 100:1 at $\leq$ 100 MHz and $\geq$ 30:1 at $>$ 100 MHz up to the rated BW					

### Offset Range

Range	1 M $\Omega$	50 $\Omega$ , 75 $\Omega$
1 mV/div to 99.5 mV/div	$\pm$ 1 V	$\pm$ 1 V
100 mV/div to 995 mV/div	$\pm$ 10 V	$\pm$ 5 V
1 V/div	$\pm$ 100 V	$\pm$ 5 V
1.01 V/div to 10 V/div	$\pm$ 100 V	NA

### Vertical System Digital Channels

Characteristic	All MSO3000 Models
Input Channels	16 Digital (D15 to D0)
Thresholds	Threshold per set of 8 channels
Threshold Selections	TTL, CMOS, ECL, PECL, User Defined
User-defined Threshold Range	-15 V to +25 V
Maximum Input Voltage	-20 V to +30 V
Threshold Accuracy	$\pm$ (100 mV +3% of threshold setting)
Maximum Input Dynamic Range	50 V <sub>pp</sub> (threshold setting dependent)
Minimum Voltage Swing	500 mV <sub>pp</sub>
Input Impedance	101 k $\Omega$
Probe Loading	8 pF
Vertical Resolution	1 bit

### Horizontal System Analog Channels

Characteristic	All MSO3000 Models All DPO3000 Models
Maximum Sample Rate (all channels)	2.5 GS/s
Maximum Record Length (all channels)	5 Mpoints
Maximum Duration of Time Captured at Highest Sample Rate (all channels)	2 ms
Time-base Range (s/div)	1 ns to 1000 s
Time-base Delay Time Range	-10 divisions to 5000 s
Channel-to-Channel Deskew Range	$\pm$ 100 ns
Time-base Accuracy	$\pm$ 10 ppm over any $\geq$ 1 ms interval

### Horizontal System Digital Channels

Characteristic	All MSO3000 Models
Maximum Sample Rate (Main, all channels)	500 MS/s (2 ns resolution)
Maximum Record Length (Main, all channels)	5 Mpoints
Maximum Sample Rate (MagniVu, all channels)	8.25 GS/s (121.2 ps resolution)
Maximum Record Length (MagniVu, all channels)	10 kpoints centered on the trigger
Minimum Detectable Pulse Width	2.0 ns
Channel-to-Channel Skew	500 ps typical



## Current Probes

### A621 & A622 Datasheet



- A622
  - AC/DC – 100 kHz
  - 50 mA to 100 A peak
  - For DMMs and oscilloscopes

#### Applications

- Motor drives
- Inverters
- Power supplies
- Avionics

#### A621 2000 Amp AC Current probe/BNC

This industrial-style clamp-on probe has a BNC connector and can be used with a shrouded banana plug adapter <sup>1</sup> so it can be used on digital multimeters, TekMeter, and oscilloscopes. The A621 can measure AC currents from 100 mA to 2000 A peak over a frequency range of 5 Hz to 50 kHz. It provides a 1 mV, 10 mV, or 100 mV output for each Amp measured.

#### A622 100 Amp AC DC Current probe/BNC

This "long nose" style clamp-on probe uses a Hall Effect current sensor to provide a voltage output to oscilloscopes. It has a BNC connector and can be used with a shrouded banana plug adapter <sup>1</sup> so it can also be used on digital multimeters, TekMeter, and oscilloscopes. The A622 can measure AC/DC currents from 50 mA to 100 A peak over a frequency range of DC to 100 kHz. It provides 10 mV or 100 mV output for each Amp measured.

#### DS\_FeaturesBenefitsContainer

The A600 Series current probes are specifically designed to support measurements with the TekMeter® or oscilloscope.

#### Features and benefits

- A621
  - AC – 5 Hz to 50 kHz
  - 100 mA to 2000 A peak
  - For DMMs and oscilloscopes
  - Clamp on

#### Recommended products

TPS2000, TDS1000B, TDS2000C, and TDS3000C Series oscilloscopes and DMM4020<sup>1</sup>, DMM4040<sup>1</sup>, and DMM4050<sup>1</sup> digital multimeters.

<sup>1</sup> For instruments with banana jack inputs, Tektronix part number 012-1450-00 Female BNC to banana lead adapter is required.

## Specifications

All specifications are guaranteed unless noted otherwise. All specifications apply to all models unless noted otherwise.

Characteristic	A621	A622
Frequency range	5 Hz to 50 kHz	DC to 100 kHz
Maximum input current	2000 A peak	100 A peak
Output	1 mV/A, 10 mV/A, 100 mV/A	10 mV/A, 100 mV/A
Maximum conductor diameter	54 mm (2.13 in.)	11.8 mm (0.46 in.)
Termination	BNC <sup>1</sup>	BNC <sup>1</sup>
Maximum bare-wire voltage	600 V (CAT III)	600 V (CAT III)
Safety	UL3111-2-032, CSA1010.2-032, EN61010-2-032, IEC61010-2-032	UL3111-2-032, CSA1010.2-032, EN61010-2-032, IEC61010-2-032

## Ordering information

A621	2000 A AC Current probe/BNC.
A622	100 A AC/DC Current probe/BNC.

## Recommended accessories

012-1450-xx	Adapter, lead; discrete – MLD, 2, 18 AWG, dual insul, BNC, female X 4 mm dual insul; banana jack X dual insul plug, shield banana
-------------	---

## Options

### Service options

Opt. R3	Repair Service 3 Years (including warranty)
Opt. R5	Repair Service 5 Years (including warranty)



Tektronix is registered to ISO 9001 and ISO 14001 by SRI Quality System Registrar.



## Zero crossing detecting circuit (SIEMENS 3RF2050-1AA02)

# SIEMENS

Product data sheet

3RF2050-1AA02



SEMICOND. RELAY 3RF2,  
1-PHASE WIDTH 45 MM,  
50 A 24-230 V / 24 V DC SCREW TERMINAL

### General technical data:

product brand name	SIRIUS	
product designation	solid-state relay	
Product function	zero-point switching	
Number of poles / for main current circuit	1	
Protection class IP	IP20	
Ambient temperature		
• during operating	°C	-25 ... +60
• during storage	°C	-55 ... +80
Installation altitude / at a height over sea level / maximum	m	1,000
Resistance against vibration / according to IEC 60068-2-6	2g	
Resistance against shock / according to IEC 60068-2-27	15g / 11 ms	
Item designation		
• according to DIN 40719 extendable after IEC 204-2 / according to IEC 750	K	
• according to DIN EN 61346-2	Q	
Number of NC contacts / for auxiliary contacts	0	
Number of NO contacts / for auxiliary contacts	0	
Number of change-over switches / for auxiliary contacts	0	

### Main circuit:

3RF2050-1AA02  
Page 1/5

03/06/2013

subject to modifications  
© Copyright Siemens AG 2013

<b>Number of NO contacts / for main contacts</b>		1
<b>Number of NC contacts / for main contacts</b>		0
<b>Operating current</b>		
• at AC-1 / at 400 V / rated value	A	50
• at AC-51 / rated value	A	50
<b>Operating current / minimum</b>	mA	500
<b>Operating voltage</b>		
• at 50 Hz / at AC / rated value	V	24 ... 230
• at 60 Hz / at AC / rated value	V	24 ... 230
<b>Working area related to the operating voltage</b>		
• at 50 Hz / for AC	V	20 ... 253
• at 60 Hz / for AC	V	20 ... 253
<b>Operating frequency</b>		
• rated value	Hz	50 ... 60
<b>Relative symmetrical tolerance / of the operation frequency</b>	%	10
<b>Insulation voltage / rated value</b>	V	600
<b>Voltage slew rate / at the thyristor / for main contacts / maximum permissible</b>	V/ $\mu$ s	1,000
<b>Block voltage / at the thyristor / for main contacts / maximum permissible</b>	V	800
<b>Reverse current / of the thyristor</b>	mA	10
<b>Derating temperature</b>	$^{\circ}$ C	40
<b>Active power loss / total / typical</b>	W	66
<b>Resistance against the impulse current / rated value</b>	A	600
<b>I<sup>2</sup>t-level / maximum</b>	A <sup>2</sup> ·s	1,800

#### Control circuit:






<b>Type of voltage / of the controlled supply voltage</b>		DC
<b>Control supply voltage / 1</b>		
• for DC		
• initial rated value	V	15
• final rated value	V	24
<b>Control supply voltage</b>		
• for DC / final value for signal<0>-recognition	V	5
<b>Relative symmetrical tolerance / of the supply voltage frequency</b>	%	10
<b>Control current</b>		
• at minimum control supply voltage / for DC	mA	2
• for DC / rated value	mA	15
<b>Fuse assignments</b>	<a href="https://www.automation.siemens.com/cc-static/material/info/3RF20_eng.pdf">https://www.automation.siemens.com/cc-static/material/info/3RF20_eng.pdf</a>	

Installation/mounting/dimensions:		
Type of mounting		screw fixing
Type of fixing/fixation / series installation		Yes
Design of the thread / of the screw for fastening of the operating resource		M4
Tightening torque / of the screw for fastening of the operating resource	N·m	1.5
Width	mm	45
Height	mm	58
Depth	mm	48

Connections:		
Design of the electrical connection / for main current circuit		screw-type terminals
Design of the thread / of the connection screw / for main contacts		M4
Tightening torque / for main contacts / with screw-type terminals		
• minimum	N·m	2
• maximum	N·m	2.5
Tightening torque (lbf·in) / for main contacts / with screw-type terminals		
• minimum	lbf·in	7
• maximum	lbf·in	10.3
Type of the connectable conductor cross-section		
• for main contacts		
• solid		2x (1.5 ... 2.5 mm <sup>2</sup> ), 2x (2.5 ... 6 mm <sup>2</sup> )
• finely stranded		
• with conductor end processing		2x (1 ... 2.5 mm <sup>2</sup> ), 2x (2.5 ... 6 mm <sup>2</sup> ), 1x 10 mm <sup>2</sup>
• for AWG conductors		
• for main contacts		2x (14 ... 10)
• for auxiliary and control contacts		1x (AWG 20 ... 12)
• for auxiliary and control contacts		
• solid		1x (0.5 ... 2.5 mm <sup>2</sup> ), 2x (0.5 ... 1.0 mm <sup>2</sup> )
• finely stranded		
• with conductor end processing		1x (0.5 ... 2.5 mm <sup>2</sup> ), 2x (0.5 ... 1.0 mm <sup>2</sup> )
• without conductor final cutting		1x (0.5 ... 2.5 mm <sup>2</sup> ), 2x (0.5 ... 1.0 mm <sup>2</sup> )
Conductor cross section that can be connected		
• for main contacts		
• solid	mm <sup>2</sup>	1.5 ... 6
• stranded wire		
• with conductor end processing	mm <sup>2</sup>	1 ... 10
• for auxiliary and control contacts		

• solid	mm <sup>2</sup>	0.5 ... 2.5
• stranded wire		
• with conductor end processing /	mm <sup>2</sup>	0.5 ... 2.5
• without conductor final cutting	mm <sup>2</sup>	0.5 ... 2.5
<b>AWG number / as coded connectable conductor cross-section / for main contacts</b>		14 ... 10
<b>Design of the electrical connection / for auxiliary and control current circuit</b>		screw-type terminals
<b>Design of the thread / of the connection screw / of the auxiliary and control pins</b>		M3
<b>AWG number / as coded connectable conductor cross-section</b>		
• for auxiliary and control contacts		20 ... 12
<b>Skinning length / of the cable / for main contacts</b>	mm	10
<b>Skinning length / of the cable / for auxiliary and control contacts</b>	mm	7
<b>Tightening torque / for auxiliary and control contacts</b>		
• with screw-type terminals	N·m	0.5 ... 0.6
<b>Tightening torque (lbf-in) / for auxiliary and control contacts</b>		
• with screw-type terminals	lbf-in	4.5 ... 5.3

#### Certificates/approvals:

General Product Approval	EMC	Declaration of Conformity	Test Certificates
 CSA	 GOST	 UR	 C-TICK
		 EG-Konf.	<a href="#">Type Test Certificates/Test Report</a>

#### other

[Environmental Confirmations](#)

#### Further information:

**Information- and Downloadcenter (Catalogs, Brochures,...)**

<http://www.siemens.com/industrial-controls/catalogs>

**Industry Mall (Online ordering system)**

<http://www.siemens.com/industrial-controls/mall>

**CAX-Online-Generator**

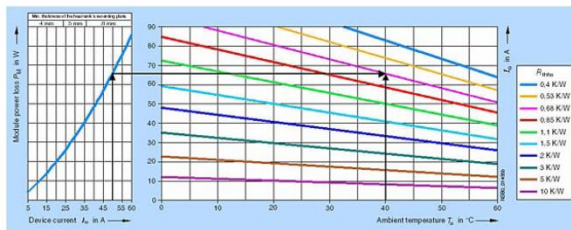
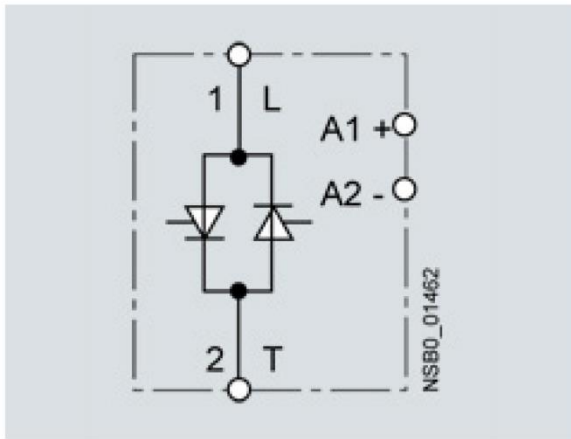
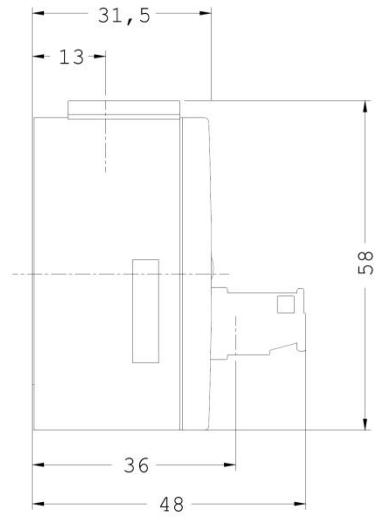
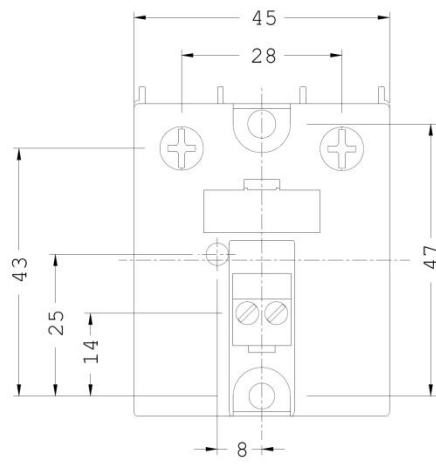
<http://www.siemens.com/cax>

**Service&Support (Manuals, Certificates, Characteristics, FAQs,...)**

<http://support.automation.siemens.com/WW/view/en/3RF2050-1AA02/all>

**Image database (product images, 2D dimension drawings, 3D models, device circuit diagrams, ...)**

[http://www.automation.siemens.com/bilddb/cax\\_en.aspx?mifb=3RF2050-1AA02](http://www.automation.siemens.com/bilddb/cax_en.aspx?mifb=3RF2050-1AA02)



last change:

Mar 4, 2013

# Sound level measuring meter (Extech SL130G)

## Sound Level Alert with Alarm

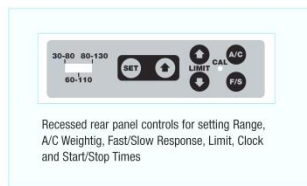
**Built-in LEDs alert user when sound level is too high or too low**  
LEDs can be read from 30m (100ft)

### Features:

- Ideal for industrial, hospital, auditoriums, schools and other areas where there is a need for being alerted when sound level reaches set point
- Meets ANSI Type 2 and EN 60651 accuracy specs compliant to OSHA
- User settable high or low limit (30 to 130dB) indication with output to drive external relay module
- Microphone rotates 180° for desired placement. Optional 5m (15ft) microphone extension cable for remote monitoring
- Complete with 100-240V AC 50/60Hz adaptor, microphone windscreen, and built-in wall, desk and tripod mount (optional Tripod TR100)

### Applications:

- Industrial, Hospitals, Classrooms, and special quiet zones – When the sound level exceeds the HI set point the RED LEDs flash and can be seen from 30m 100ft.
- Speakers/Educators/Instructors, Auditoriums and Theaters – The user can set the SL130 so the RED LEDs flash when the sound level is below the LO set point where people in the audience may not be able to hear. When the sound level is above the LO set point, the GREEN LEDs indicate the sound level is acceptable. The user can reverse the Red and Green LEDs activation per user color preference.



Specifications	
Display	4.6 x 3.125" multifunction LCD
Frequency bandwidth	31.5 Hz to 8 kHz
Microphone	0.5" Electret Condenser Microphone (removable)
Measurement ranges	30 to 80dB, 60 to 110dB, 80 to 130dB
Frequency weighting	'A' and 'C' (Programmable)
Response time	Fast (125ms) / Slow (1s) (Programmable)
Resolution	0.1dB
Alarm output	3.5mm Mono Phone Plug, Maximum: 3.4mA @ 5 VDC
Minimum Output	Voltage: 2.5 VDC
Power	AC/DC Adaptor for full functions; 8xAA batteries for monitoring function only without LED alert
CE/Warranty	CE approved/ 1 year warranty
Dimensions / Weight	8.75 x 7.1 x 1.25" / 0.63 lbs. (22 x 18 x 3.2mm / 285g)

### Ordering Information:

- SL130G ..... Sound Level LED Alert
- SL130G-NIST ..... SL130G with Calibration Traceable to NIST.
- SL125 ..... Remote Microphone Cable 15'
- TR100 ..... Tripod (for meters with Tripod mount feature)
- 407766 ..... Sound Level Calibrator, 94/114dB



YOKOGAWA 

**ENERGY SAVING TOOLS**  
**Digital Sampling Power Meters**  
**with Superior Cost Performance**

Digital Power Meters

# WT 210/WT 230



- Basic power accuracy: 0.1%
- DC measurement, 0.5 Hz to 100 kHz power frequency range
- Compact design (half-rack size)
- 5 mA range for very low current measurements (model WT210 only)
- Line filter function
- High-speed data update (as fast as 10 readings per second)
- Harmonic measurement function available
- User calibration capability

Maximum input with assured accuracy

# 26A

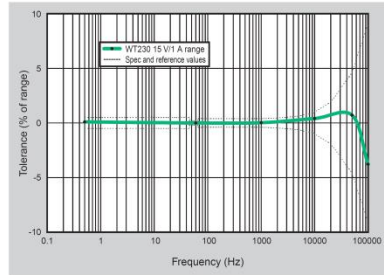
Maximum Display: 28 A

[www.yokogawa.com/tm/](http://www.yokogawa.com/tm/)  
... and subscribe to "Newswave,"  
our free e-mail newsletter

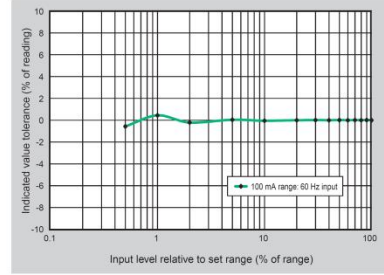
Bulletin 7604-00E

# Basic Characteristics

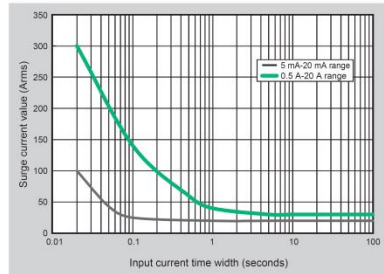
Example of Frequency-power Accuracy Characteristics



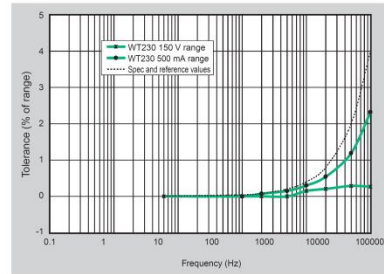
Example of WT210 Current Accuracy



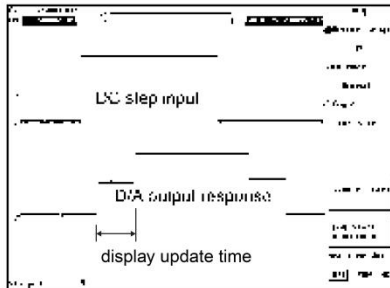
Current Input Surge Withstanding Ability



Example of Influence of Common Mode Voltage



Example of D/A Output Response



Comparison with Former Models

	WT200/WT130	WT210/WT230
Voltage input terminal	Bending post	Plug-in terminal (safety terminal)
External output terminal	Plug-in terminal (safety terminal)	BNC
Voltage and current basic accuracy	0.25% of mg	0.2% of mg
Power basic accuracy	0.3% of mg (WT200) 0.25% of mg (WT130)	0.2% of mg
Frequency range	DC, 10 Hz to 20 kHz	DC, 0.5 Hz to 100 kHz
Assured accuracy range	10% to 130% of range rating	1% to 130% of range rating
Display updating interval	0.25 second (fixed)	0.1/0.25/0.5/1/2/5 seconds
V, A, W display digits	4 digits (WT130) 5 digits (WT200)	5 digits
Line filter function	No	Yes (f <sub>c</sub> = 500 Hz)
Frequency filter function	Yes (f <sub>c</sub> = 300 Hz)	Yes (f <sub>c</sub> = 500 Hz)
Key lock	No	Yes
Harmonic measurement display updating interval	Approximately 3 seconds	0.25/0.5/1/2/5 seconds
Remote signals when comparator is installed	EXT HOLD and EXT TRIG are added. EXT START, EXT STOP, EXT RESET, and INTEG BUSY are not added.	All six signals listed to the left are added. Pin assign is changed.
Online data format	ASCII	ASCII, binary
Wireless data communications output	No	Yes (need HRM)
Addressable mode B for GPRS communications	Yes	No
Display digits (factory default)	4 digits	5 digits
Online output data digits (factory default)	4 digits	5 digits

Functions Included with the WT200 (but Not Included with the WT130) and Included with the WT210/WT230

- MAX hold function
- Moving decimal point display based on integrated power value
- 10,000-hour maximum integration time
- Integration with few data omissions
- Average active power display



WT230



WT210



# Specifications

The latest product information is available at our web site <http://www.yokogawa.com/tm/>. Review the specifications to determine which model is right for you.

Input Specifications		
Parameter	Voltage	Current
Input type	Resistance voltage divider	Floating input Shunt input system
Rated values (ranges)	15/30/60/150/300/600 V	Direct input: 5/10/20/50/100/200 mA (WT210 only) <sup>1</sup> : 0.5/1/2/5/10/20 A (WT210/WT230) External input (optional): 2.5/5/10 V or 50/100/200 mV
Measuring instrument loss (input resistance)	Input resistance: Approximately 2 M $\Omega$ Input capacitance: Approximately 13 pF	Direct input: Approximately 500 m $\Omega$ + approximately 0.1 $\mu$ H (5-20 mA; WT210) Approximately 6 m $\Omega$ + 10 m $\Omega$ (max) <sup>2</sup> + approximately 0.1 $\mu$ H (0.5-20 A; WT230) External input: Approximately 100 k $\Omega$ (2.5/5/10 V), approximately 20 k $\Omega$ (50/100/200 mV)
Maximum instantaneous allowed input (1 cycle, 20 ms duration)	Peak voltage of 2.8 kV or rms value of 2.0 kV (whichever is less)	0.5-20 A (WT210/WT230): Peak current of 450 A or rms value of 300 A (whichever is less) 5-200 mA (WT210): Peak current of 150 A or rms value of 100 A (whichever is less) External input: Peak value of 10 times range or less
Maximum instantaneous allowed input (1 second duration)	Peak voltage of 2.0 kV or rms value of 1.5 kV (whichever is less)	0.5-20 A (WT210/WT230): Peak current of 150 A or rms value of 40 A (whichever is less) 5-200 mA (WT210): Peak current of 30 A or rms value of 20 A (whichever is less) External input: Peak value of 10 times range or less
Maximum continuous allowed input	Peak voltage of 1.5 kV or rms value of 1.0 kV (whichever is less)	0.5-20 A (WT210/WT230): Peak current of 100 A or rms value of 30 A (whichever is less) 5-200 mA (WT210): Peak current of 30 A or rms value of 20 A (whichever is less) External input: Peak value of 5 times range or less
Maximum continuous common mode voltage (with 50/60 Hz input)	600 Vrms (with output connector protective cover), CAT II / 400 Vrms (without output connector protective cover) CAT II	
CMRR 600 Vrms across input terminal and case	50/60 Hz, -80 dB or higher ( $\pm 0.01\%$ of range or less) with voltage input terminals shorted and current input terminals open and external input terminals shorted Reference value (up to 100 kHz): $\pm[(\text{Maximum range rating})/(\text{Range rating}) \times 0.001 \times \%$ of range] or less (voltage range and 0.5-20 A current range and external input range) $\pm[(\text{Maximum range rating})/(\text{Range rating}) \times 0.0002 \times \%$ of range] or less (WT210: 5-200 mA range) Note: 0.01% or higher, f is in kHz. 3 Decouple the above-formula about the external input range.	
Input terminal type	Plug-in terminal (safety terminal)	Direct input: Large binding post External input: BNC connector (insulation type)
A/D converter	Simultaneous conversion of voltage and current inputs Resolution: 16 bits Maximum conversion speed: Approximately 20 $\mu$ s (approximately 51 kHz)	
Range switching	Ranges can be set manually, automatically, or through online controls. Auto-range function Range raising: When a measurement exceeds 130% of the rating, or when the peak value exceeds approximately 300% of the rating Range lowering: When a measurement falls to 30% or less of the rating, and the peak value falls to approximately 300% or less of the rating for the low range	
Measurement mode switching	Any of the following, selected manually or through online controls: RMS (true rms value measurements for both voltage and current), V MEAN (calibration of average-value-rectified rms value for voltage; true rms value measurement for current), DC (simple averages for both voltage and current)	

Note: Current direct input and external sensor input cannot both be used at the same time. When you operate current input terminals and external input terminals, please be careful.  
Since these terminals are electrically connected inside the instrument.  
1. Connect wires that match the size of the measurement current.  
2. Factory setting

Measurement Functions		
Parameter	Voltage/current	Active power
System	Digital sampling, sum of averages method	
Frequency range	DC, and 0.5 Hz to 100 kHz	
Crest factor	3 (with rated input) 300 (with minimum effective input)	
Accuracy (three months after calibration) (Conditions) Temperature: 23 $\pm$ 5 $^{\circ}$ C Humidity: 30-75% RH Input waveform: Sine wave Power factor: $\cos\phi = 1$ In-phase voltage: 0 V DC Frequency filter: ON at 200 Hz or less Scaling: OFF Display digits: 5 digits After CAL is executed	DC: $\pm(0.2\%$ or rdg + 0.2% of rng) <sup>*</sup> 0.5 Hz $\leq f < 45$ Hz: $\pm(0.1\%$ of rdg + 0.2% of rng) 45 Hz $\leq f \leq 66$ Hz: $\pm(0.1\%$ of rdg + 0.1% of rng) 66 Hz $< f \leq 1$ kHz: $\pm(0.1\%$ of rdg + 0.2% of rng) 1 kHz $< f \leq 10$ kHz: $\pm[(0.07 \times f)\%$ of rdg + 0.3% of rng]	DC: $\pm(0.3\%$ or rdg + 0.2% of rng) <sup>*</sup> 0.5 Hz $\leq f < 45$ Hz: $\pm(0.3\%$ of rdg + 0.2% of rng) 45 Hz $\leq f \leq 66$ Hz: $\pm(0.1\%$ of rdg + 0.1% of rng) 66 Hz $< f \leq 1$ kHz: $\pm(0.2\%$ of rdg + 0.2% of rng) 1 kHz $< f \leq 10$ kHz: $\pm(0.1\%$ of rdg + 0.3% of rng) 10 kHz $< f \leq 100$ kHz: $\pm(0.067 \times (f-1))\%$ of rdg 10 kHz $< f \leq 100$ kHz: $\pm(0.5\%$ of rdg + 0.5% of rng) $\pm[(0.09 \times (f-10))\%$ of rdg]
Note: In the accuracy calculation formula, f is in kHz.	<sup>*</sup> Add $\pm 10 \mu$ A to the current DC accuracy.	
Power factor effect	For $\cos\phi = 0$ 45 Hz $\leq f \leq 66$ Hz: $\pm 0.2\%$ of VA (VA is a reading value of apparent power) Reference data (up to 100 kHz): $\pm[(0.2 + 0.2 \times f)\%$ of VA) Indicated value tolerance for $0 < \cos\phi < 1$ Add (rate $\times$ effect when $\cos\phi = 0$ )% of power reading to the above power accuracy. Note: $\phi$ is the phase angle between voltage and current.	
Note: In the accuracy calculation formula, f is in kHz.		
Effective input range	1-130% of voltage/current range rating (for accuracy at 110-130%, add the reading tolerance $\times 0.5$ to the above accuracy)	
Accuracy (12 months after calibration)	Add the accuracy's reading tolerance (three months after calibration) $\times 0.5$ to the accuracy three months after calibration.	
Line filter function	A low-pass filter can be inserted in the input circuit for measurement. The cutoff frequency (fc) is 500 Hz.	
Accuracy with line filter on	Voltage and current: Add 0.2% of rdg at 45-66 Hz. Add 0.5% of rdg below 45 Hz. Power: Add 0.3% of rdg at 45-66 Hz. Add 1% of rdg below 45 Hz.	
Temperature coefficient	$\pm 0.03\%$ of range/ $^{\circ}$ C at 5-18 $^{\circ}$ C and 28-40 $^{\circ}$ C.	
Display updating intervals	0.1/0.25/0.5/1/2/5 seconds	
Lead/lag detecting	Lead/lag is detected correctly when phase difference equal to or greater than $\pm 5^{\circ}$ with both voltage and current inputs as sine waves equal to or greater than 50% of rated range-value, and the frequency is between 20 Hz to 2 kHz.	
Measurement lower limit frequency	Data updating rate: 0.1 second, 0.25 second, 0.5 second, 1 second, 2 seconds, 5 seconds Measurement lower limit frequency: 25 Hz, 10 Hz, 5 Hz, 2.5 Hz, 1.5 Hz, 0.5 Hz	

## Frequency Measurements

Measurement inputs: V1, V2, V3, A1, A2, or A3 (select one)  
Measurement system: Reciprocal system

Measurement frequency ranges  
100 ms: 25 Hz  $\leq f \leq 100$  kHz  
250 ms: 10 Hz  $\leq f \leq 100$  kHz  
500 ms: 5 Hz  $\leq f \leq 100$  kHz  
1 sec: 2.5 Hz  $\leq f \leq 100$  kHz  
2.5 sec: 1.5 Hz  $\leq f \leq 50$  kHz  
5 sec: 0.5 Hz  $\leq f \leq 20$  kHz

Accuracy:  $\pm(0.06\%$  of rdg)  
Conditions: Input equal to at least 30% of voltage/current rated range.  
Frequency filter function ON at 200 Hz and below.  
Frequency filter cutoff frequency: 500 Hz

## Communication Functions (Optional for the WT210)

GP-IB or serial interface (RS-232-C) (select one)

GP-IB  
Electrical and mechanical specifications:  
Conform to IEEE Standard 488-1978 (JIS C1901-1987).

Functional specifications:  
SH1, AH1, T5, L4, SR1, RL1, PR0, DC1, DT1, C0  
Protocol: Conforms to IEEE Standard 488.2-1992.  
Code used: ISO (ASCII) code  
Addresses: 0-30 talker/listener addresses can be set.

Serial interface (RS-232-C)  
Transmission mode: Asynchronous  
Baud rates: 1200, 2400, 4800, 9600 bps

# Specifications

## Calculation Functions

	Single-phase 3-wire (2 voltages, 2 currents)	Three-phase 3-wire (3 voltages, 3 currents)	Three-phase 3-wire (3 voltages, 3 currents)	Three-phase 4-wire
Voltage $\Sigma V$	$(V1 + V2)/2$	$(V1 + V2 + V3)/3$	$(V1 + V2 + V3)/3$	
Current $\Sigma A$	$(A1 + A2)/2$	$(A1 + A2 + A3)/3$	$(A1 + A2 + A3)/3$	
Active power $\Sigma W$	$W1 + W2$	$W1 + W2 + W3$	$W1 + W2 + W3$	
Reactive power var, $\Sigma var$	$var1 = \sqrt{(VA^2 - W^2)}$	$var1 + var2 + var3$	$var1 + var2 + var3$	
Apparent power VA, $\Sigma VA$	$VA = W/V$	$\sqrt{VA1^2 + VA2^2}$	$\sqrt{VA1^2 + VA2^2 + VA3^2}$	$VA1 + VA2 + VA3$
Power factor PF, $\Sigma PF$	$PF = W/VA$	$\Sigma W/\Sigma VA$		
Phase angle deg, $\Sigma deg$	$deg = \cos^{-1}(W/VA)$	$\cos^{-1}(\Sigma W/\Sigma VA)$		

- Notes**
- This equipment's apparent power (VA), reactive power (var), power factor (PF), and phase angle (deg) are calculated from voltage, current, and active power. (Therefore, if the input contains a distorted wave, the values may not match those of other measuring instruments based on different measurement principles.)
  - If either voltage or current falls to 0.5% of the range rating or less, then the apparent power (VA) and reactive power (var) are displayed as zero, and errors are displayed for power factor (PF) and phase angle (deg).
  - The sign of the var of each phase is displayed with + (positive). In the  $\Sigma var$  calculation, the var value for each phase is calculated with a negative sign if the current input leads the voltage input, and with a positive sign if the current input lags the voltage input. Then the value of  $\Sigma var$  may be displayed with - (negative).
  - Apparent power (VA) and reactive power (var) cannot be calculated and displayed at the harmonics measurement mode.

## Display Functions

Display unit: 7-segment LED (light-emitting diode)

Display areas: 3

Display area	Displayed information
A	V, A, W, VA, var (for each element), integration elapsed time
B	V, A, W, PF, deg (for each element, percentage (content percentage, THD))
C	V, A, W, V/AHz, Vpk, Apk, $\pm Wh$ , $\pm Ah$ (for each element), MATH

Measurement parameters	Maximum display	Display resolution
V, A, W, VA, var	99999	0.001%
PF	$\pm 1.0000$	0.01%
deg	$\pm 180.0$	0.1°
$\pm Wh$ , $\pm Ah$	999999	0.0001%
VHz, AHz	99999	Input frequency/20,000

Display digits: 4 or 5 digits (selectable by user).  
Factory default setting is 5 digits.

- Units:** m, k, M, V, A, W, VA, var, Hz, ht, deg, %
- Display updating intervals:** 0, 1/10, 25/10, 5/1/2/5 seconds
- Response time:** Maximum 2 times the display updating interval (time required for display value to enter accuracy range of final value with line filter off, when range rating abruptly changes from 0% to 100%, and from 100% to 0%)
- Maximum display:** 140% of voltage/current range rating
- Minimum display:** About  $V_{rms}$ ,  $A_{rms}$ , and  $Ah$ , 0.5% of range rating. Less than 0.5% is zero suppression.
- Display scaling function:** Effective digits: Selected automatically according to the digits in the voltage and current ranges.
- Setting range:** 0.001 to 9999
- Averaging function:** There are two averaging methods (selectable by user): Exponential average, Moving average
- In cases where response can be set and exponential average is used, the attenuation constant can be selected. In cases where a moving average is used, the number of averages N can be selected from 8, 16, 32, and 64.
- Auto-range monitor:** An LED turns on when the input value is outside the range set for the auto-range.
- MAX hold function:** This function can be used to hold V, A, W, VA, var, Vpk, and Apk at maximum values.
- MATH functions:** System: When a function key on DISPLAY C is pressed to select the MATH functions, it is possible to perform efficiency (WT230 only) and input crest factor measurements, as well as arithmetic calculations on DISPLAY A and B measurements. In addition, it is possible to display average active power for time-converted integrated power.

## Integration Functions

- Display resolution:** The minimum display resolution changes together with the integrated value.
- Maximum display:** -99999 to 999999 MWh/MAh
- Modes:** Standard integration mode (timer mode), continuous integration mode (repeat mode), manual integration mode
- Automatic integration start/stop based on timer setting.**
- Timer:** Setting range: 0:00 min:00 sec to 10000 h:00 min:00 sec (If the time is set to zero, manual mode is automatically set.)
- Count over flow:** When the integrated value exceeds 999999 MWh/MAh or falls to at least -99999 MWh/MAh, the elapsed time is saved and the operation is stopped.
- Accuracy:**  $\pm$ (display accuracy + 0.1% of rdg)
- Timer accuracy:**  $\pm 0.02\%$
- Remote control:** Starting, stopping, and resetting can be controlled through external control signals. This function is only available when option /DA4, /DA12 or /CMP is installed.

## Internal Memory Functions

### Measurement data

Stored data	Normal measurement	Harmonic measurement
WT210 (760401)	Data for 600 samples	Data for 30 samples
WT230 (760502)	Data for 300 samples	Data for 30 samples
WT230 (760503)	Data for 200 samples	Data for 30 samples

**Store interval:** Display updating interval and 1 second to 99 hours, 59 minutes, and 59 seconds

**Recall interval:** Display updating interval and 1 second to 99 hours, 59 minutes, and 59 seconds  
(Both can be set in 1-second increments.)

**Panel setting information:** Four different patterns of panel setting information can be written/read.

### Harmonic Measurement Function (optional)

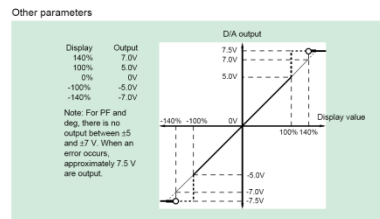
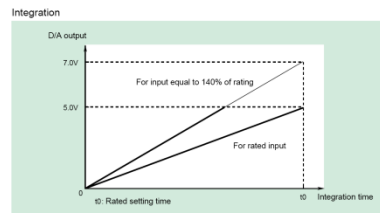
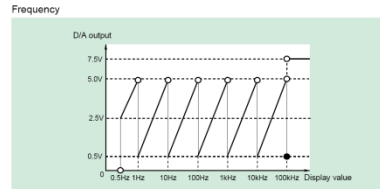
- System:** PLL synchronization
- Measurement frequency range:** Fundamental frequency in range of 40-440 Hz
- Maximum display:** 99999
- Display digits:** 4 or 5 digits (selectable by user).  
Factory default setting is 5 digits.
- Measurement parameters:** V, A, W, deg (WT210), V1, V2, V3, A1, A2, A3, W1, W2, W3, deg1, deg2, deg3 (WT230), individual harmonic levels, rms voltage, rms current, active power, fundamental frequency PF, harmonic distortion rate, individual harmonic content
- Measurement element:** These parameters can only be measured simultaneously for a single specified input element.

- Sampling speed, window width, and analysis orders**  
The values for these parameters vary according to the input fundamental frequency as shown below:
- | Fundamental frequency    | Sampling speed    | Window width    | Analysis orders |
|--------------------------|-------------------|-----------------|-----------------|
| $40 \leq f < 70$ Hz      | $f \times 512$ Hz | 2 periods of f  | 50              |
| $70 \leq f < 130$ Hz     | $f \times 256$ Hz | 4 periods of f  | 50              |
| $130 \leq f < 250$ Hz    | $f \times 128$ Hz | 8 periods of f  | 50              |
| $250 \leq f \leq 440$ Hz | $f \times 64$ Hz  | 16 periods of f | 30              |

- FFT data length:** 1024
- FFT processed word length:** 32 bits
- Window function:** Rectangular
- Display updating interval:** 0.25/0.5/1/2/5 seconds Updating is slower during online output according to the communication speed and the number of parameters transferred.
- Accuracy:** Add  $\pm 0.2\%$  of range to normal measurement accuracy.  
Note: For nth-order component input, add ((nth order reading)  $\times$  (10/(n+1)))% to the n+1th order and n-mth order.

## D/A Output (optional)

- Output voltage:**  $\pm 5$  V FS (maximum approximately  $\pm 7.5$  V) for each rated value
- Number of outputs:** 12 parameters with /DA12 option; 4 parameters with /DA4 option
- Output data selection:** Can be set separately for each channel.
- Accuracy:**  $\pm$ (equipment accuracy + 0.2% of FS)
- D/A converter:** 12-bit resolution
- Response time:** Maximum 2 times the display updating interval
- Updating interval:** Same as the equipment's display updating interval
- Temperature coefficient:**  $\pm 0.05\%$  C of FS
- Output type**



### External Input (Optional)

Select either /EX1 or /EX2 for the voltage output-type current sensor.  
 /EX1: 2.5/5/10 V  
 /EX2: 50/100/200 mV  
 Specifications: See the section on input specifications.

### Comparator Output (Optional)

Output method: Normal-open and normal-close relay contact output (pair)  
 Number of output parameters and settings: Four parameters; can be set separately on each output channel.  
 Contact capacitance: 24 V/0.5 A  
 D/A output (4-channel); See section on D/A output (optional)

### External Control Signal (with D/A or /CMP Option Only)

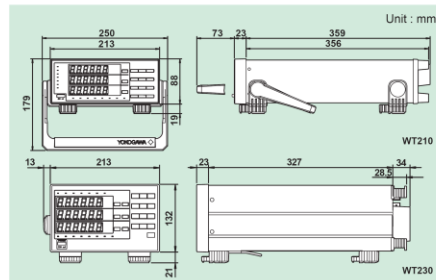
External control signals: EXT-HOLD, EXT-TRIG, EXT-START, EXT-STOP, EXT-RESET, INTEG-BUSY  
 Input: TTL level negative pulse

### General Specifications

Warmup time: Approximately 30 minutes  
 Operating temperature and humidity ranges: 5-40 °C, 20-80% RH (no condensation)  
 Storage temperature: -25-60 °C (no condensation)  
 Maximum operating elevation: 2000 meters  
 Insulating resistance: 50 MΩ or higher at 500 V DC across all of the following areas:  
 Voltage input terminals (ganged) and case  
 Current input terminals (ganged) and case  
 Voltage input terminals (ganged) and current input terminals (ganged)  
 Voltage input terminals (ganged) of each element  
 Current input terminals (ganged) of each element  
 Voltage input terminals (ganged) and power plug  
 Current input terminals (ganged) and power plug  
 Case and power plug  
 Insulating withstand voltage:  
 3700 V for one minute at 50/60 Hz across all of the following areas:  
 Voltage input terminals (ganged) and case  
 Current input terminals (ganged) and case  
 Voltage input terminals (ganged) and current input terminals (ganged)  
 Voltage input terminals (ganged) of each element  
 Current input terminals (ganged) of each element  
 Voltage input terminals (ganged) and power plug  
 Current input terminals (ganged) and power plug  
 1500 V for one minute at 50/60 Hz across case and power plug

Power supply: Free power supply (100-240 V), 50/60 Hz frequency  
 Consumed power: Max 35 VA for WT210, max 55 VA for WT230  
 External dimensions for WT210: Approximately 213 × 88 × 379 mm (WHD) (excluding projections)  
 External dimensions for WT230: Approximately 213 × 132 × 379 mm (WHD) (excluding projections)  
 Weight: Approximately 3 kg for WT210, approximately 5 kg for WT230  
 Safety standard: Complying standard EN61010-1  
 Overvoltage category (Installation category) II  
 Pollution degree 2  
 Emission: Complying standard EN61326 Class A  
 EN61000-3-2  
 EN61000-3-3  
 AS/NZS 2064 Class A  
 Immunity: Complying standard EN61326 Annex A

### Exterior View



### Model Numbers and Suffix Codes

Model number	Suffix code	Description	
760401		WT210 single-input element model	
Power cord	-D	UL/CSA standard	
	-F	VDE standard	
	-R	AS standard	
	-Q	BS standard	
Options	/C1	GP-IB communication interface	Select one
	/C2	Serial (RS-232-C) communication interface	Select one
	/EX1	External input 2.5/5/10 V	Select one
	/EX2	External input 50/100/200 mV	Select one
	/HRM	Harmonic measurement function	Select one
	/DA4	4-channel DA output	Select one
/CMP	Comparator and D/A, 4 channels each	Select one	

Note: The WT210 communication interface cannot be changed or modified after delivery.

Model number	Suffix code	Description	
760502		WT230 2-input element model	
760503		WT230 3-input element model	
Interface	-C1	GP-IB communication interface	Select one
	-C2	Serial (RS-232-C) communication interface	Select one
Power cord	-D	UL/CSA standard	
	-F	VDE standard	
	-R	AS standard	
	-Q	BS standard	
Options	/EX1	External input 2.5/5/10 V	Select one
	/EX2	External input 50/100/200 mV	Select one
	/HRM	Harmonic measurement function	Select one
	/DA12	12-channel DA output	Select one
	/CMP	Comparator and D/A, 4 channels each	Select one

### Standard Accessories

Power cord, Power fuse, Current input protective cover, Rubber feet for the hind feet, 24-pin connector (provided only on options/DA4, /DA12, and /CMP), User's manual

### Wiring Types and Model Numbers

Wiring	Model	760401	760502	760503
Single-phase 2-wire		✓	✓	✓
Single-phase 3-wire		-	✓	✓
Three-phase 3-wire (2 voltages, 2 currents)		-	✓	✓
Three-phase 3-wire (3 voltages, 3 currents)		-	-	✓
Three-phase 4-wire		-	-	✓

### Rack mounts

Product	Model or part number	Specification	Order quantity
Rack mounting kit	751533-E2	For WT210 EIA standalone installation	1
Rack mounting kit	751533-J2	For WT210 JIS standalone installation	1
Rack mounting kit	751534-E2	For WT210 EIA connected installation	1
Rack mounting kit	751534-J2	For WT210 JIS connected installation	1
Rack mounting kit	751533-E3	For WT230 EIA standalone installation	1
Rack mounting kit	751533-J3	For WT230 JIS standalone installation	1
Rack mounting kit	751534-E3	For WT230 EIA connected installation	1
Rack mounting kit	751534-J3	For WT230 JIS connected installation	1

Ask Yokogawa for information on rack mounts in which WT210 and WT230 are combined.

### Accessories (sold separately)

Model number	Description
B9317WD	1.5 mm hex wrench For fastening cable on 758931
B9284LK	External sensor cable For external input; 50 cm